For Reference

NOT TO BE TAKEN FROM THIS ROOM

For Reference

NOT TO BE TAKEN FROM THIS ROOM

Ex libris
universitatis
albertaensis

University of Alberta
Printing Department

Digitized by the Internet Archive
in 2019 with funding from
University of Alberta Libraries

https://archive.org/details/Hutchinson1965

UNIVERSITY OF ALBERTA

A STUDY OF CARBON TRANSPORT IN Fe, Fe-Mn, AND Fe-Si ALLOYS UNDER THE INFLUENCE OF AN ELECTRIC FIELD

A THESIS
SUBMITTED TO THE FACULTY OF GRADUATE STUDIES
IN PARTIAL FULFILMENT OF THE REQUIREMENTS
FOR THE DEGREE OF MASTER OF SCIENCE

by

Lew Cameron Hutchinson

DEPARTMENT OF MINING AND METALLURGY

EDMONTON, ALBERTA

MAY 1965

THE UNIVERSITY OF ALBERTA

FACULTY OF GRADUATE STUDIES

The undersigned certify that they have read, and recommend to the Faculty of Graduate Studies for acceptance, a thesis entitled: "A Study of Carbon Transport in Fe, Fe-Mn, and Fe-Si Alloys Under the Influence of an Electric Field", submitted by Lew Cameron Hutchinson in partial fulfilment of the requirements for the degree of Master of Science.

ABSTRACT

The migration of carbon ions in Fe, Fe-4 %Mn, and Fe-2 %Si Alloys under the influence of an electric field was studied at 950° C with a field strength of approximately 0.24 V/cm. The carbon concentration distribution curves in the diffusion couples were determined using a microhardness technique. The measured electro-migration was related to an effective charge by the Einstein equation. The effective charge of 6.69 ± 0.22 for carbon in Fe was increased to 9.19 ± 0.34 in Fe-4 %Mn and decreased to 4.73 ± 0.38 in Fe-2 %Si. The results have been qualitatively explained using Pauling's theory on the valencies of transition metals.

ACKNOWLEDGEMENTS

The author wishes to express his gratitude to Dr. W.V. Youdelis for his guidance and contributions during the course of this project. He is also indebted to Mr. Malcolm Bibby, M. Sc. for his encouragement and suggestions in carrying out the work, and to his wife, Marilyn, and Mrs. Trahan who typed the manuscript. The photography by Mr. R.M. Scott and departmental supervision by Professor E.O. Lilge are gratefully acknowledged.

The author is grateful to the Defence Research Board who furnished the grant making this project possible.

TABLE OF CONTENTS

LIST OF FIGURES AND ILLUSTRATIONS

Page

Page

LIST OF TABLES

I. INTRODUCTION

A satisfactory model to adequately explain the electronic structure and mechanism of bonding in alloys is still being sought. There have been some models proposed to explain this, but none that have satisfied all the experimental results that have been gathered. X-ray diffractions, neutron diffraction, and experiments on magnetic properties and the effects of a magnetic field have produced many results to support or contradict the different electronic models proposed. One approach that produces useful information about electronic structure and bonding between solute and solvent atoms is the study of migration of both the base metal and impurity ions under the influence of an electric field.

When an electric field is applied to a metal there is a flow of current carrying electrons. There is also a movement or transport of the metal and impurity ions in an attempt to carry some of the current. Studying the migration and conditions necessary for migration of these ions offers information regarding an acceptor-donor relationship between the elements involved as well as ideas concerning the types of carriers in metals. Ion transport under the influence of an electric field is frequently referred to as electro-transport,

electro-diffusion, or electro-migration.

The electro-migration of a metal ion through a medium of like ions is very slow because of the high activation energy required for an atom jump. Thus, it is found that electro-transport of iron atoms in an iron bar subjected to an electric field is small. Interstitial atoms present would tend to be transported at a much faster rate because of the relative ease with which they pass through the parent lattice. The electro-migration of carbon in iron is a good example of interstitial ion transport. Conditions favouring electro-transport are a sufficiently high electric field to cause a measurable ion migration and a high enough temperature to facilitate the diffusion process.

The electro-migration of carbon in iron has been studied with varying degrees of success in the past. In the present work a technique has been developed to determine the electric mobility of carbon ions in iron. The electro-migration of carbon is studied by observing the shift, under the influence of an electric field, of the carbon distribution curve. The magnitude of the shift is related to an effective valency for the carbon ions using the Einstein equation

$$B = \frac{D}{kT} ,$$

where B is the mobility (velocity per unit force), D is the diffusion coefficient, k is Boltzman's constant, and T is the absolute temperature.

It is known that manganese and silicon, as alloy additions to steel, have opposite effects on the extent of the γ field, with manganese opening and silicon closing the γ field. As a result, it is interesting to determine the effect of each of these elements on the electro-migration of carbon in steel. The effects may be explained in terms of an altered electronic structure.

The success of an investigation of this type depends on the ability to determine the carbon concentration distribution curves over a distance of approximately one millimeter. The small size of samples used limited the methods of analysis available. A calibration curve of hardness vs. carbon content has been determined to permit the use of micro-hardness measurements for determining carbon concentration.

II. LITERATURE REVIEW

(1) The Hardness vs. Carbon Concentration Curve

Bain[1] has shown that for steel with 0.1 to 0.6%[*] carbon in the martensitic condition there is a reproducible relationship between the hardness and the carbon concentration. Bain has also shown that additions of Cr, Mo, Si, Mn, and Ni will increase the maximum attainable hardness by a small amount. The increased maximum hardness by alloy additions was not noticed in the work of Nehrenberg et al.[2] The alloys tested by Nehrenberg et al. were Ni (0.13%-6.28%), Cr (0.43%-0.77%), Si (0.13%-1.36%), and Mn (0.33%-3.41%) in steel. He suggested that the increase in maximum hardness that Bain found for chromium was due to an increased nitrogen content as the chromium was increased. It is noted in the ASM Metals Handbook (1948) that silicon and manganese do appreciably increase the hardness in the tempered condition.

The effect of manganese on the M_s temperature has been investigated.[3] Steel containing 4% Mn and 0.5% C has the M_s and M_f temperatures lowered to approximately 225° C and -70°C respectively. Bain[1] found that the presence of some retained austentite does not affect the aggregate hardness of a sample.

---

[*] All concentrations are in weight percent unless otherwise noted.

The addition of silicon should tend to raise the M_s and M_f temperatures of steel since it is an α-iron stabilizer.

(2) Electro-Migration

The first reported experimental work on electro-migration appeared in the 1930's.[4] At that time some qualitative experiments were performed which indicated an increased directed self diffusion of metal atoms under the influence of an electric field. There were also studies done on the electromigration of interstitial atoms in metals. The quantitative results were recorded as electric mobilities of the interstitial atom or as a transference number.

Experiments indicating self diffusion in metals under the influence of an electric field consisted of heating wires in a vacuum by passing a direct current through them.[5] There was a surface change observed at each end of the hot zone in the wire. There appeared to be a transport of material to the negative end of the sample and a corresponding shrinkage at the positive end. This indicates the movement of the metal atoms as though they were positively charged ions. This was found with W, Ta, Mo, Pt, Fe, and Ni. When these same wires were heated by an alternating current there was no apparent change in surface structure. It was difficult to

obtain quantitative results from these experiments, but they do indicate a significant metal transport in a direct electric field.

Studies of the electro-transport of interstitial atoms were performed on H-Pd, C-Fe, N-Fe, and B-Fe, the first component named being the interstitial solute. These interstitial elements, with the exception of N, were found to migrate towards the cathode. Nitrogen migrated towards the anode as though it possessed a negative charge.

In 1935 Seith and Kubaschewski[6] showed that carbon migrated to the cathode in iron at 1000° C under the influence of an electric field. For their experiments they used a 1.5 millimeter diameter, low-carbon iron wire. They coated the wire with copper and then removed about 1 centimeter of the coating from the central portion. The unprotected part of the wire was then carburized and recoated. A direct current power source was used to heat the wire to 1000° C in a vacuum. With a reported current of approximately 25 amps and a field strength of 0.1 volts per centimeter, they found an average electronic mobility for the carbon ions of 2×10^{-5} cm/sec. per V/cm.

(3) Fiks' Theory

In the latest surge of work on electro-transport there

have been efforts to present a quantitative theory explaining electro-transport in metals. In electro-transport, the electric field is not the only force on the ions. There is also a force due to momentum transfer between the current carriers and the migrating ions. The object of the theories is to define the forces which act on the migrating ions and to relate these forces to the velocities of the various ions. The theory proposed by Fiks[7] appears to be the most generally accepted one.

Fiks assumes the electrons to be the current carriers. He examines the interaction of electrons with ions in the framework of the electron theory of metals, and considers that the theory should establish a connection between the mobility of an ion in a metal, the diffusion coefficient of the ion, the electrical properties of the metal, and the physical parameters of the ion which characterize its interaction with the electrons.

When an electric field, E, is applied to the metal, an ion of charge (+)q will have a force

$$F = eEq \qquad (1)$$

acting on it in the direction of the field. There will be a force in the opposite direction as well due to the electron wind. If the mean free path of electrons in the metal is l,

an electron having velocity v will move for a time interval $t = l/v$, and the added momentum picked up by the electron due to the field is

$$\Delta p = eEl/v \tag{2}$$

The number of electrons per unit volume whose momenta lie between p and p+dp is $(2/h^3)\, f dP$, where f is the distribution function of electrons with regard to momentum and dP is the volume element in momentum space. The number of collisions per second for these electrons is $v\sigma_i(2/h^3) f dP$, where σ_i is the scattering cross section of the ions for the electrons. The momentum imparted to the ion in one second is equal to the force the electrons exert on the ion, viz.,

$$\begin{aligned} F_{ei} &= (\text{no. of collisions/sec.})(\text{momentum/collision}) \\ &= \int v\sigma_i (2/h^3)\, f dP \cdot eEl/v \\ &= (2/h^3)\int eEl\sigma_i\, f dP \\ &= eEnl\sigma_i\,. \qquad (3) \end{aligned}$$

This force is directed against the field because of the electron's negative charge. From equations (1) and (3) it is seen that the resultant force on the ion is

$$F = eE(q - nl\sigma_i)\,. \tag{4}$$

Fiks' uses Mott's[8] expression for the residual resistance of a metal due to scattering of electrons at impurity ions,

is

$$\Delta\rho_0^i = \frac{m\bar{v}}{e^2} c_i \sigma_i \quad , \tag{5}$$

where c_i is the relative concentration of impurity ions, $\bar{v}$ is the mean velocity of the electrons, and the expression for the specific resistance of a pure metal,

$$\rho = \frac{m\bar{v}}{e^2 n l} \tag{6}$$

to give the expression relating scattering cross section and resistivity, thus:

$$\sigma_i n l = \frac{1}{c_i} \frac{\Delta\rho_0^i}{\rho} \quad . \tag{7}$$

The resultant force on the ion can now be written

$$F = eE\left(q - \frac{1}{c_i} \frac{\Delta\rho_0^i}{\rho}\right) . \tag{8}$$

It can be seen from expression (4) that the direction of the force on the ion depends on the magnitude of the electron momentum exchange relative to the charge q of the impurity ion. It is also seen from equations (4) and (8) that the coefficient of eE is what can be termed the effective charge on the ion.

Fiks then uses Frenkel's[9] kinetic expressions for the effect of an electric field on the velocity of ion migration to derive the Einstein equation, which relates the velocity of ion migration to the diffusion constant.

Consider the motion of a particle that requires an activation energy U to jump from one site to another. If an external force F acts on the ions in the positive x direction, the change in potential energy will be $\Delta U = -Fx$. In the absence of the external force the probability of an atom making a jump per unit time is

$$\alpha = \nu_0 \exp. (-U/kT), \tag{9}$$

where ν_0 is the vibration frequency of the particle in the potential well. When an external force is applied in the positive x direction, the probability of a jump per unit time in the negative x direction will be

$$\alpha_- = \frac{1}{2} \nu_0 \exp. -(U + 1/2\, \delta F)/kT , \tag{10}$$

where δ is the distance from one potential well to the next. The probability of a jump per unit time in the positive x direction will be

$$\alpha_+ = \frac{1}{2} \nu_0 \exp. -(U - \tfrac{1}{2} \delta F)/kT . \tag{11}$$

Thus the mean velocity of the motion is given by

$$\begin{aligned} \bar{v} &= (\alpha_+ - \alpha_-) \\ &= \frac{1}{2} \delta\alpha \left[\exp.(\delta F/2kT) - \exp.(-\delta F/2kT)\right] \\ &= \delta\alpha \sinh \delta F/2kT . \end{aligned} \tag{12}$$

If $\frac{1}{2}\delta F \ll kT$ the hyperbolic sine can be replaced by $\delta F/2kT$. The quotient of the velocity divided by the force causing the velocity is the mobility, and from the above expression is

seen to be

$$B = \delta^2\alpha/2kT\,. \qquad (13)$$

Frenkel has shown that $\frac{\delta^2\alpha}{2}$ is equal to the diffusion coefficient D. The mobility is thus related to the diffusion coefficient by the expression

$$B = D/kT, \qquad (14)$$

which is the expression derived by Einstein[10] in his theory of Brownian motion.

At this point it is interesting to point out that Glinchuk[11] considers momentum transferred to ions from positive electronic charge carriers or holes as well. The force exerted would be in the opposite direction to that of electrons. Fiks' equation is modified thus:

$$F = eE(q - n_e l_e \sigma_{ie} + n_p l_p \sigma_{ip}), \qquad (15)$$

where p refers to the positive charge carriers and e refers to the electrons. The momentum transfer from positive charge carriers has been referred to as hole momentum by those using it.[12]

(4) Experimental Results

Next, it is of interest to consider some of the investigations on electro-migration in pure metals and alloys. Wever[13] has investigated electro-migration in the pure metals

iron, copper and nickel. For iron he finds that there is a mass transport towards the cathode, suggesting a large positive charge for the iron ions, which would indicate a force over and above that of the electric field force. Momentum imparted to the iron ions by a positive charge carrier would have this effect. (cf. Glinchuk)

Frantsevich[14] studied the migration of iron atoms in a Fe-1%C alloy. He found that the iron migrated to the anode up to the temperature of 1150° C, above which he found no migration. Gertsriken[15] also studied the electro-migration of iron in a Fe-C alloy using alloys containing 0.35%C and 0.70%C, and found that the iron migrated to the anode in these alloys as it did in the 1%C alloy used by Frantsevich.

There has been a fair amount of work reported on electro-migration of interstitial atoms. Interstitial migration is more suitable experimentally because of the high migration velocity of the interstitial ions relative to the lattice ions. The results reported for the electro-migration of carbon in iron have been consistent in recording the same direction of migration but variations in the magnitude of migration are noted. Dayal and Darken[16] studied electro-migration of carbon in iron by measuring the amount of carbon passing a central plane per unit time; the central plane

being perpendicular to the direction of the applied field. Their sample was initially of uniform carbon concentration, and after applying the field for a suitable length of time the sample was cut in half at the central plane. Each side was analyzed for carbon by a combustion analysis technique. This method of studying carbon ion migration was thought to be good because the effect of diffusion down a concentration gradient at the central plane was not encountered as it was in methods where carbon diffused from a high carbon zone to a low carbon zone under the influence of an electric field. They did not consider any momentum exchange between the carbon ions and the current carriers in the interpretation of their results, and reported an average charge of +3.7 for the carbon ions.

Hume-Rothery[17] commented on Dayal and Darken's interpretation of their results. He criticized the concept of carbon having a +4 charge at all times in the iron lattice. He pointed out that the sum of the first four ionization potentials for the carbon atom was 147 volts. Considering iron atoms as poor acceptors, he found it difficult to visualize the stripping of four electrons from the carbon atom. Hume-Rothery's alternate suggestion was that the carbon was bound by forces resembling covalent linkages. These covalent

linkages would be fractional because carbon has only four valence electrons to share with the six nearest iron neighbors. At the high temperatures used for electro-migration some of these bonds would be broken. The situation now would be a deficiency of electrons around some of the carbon ions, resulting in a positively charged ion, and a preponderance of electrons around the other carbon ions resulting in negative carbon ions. The small positive carbon ions would readily migrate through the lattice towards the cathode while the negative ions would be tied up because of their increased size, and also because they would still be bound to their iron neighbors. Hume-Rothery criticizes the electro-migration experiments in that the positive ion is indicated by its ability to migrate but no information is attainable about the negative carbon ions, and contends that it is thus incorrect to suggest that, on the whole, the carbon ions have a positive charge in iron.

Frantsevich et al.[14] studied the migration of both iron and carbon in Fe-C alloys. The direction and magnitude of migration was determined by using radioactive isotopes of the migrating ion. Using Frenkel's theory of ion migration they calculate a charge and transport number for the ion. However, variables such as field, current, cross-sectional area of the

sample and the velocity of migration were not given, so consequently, it is not possible to check their results. There was no indication of the effect of momentum exchange between the migrating ions and the current carriers. An average charge of +1.4 was reported for the carbon ions.

Within a few years of the above report, Kalinovich[12] reconsidered the results of Frantsevich et al.[14] in view of the momentum exchange existing between the current carriers and the carbon ions. He used the Einstein relation to relate the reported velocities to the effective charge on the ion. Kalinovich reported an effective charge of +13.4 for carbon at 950° C and a velocity of 8.1×10^{-6} cm/sec.

Frantsevich et al.[18] published a paper in 1958 discussing the donor-acceptor relationship of carbon and iron. On the strength of their work with radioactive tracers, they dispute Hume-Rothery's remarks about some carbon ions having a negative charge while others have a positive charge. They found that all the carbon atoms were shifted by the electric field. Hume-Rothery suggested that only some of the atoms were involved in the migration. They apparently make the assumption that Hume-Rothery intends each carbon ion to maintain its assumed charge, positive or negative, for the full length of the experiment. It would seem more reasonable that

the charges would move from one carbon atom to another giving each carbon atom an equal chance to have a positive charge and migrate to the cathode. They also found that not all of the iron atoms in a Fe-C alloy moved under the influence of the electric field. This was attributed to the probability that only the iron atoms associated with carbon would assume a negative charge and would migrate to the anode. Frantsevich et al.[18] suggest that the donor or acceptor role of impurity atoms in a metal is determined by the reciprocal distribution of the energy levels of the electrons in the outer shell of the impurity ion and of the Fermi level of the electron spectrum of the metal. The introduction of impurity atoms with a donor capacity to the metal results in deformation of the conduction band in the region of the impurity atom. This conduction band deformation will help screen the excess charge of the impurity ion. It is suggested that the screening charge is distributed partly in the conduction band and partly in the inner incomplete 3d shell of the metal atom. The thermal motion of the lattice ion results in a diffusing of the conduction zone electrons. Frantsevich et al. refers to W.F. Mott and H.H. Wils to show that in all probability the diffusion of electrons occurs not as $s \rightarrow s$ migrations but as $s \rightarrow d$ migrations. The probability of these migrations near the

impurity ion is shown to be appreciable.

The literature review indicates that at this time there is no great degree of consistency in results reported for electro-migration. Different experimental techniques and varying methods of interpreting the experimental results are responsible for much of the disagreement. It is apparent that more accurate experimental results are necessary if the various theories and mechanisms proposed for electro-migration are to be accurately assessed.

III. EXPERIMENTAL

A. Apparatus

A fifteen inch tube furnace was used for carburizing, homogenizing, and heating the samples for quenching. A twenty-four inch long, one inch I.D. vitreosil tube was used in the furance to hold the samples and to pass the required atmosphere gas through. Temperature readings were obtained using a thermo-couple coated with zirconium base cement for protection against the carburizing atmosphere. The thermo-couple wires were passed through a rubber stopper to enter the tube, thus preventing any leakage of atmosphere. Atmosphere gas entered one end and then bubbled through an oil pot on the exit end of the tube. Figure 1 shows a schematic arrangement of the furnace and atmosphere control.

The furnace was used in the horizontal position for carburizing, and in the vertical position for homogenizing and quenching. The temperature of the furnace was controlled to $\pm 5^{\circ}$ C using a Honeywell control unit. A water bath containing twelve inches of water was used for quenching.

The Fe-Mn and Fe-Si alloys were prepared in an argon atmosphere by high frequency induction melting in alumina crucibles. The high frequency furnace and the vacuum system

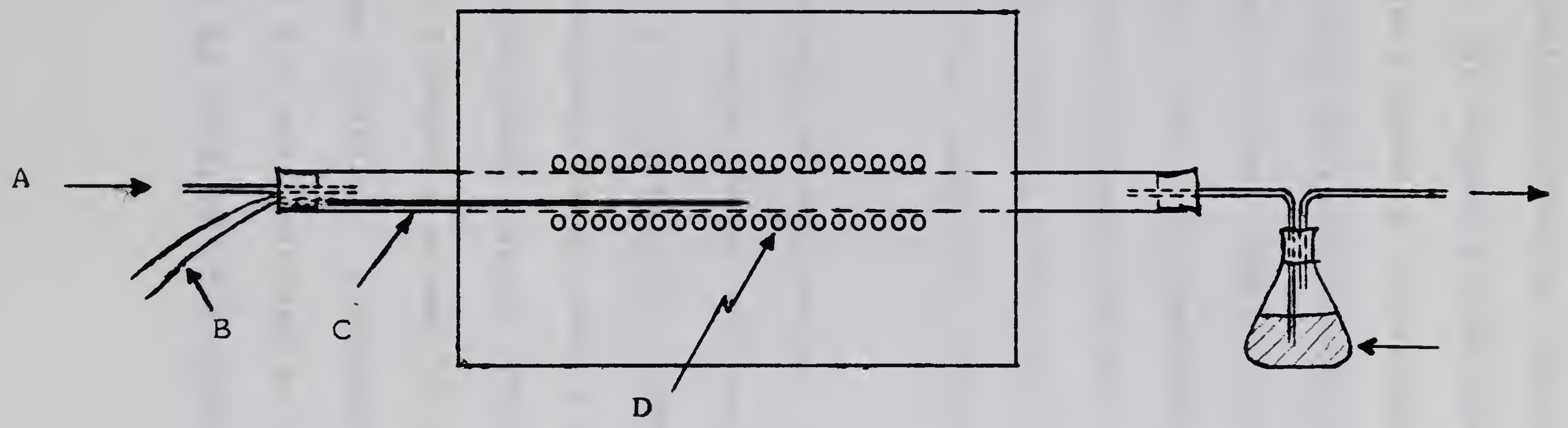

A	Gas inlet
B	Chromel-Alumel thermocouple
C	Vitreosil tube
D	Heating element
E	Oil bubble pot
F	Gas outlet

Figure 1. Tube Furnace Used for Carburizing and Homogenizing.

[illegible]

[illegible]

[illegible]

[illegible]

[illegible]

[illegible]

[illegible]

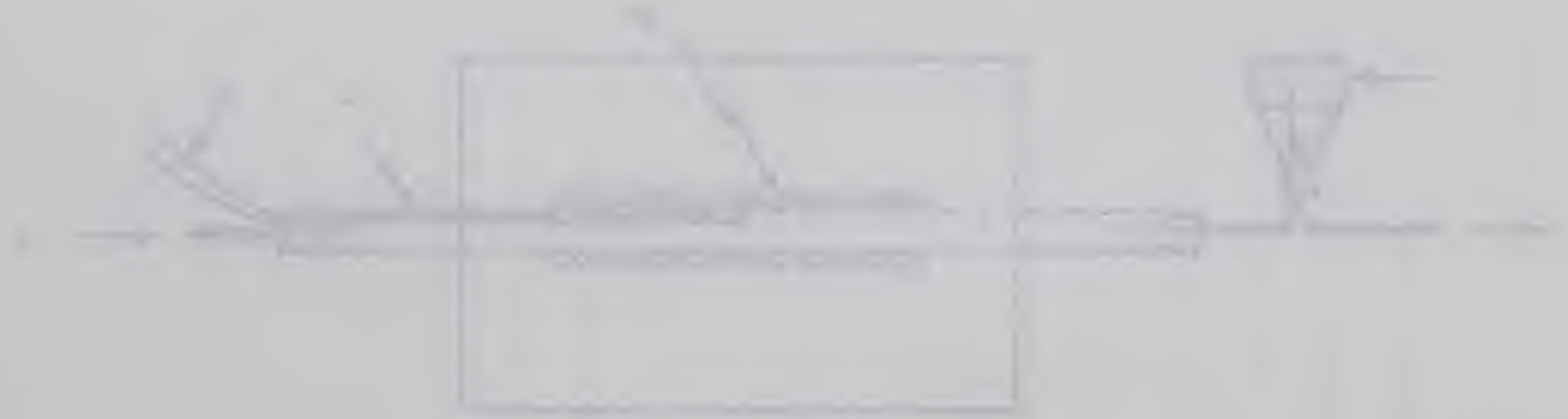

are shown in Figure 2.

The electro-diffusion apparatus consisted of an eighteen inch bell jar vacuum system admitting two water cooled electrode inlets capable of carrying about 500 amps (Figure 3). Twelve electrical outlets suitable for thermo couple leads, voltage probes or other similar connections were attached to the base plate. Power was supplied by a rectifier type direct current welding generator with a ten percent ripple in the current. The vacuum was obtained using a Duo-Seal Vacuum pump, with the gas inlet opened or closed by means of a solenoid valve.

A Honeywell potentiometer, Model 2745, was used for measuring the temperature, voltage and current. For current measurements, a fifty millivolt shunt was put in the circuit.

Microhardness measurements were obtained using a Reichert microhardness tester (Figure 4).

Figure 5 shows a schematic drawing of the apparatus used for copper coating. A variable resistor was placed in series with a 1.5 volt battery so that a suitable current density could be obtained for electroplating.

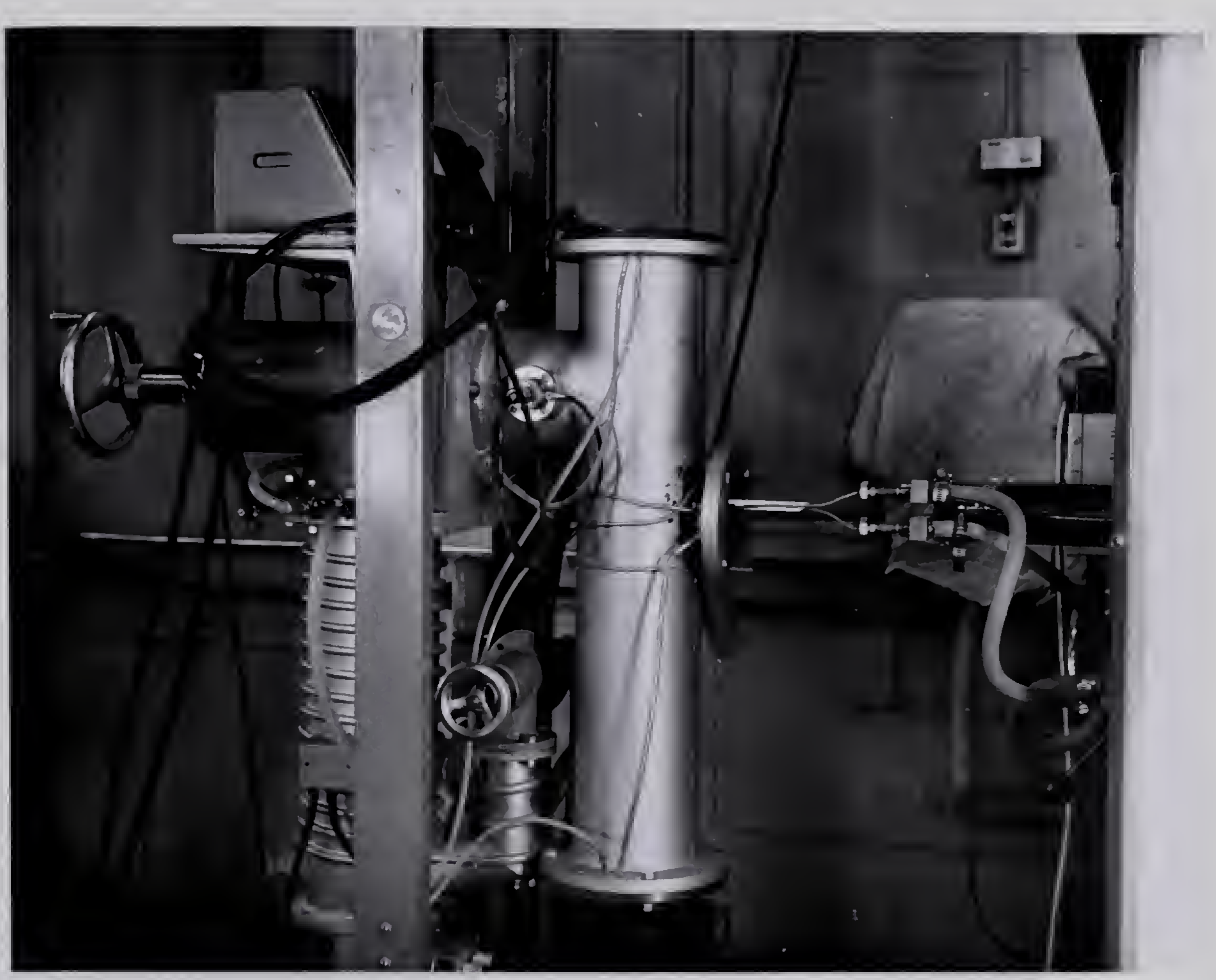

Figure 2. High Frequency Unit and Vacuum System.

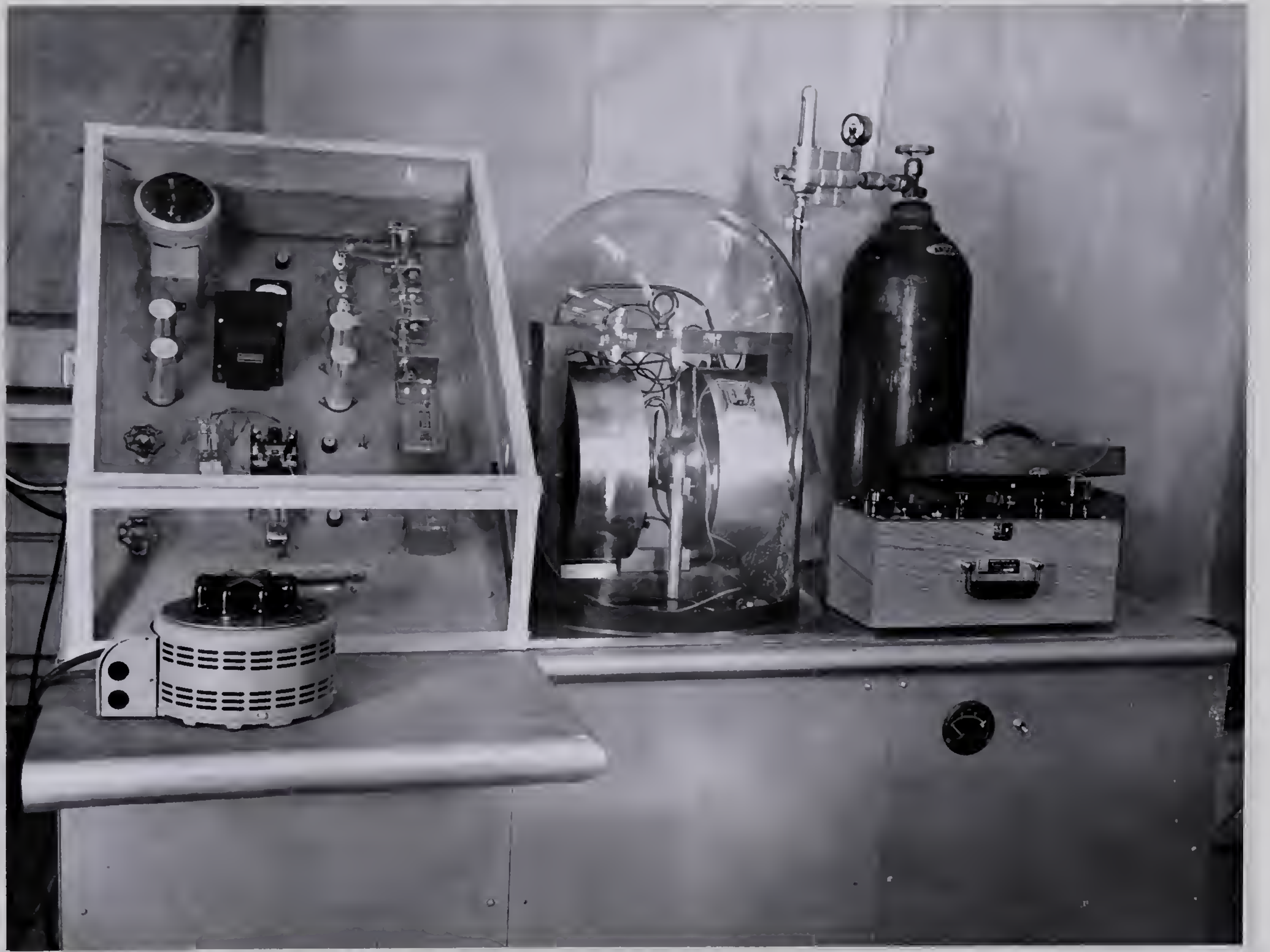

Figure 3. Electro-Diffusion Apparatus.

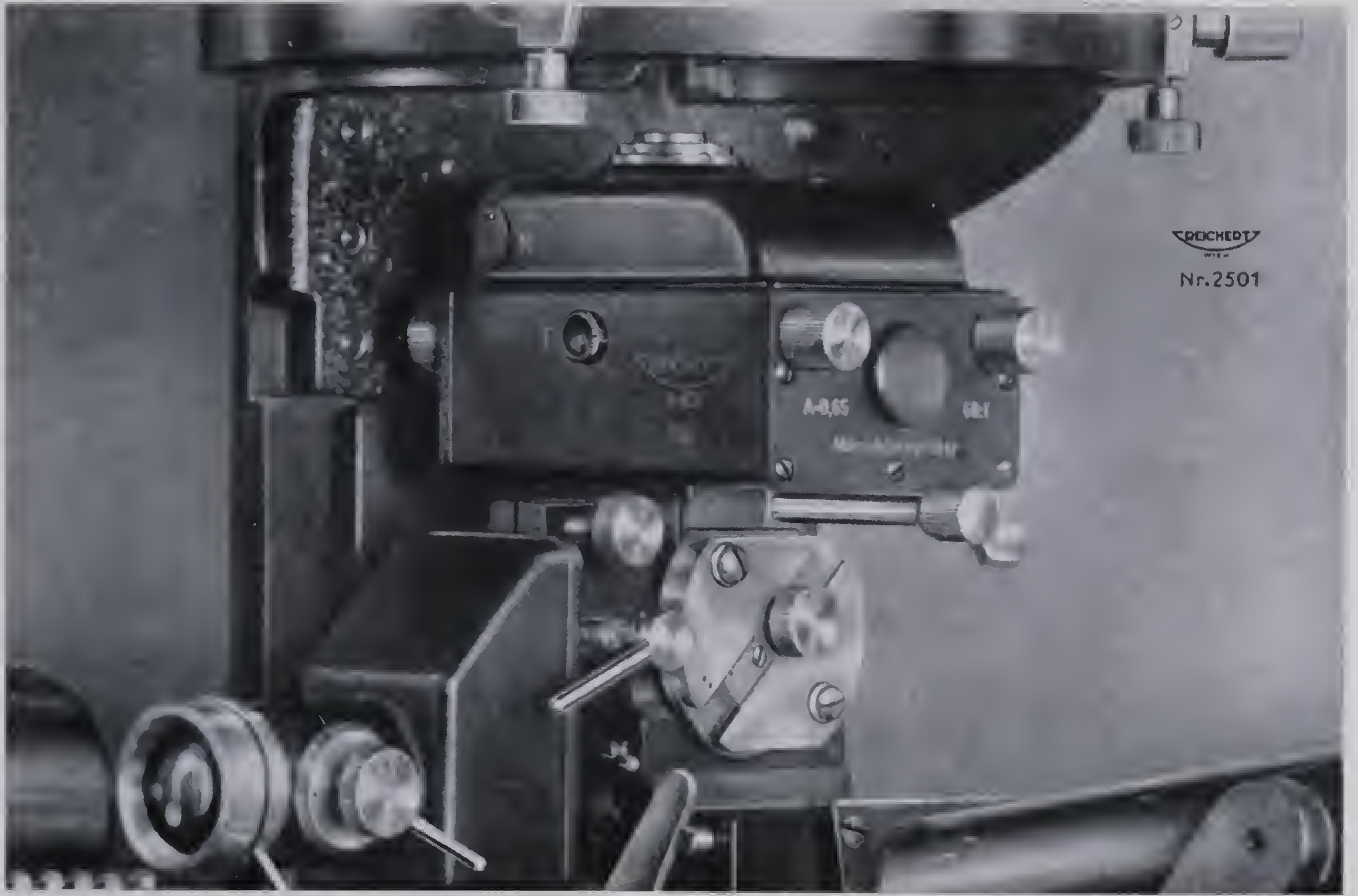

Figure 4. Reichert Microhardness Tester.

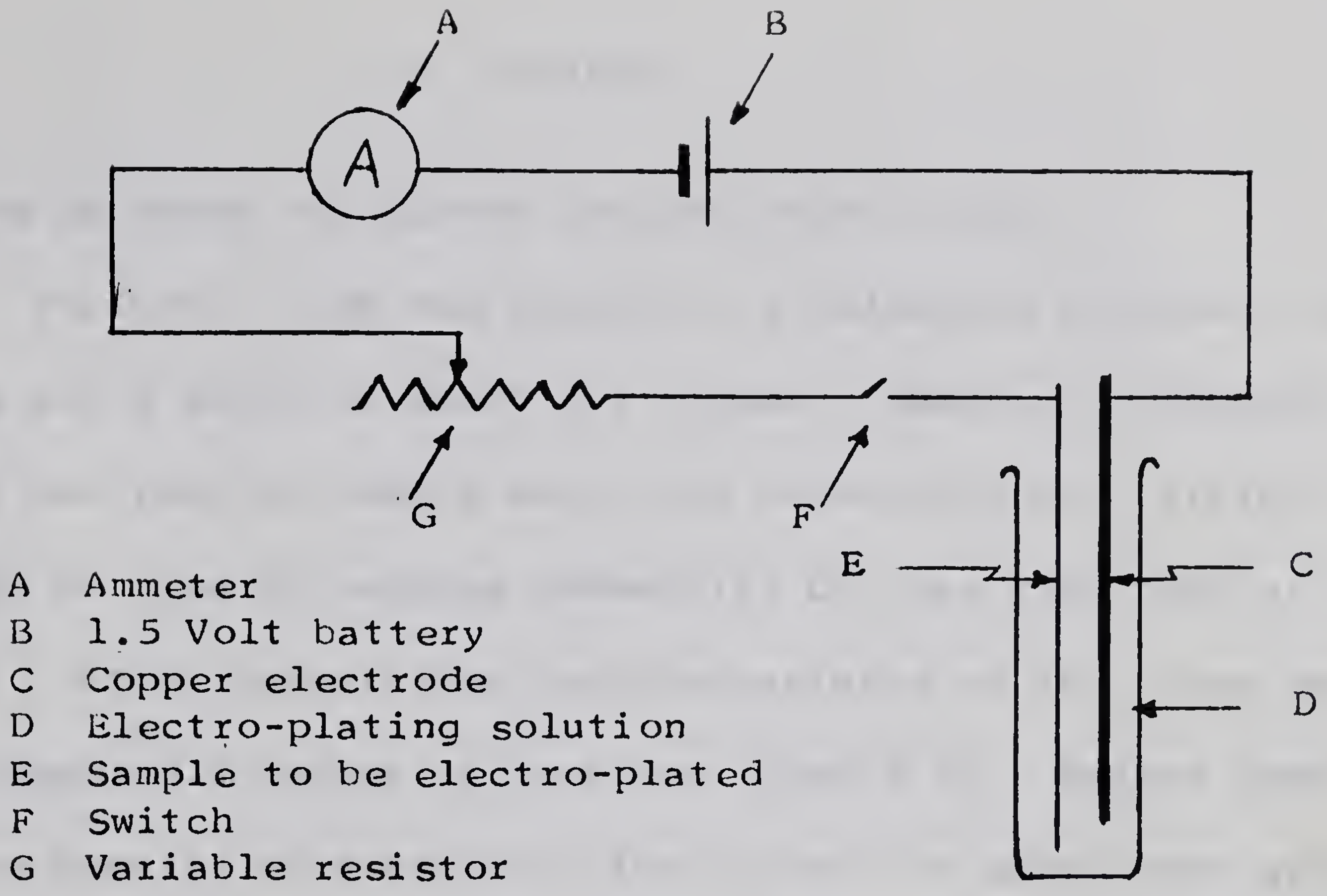

A	Ammeter
B	1.5 Volt battery
C	Copper electrode
D	Electro-plating solution
E	Sample to be electro-plated
F	Switch
G	Variable resistor

Figure 5. Schematic Diagram of Copper Coating Apparatus.

Figure 6. Cross Section of Carburized Sample Showing Boarder of Pearlite.

B. Method

(1) The Hardness vs. Carbon Concentration Curve.

Ferrovac* iron was rolled to a thickness of about 0.080 inches and a width of about 0.5 inches. Samples of approximately one inch in length were then carburized for varying lengths of time by passing commercial CH_4 gas over them at 900° C. After Carburizing, microstructures of the cross section revealed a border of pearlite (Figure 6). Before soaking the samples to distribute the carbon the edges were ground off so that the only source of carbon for distribution was the flat faces of the sample. This allowed a shorter soaking time by eliminating what would have been high carbon zones along the edges. A two hour soaking time at 1000° C was found to be sufficient to insure homogeneity (Figure 7). A tantalum lining in the vitreosil tube was necessary to prevent decarburization of the sample during soaking. If a sample was slowly cooled the microstructure would show whether the sample was homogeneous. A constant hardness diagonal across the sample in the martensite condition also indicated homogeneity. If the sample was slowly cooled after homogenizing it was heated to over

---

*For analysis of Ferrovac see Table 1.

1000° C and held there at least ten minutes before quenching. The procedure for quenching was to drop the sample directly down the vitreosil tube into twelve inches of water at 15° C.

Microhardnesses were taken on all four sides of the specimen to insure homogeneity. Before taking microhardnesses, the sample was polished until there were no scratches on the surface visible at 350 magnification and then etched with 2% Nital to reveal an undistorted microstructure of martensite (Figure 8). Microhardness indentations were made using a 35.5 gm load for 10 seconds. The indentation diagonals were recorded as the number of units on the diagonal-measuring drum. Samples were sent to Chicago Spectro Service Laboratory for carbon analysis after the hardness was determined.

(2) Alloy Preparation

Ferrovac iron was used for the Fe-Mn and the Fe-Si alloys. The 4% Mn alloy was prepared by placing the manganese adjacent to the iron in an alumina crucible and melting by high frequency induction heating. The 2% Si alloy was made in a similar manner by placing the silicon in holes drilled in the iron. This procedure was necessary to enable the silicon to properly mix with the molten iron.

To insure an inert atmosphere for melting, the alloy

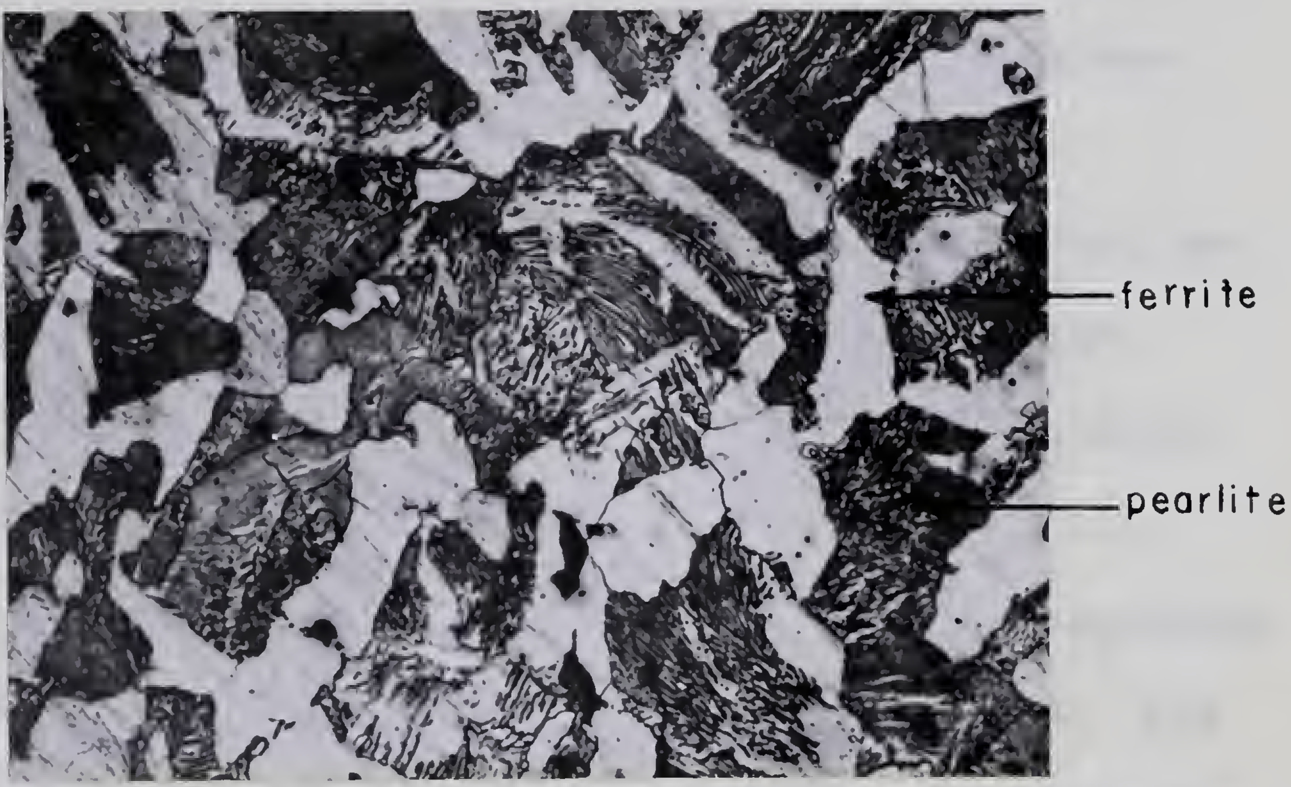

Figure 7. Evenly Distributed Pearlite Indicating Homogeneity of the Sample x275.

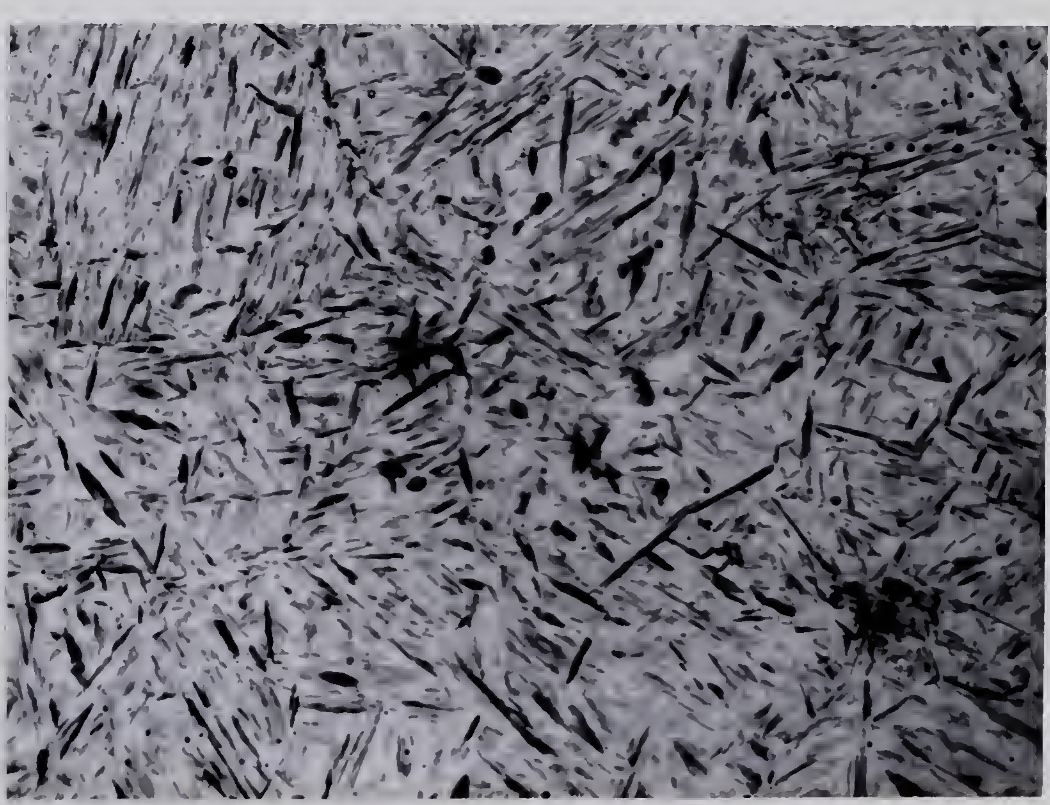

Figure 8. Martensite in Fe-C x 550.

was placed in a vacuum system. A vacuum of 2×10^{-5} mm of mercury was obtained before admitting argon to a positive pressure of about two psi.

Good convective mixing was evident when the alloy was in the molten state. After freezing, cold rolling, and annealing, hardness measurements were taken to insure homogeneity.

The ingots were rolled to a thickness of approximately 0.025 inches and sheared into strips 0.07 inches wide. The Fe-Mn and Fe-Si alloys were carburized in the same manner as the iron samples.

Armco iron wire was used for the iron-carbon experiments. The wire was 0.050 inches in diameter. A complete analysis of the wire is given in Table 2.

(3) Sample Preparation

A typical couple design was a 1/8 inch piece of Fe-C butt welded between two 3¼ inch pieces of iron, all of the same cross sectional area and shape.

The couples were welded by a resistance butt welding technique. This was accomplished by replacing the electrodes of the spot welder with the two pieces of sample to be welded. A clean, sound weld was insured by polishing and etching the surfaces to be welded.

The Fe-Mn couples were made in a manner similar to the pure iron couples. A section of Fe-Mn-C strip was welded between two pieces of Fe-Mn.

It was necessary to adopt a more elaborate couple design for the Fe-Si alloy. From the phase diagram (Figure 9) for Fe-2% Si-C, it is noted that at 950° C., 0.18% C is the minimum carbon concentration for the γ region; the region in which carbon ion migration was to be studied. Thus, to keep the sample in the γ region at 950° C. it was necessary to diffuse carbon from a high carbon zone to a low carbon zone on each end (low carbon being greater than 0.18%).

Another complicating factor was the alloying of the Chromel-Alumel thermo-couple wires with carbon. This was avoided by using the following couple arrangement: Fe-Si, Fe-Si-C, Fe-Si-C, Fe-Si-C, with the thermo-couples being welded to the Fe-Si section of the sample.

To prevent decarburization during a run, a copper coating was electroplated on the sample. A cyanide electroplating bath was used with a current density of approximately 0.4 amps per square foot. An electroplating time of 1/2 - 3/4 of an hour gave an adequate copper coating of 0.0005-0.001 inches. The electroplating bath contained:

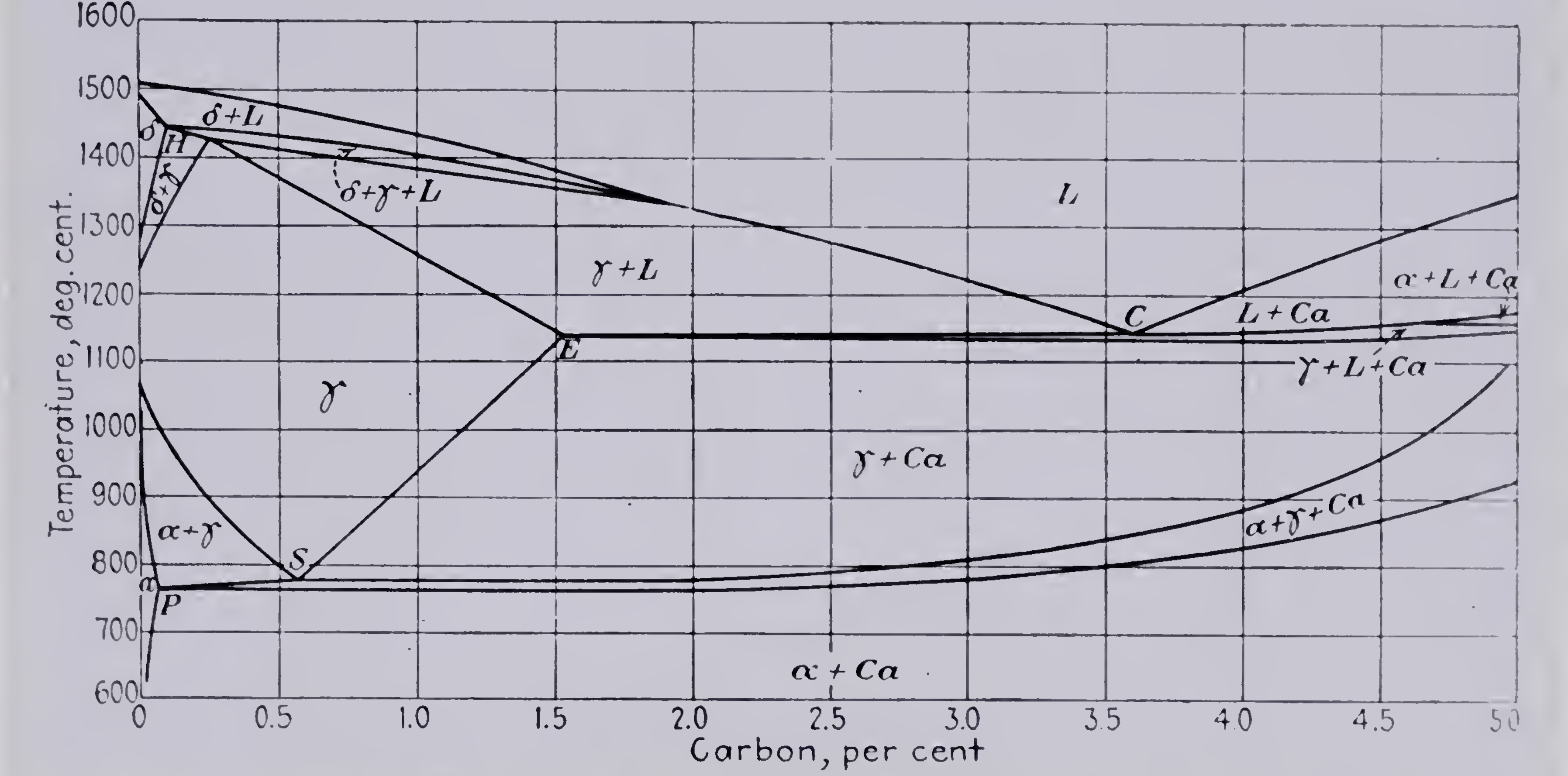

Figure 9. Fe-2% Si-C Phase Diagram.

		Oz. per gal.
Copper (cuprous) cyanide	CuCN	3.0
Sodium Cyanide	NaCN	4.5
Sodium Carbonate	Na_2CO_3	2.0
(Free Sodium Cyanide)	NaCN	1.0

Chromel-Alumel thermocouples were used for temperature readings. When attaching thermocouples to a couple that is carrying a current it is impossible to get a true temperature reading because of the "IR" drop or pick up across the thermocouple wires. To eliminate this effect a balancing circuit devised by Boedtker and Duwez[19] (shown schematically in Figure 10) was used. Three thermocouple wires were welded to the specimen at a distance of approximately 0.020 inches (Figure 11). If the two outside wires were Alumel and the third wire was Chromel, the arrangement would constitute a double thermocouple. The two outer wires were connected to the fixed contacts of a 100 ohm potentiometer (Heliopot, Model A) and the movable contact was adjusted until on passing a current through the sample there was no change in the e.m.f. reading between the movable contact and the Chromel wire when the current direction was reversed. At this setting of the movable contact the "IR" drop and "IR" pick up over the double thermocouple arrangement cancel one another. The balance of the circuit can also be checked at high temperatures to insure that the temperature recorded is correct.

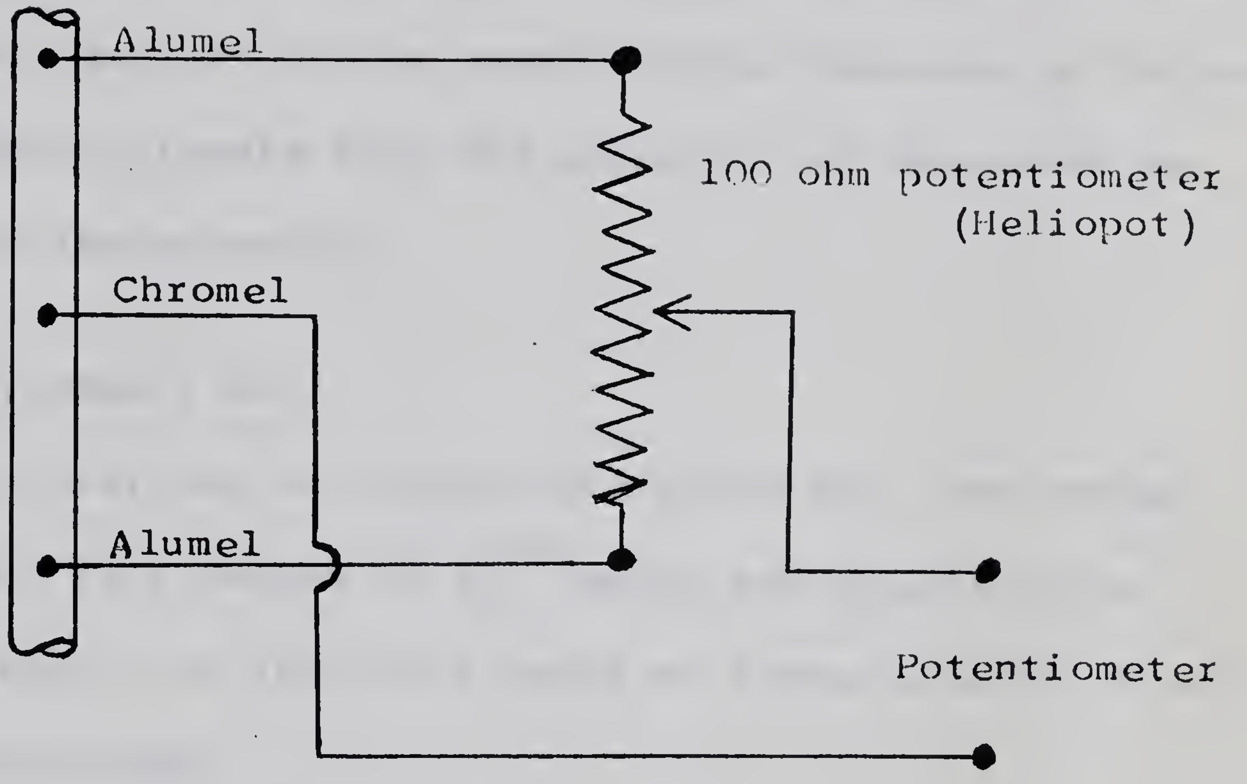

Figure 10. Balancing Circuit (after Boedtker and Duwez).

Figure 11. Photomacrograph of Three Thermocouple Wires Welded to Sample.

[illegible]

[illegible]

Chromel-Alumel thermocouples alloy with carbon resulting in a change of e.m.f. This necessitated welding the thermocouples on a section of the sample where there was no carbon. Care was taken to insure that the direction of migration was away from the thermocouples.

(4) Carbon Transport Run

Before starting an electro-diffusion run, the system was pumped out to a vacuum of 10^{-3} mm Hg and purged three times with argon. On the third purge an atmosphere of -2 psi gauge was maintained.

The non-temperature electrical effects of the thermocouple readings were balanced out at relatively low temperatures. This was accomplished by reversing the direction of the current by means of a double pole-double throw switch and adjusting the movable contact on the Heliopot until the e.m.f. was constant.

The two Alumel thermocouple leads were used for measuring the voltage drop across the sample. The distance between the Alumel wires was measured by a micrometer with the aid of laboratory binoculars.

The temperature was held at 950° C by adjusting the current at the power source.

To determine the carbon concentration distribution curve the sample had to be in the martensitic condition. This was accomplished by holding the sample at 1000° C. for five minutes in an argon atmosphere and quenching in water.

A one inch piece of the sample containing the diffusion couple was mounted in thermosetting bakelite to facilitate handling. The sample was then polished and etched before taking microhardness readings. Microhardness traverses were taken in the direction parallel to the direction of the current.

IV. RESULTS

The relationship between carbon concentration and hardness is illustrated in Figure 12. The carbon concentrations are plotted as weight percent. Multiplying the weight percent by 4.54 will give the approximate atomic percent of carbon for the composition investigated.

Two weld zones constitute each couple. The weld on the cathode side of the high carbon zone is referred to as the negative (-) weld, and the weld on the anode side of the high carbon zone as the positive (+) weld. The hardness traverse was taken along the sample parallel to the direction of the applied field. The hardness traverses for Fe-C Couple A are plotted in Figure 13. The weld interfaces were detected metallographically and are marked at appropriate positions on the hardness plot.

It was possible to construct concentration-penetration curves for the iron-carbon electro-migration couples. The weld position and penetration curve for the Fe-C Couple A, at the (-) weld, is shown in Figure 14. Diffusion constants were then determined from the concentration-penetration curves for Fe-C Couples A, B, and C. The concentration-penetration curves were constructed from C/C_0 values taken from a best fit

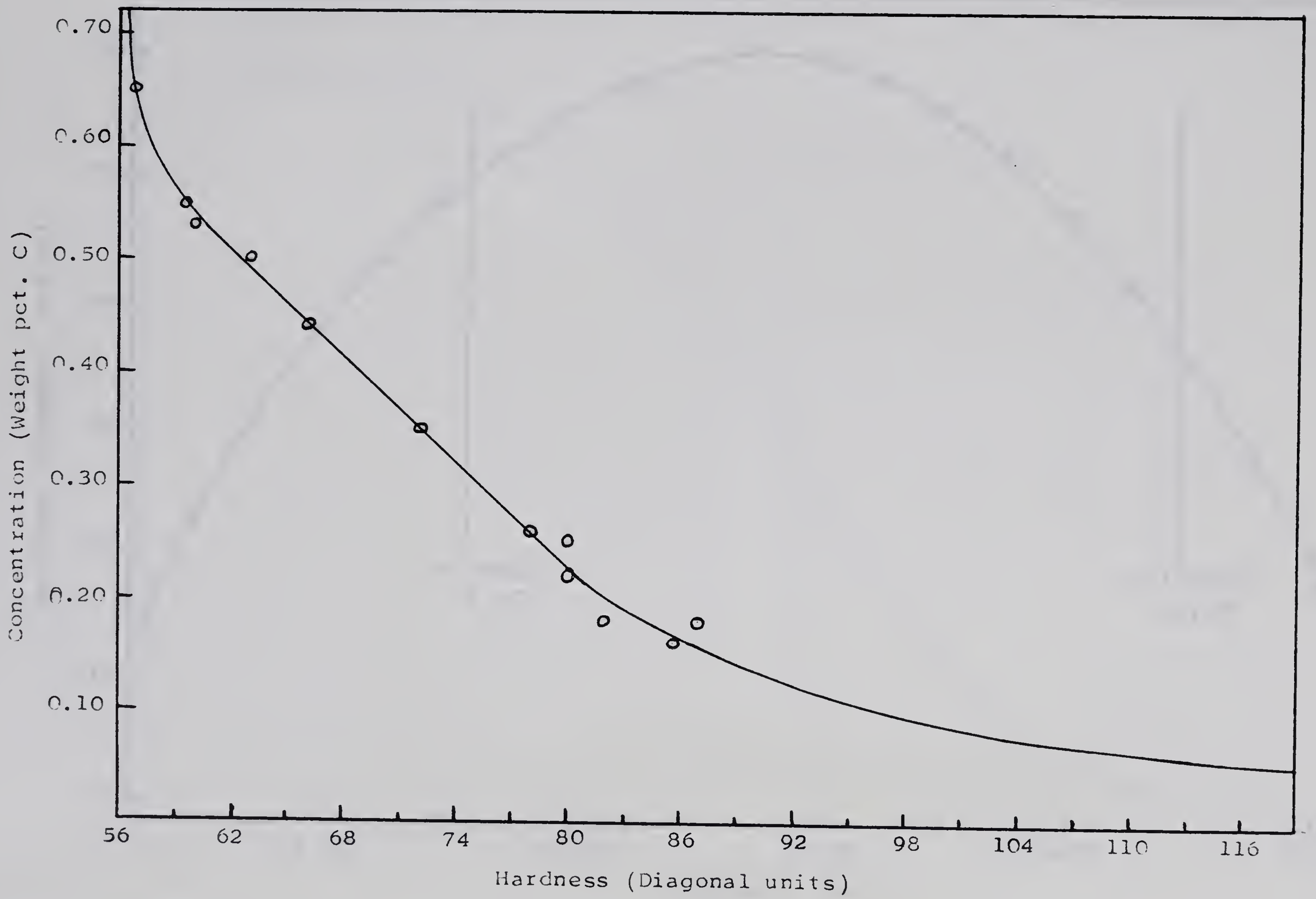

Figure 12. Carbon Concentration vs. Hardness of Iron-Carbon Martensite.

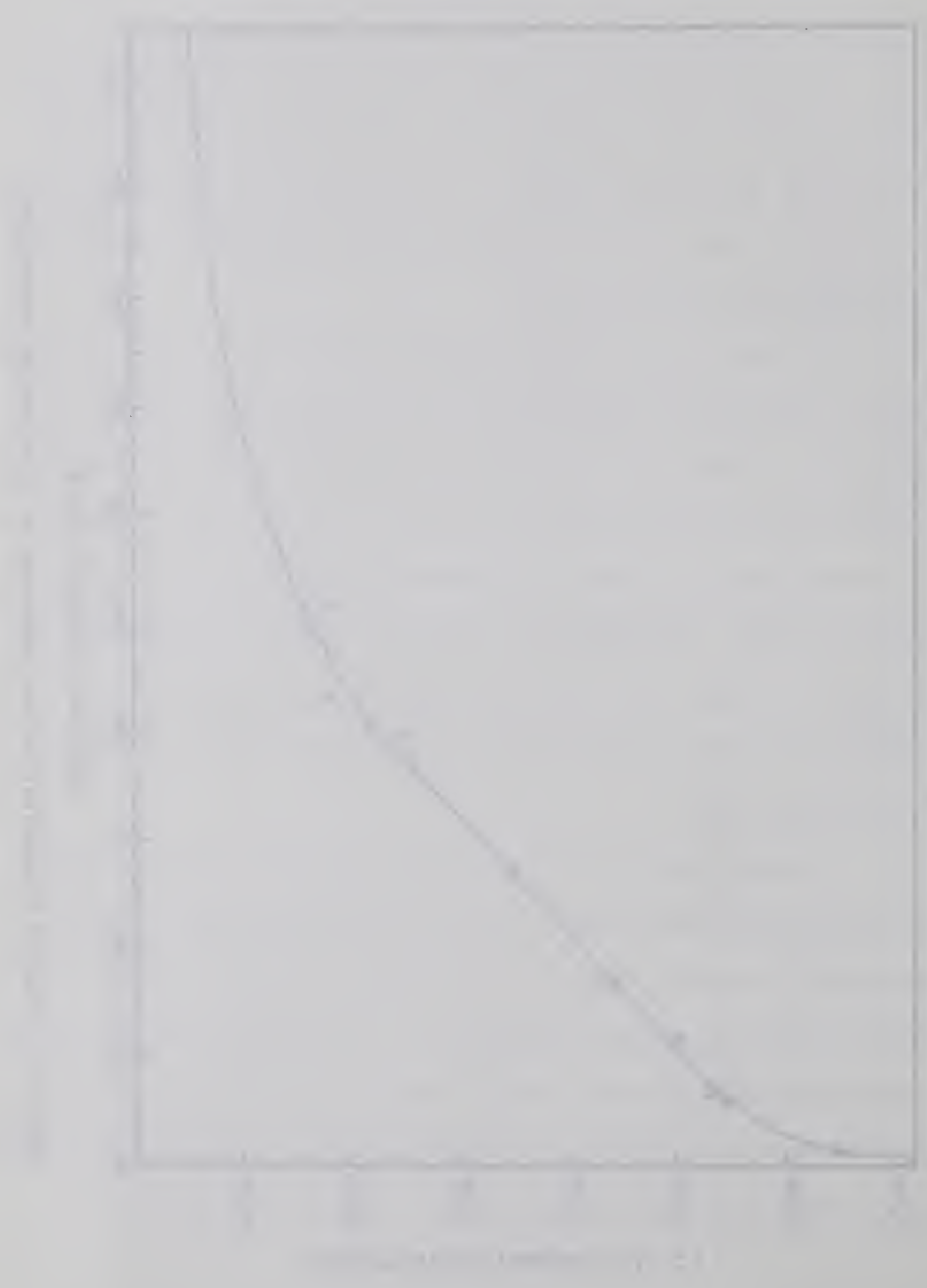

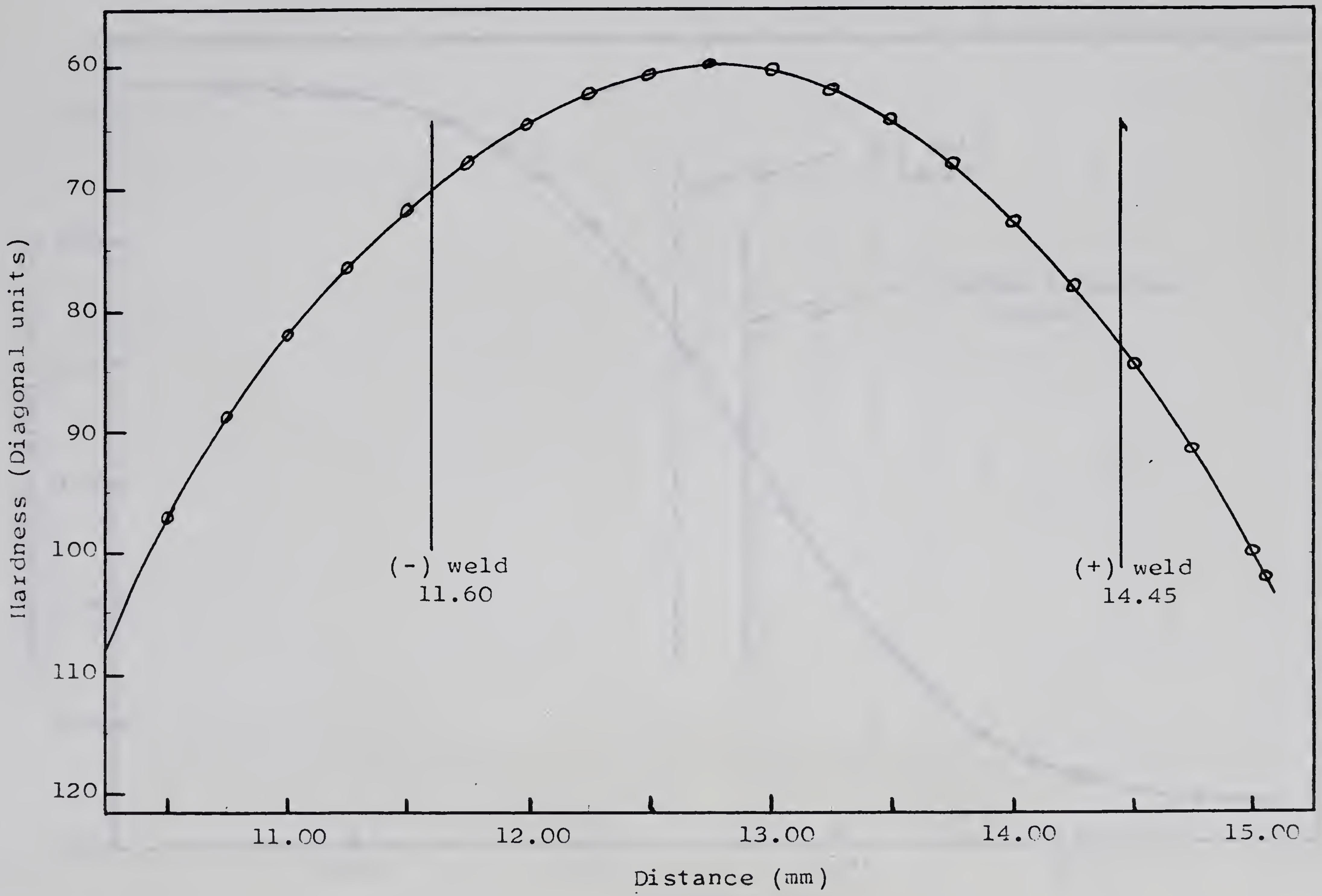

Figure 13. Hardness Traverse for Fe-C Couple A

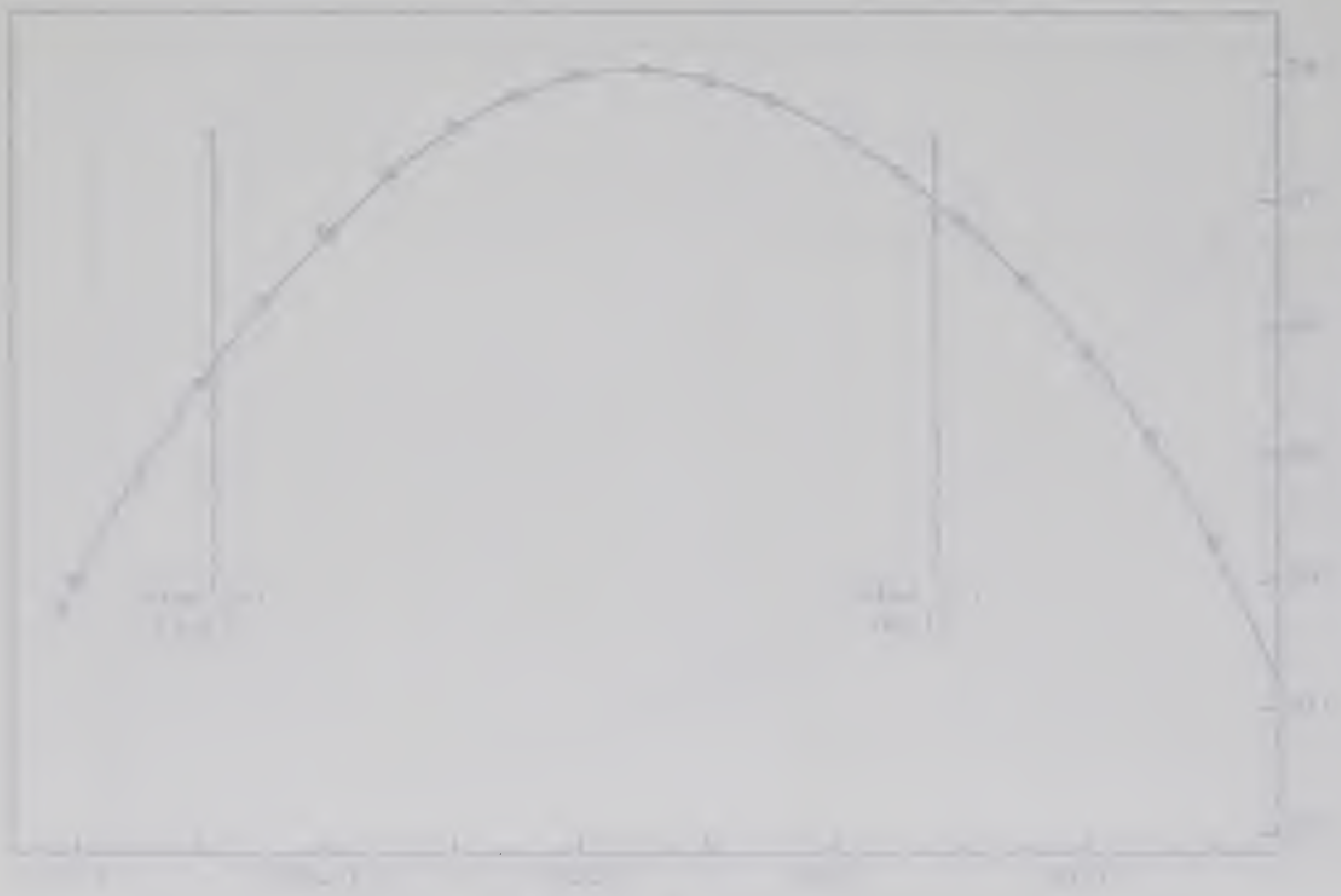

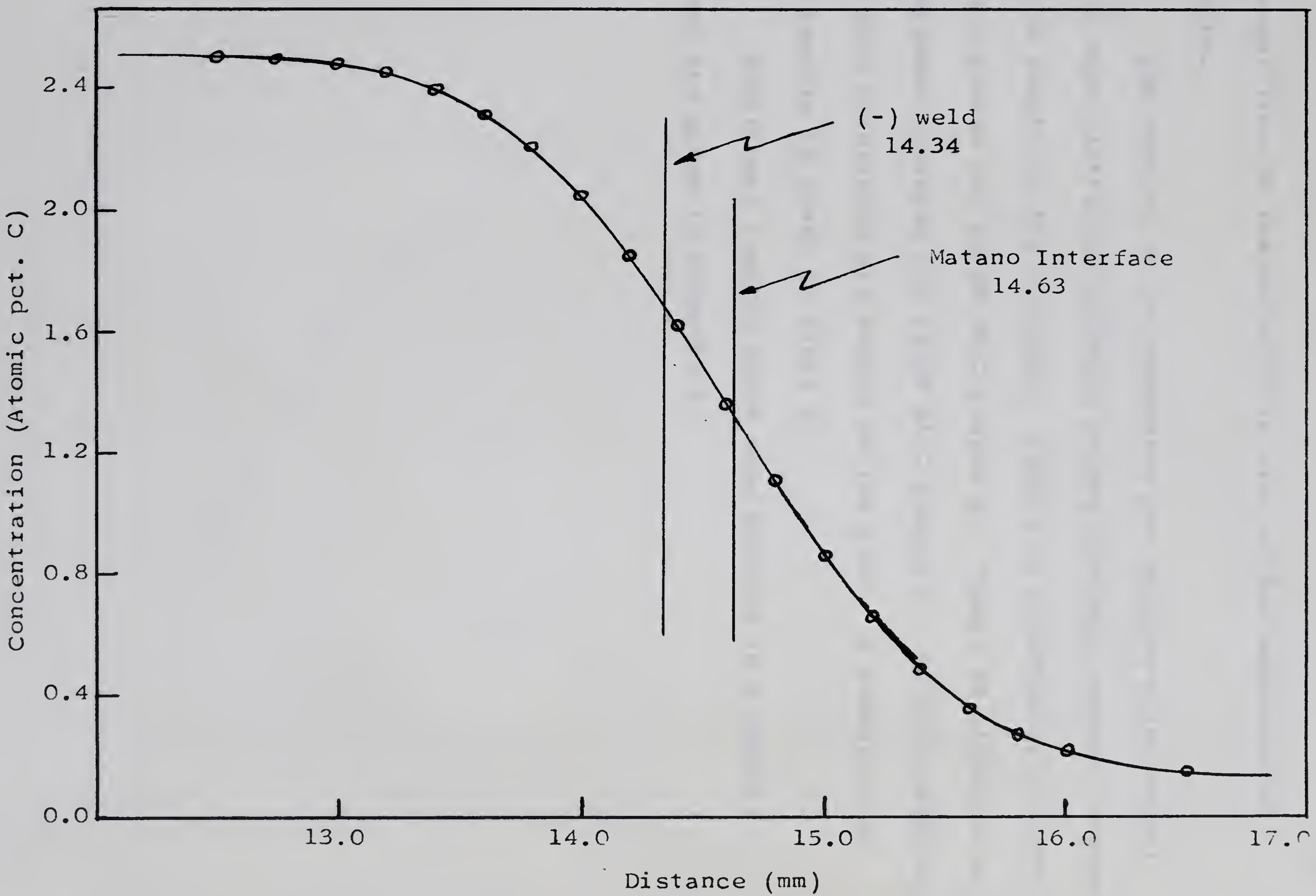

Figure 14. Concentration-Penetration Curve for Fe-C Couple A, (-) weld.

straight line of the probability plot of the experimental results.

The results of the manganese and silicon alloy experiments were plotted as hardness versus distance, where distance is the length of the traverse. Figure 15 illustrates a hardness traverse for Fe-4% Mn-C Couple D. Figure 16 illustrates a hardness traverse for Fe-2% Si-C Couple F. In both samples, the weld interfaces are marked on the plot. A summation of the results is given in Table 3.

Additional results which were plotted in a similar manner are given in Appendix I.

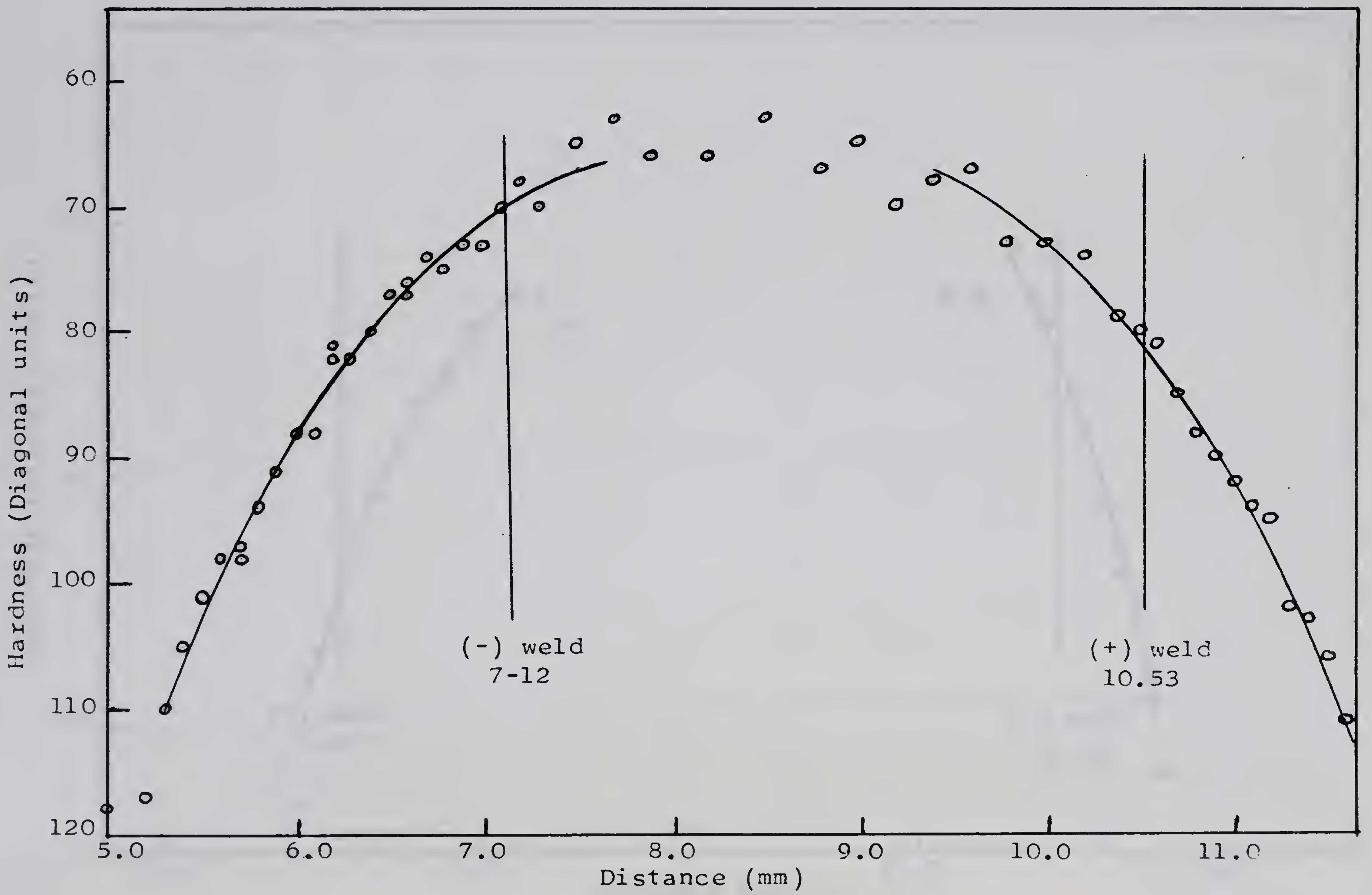

Figure 15. Hardness Traverse for Fe-4% Mn-C Couple D, Traverse (a)

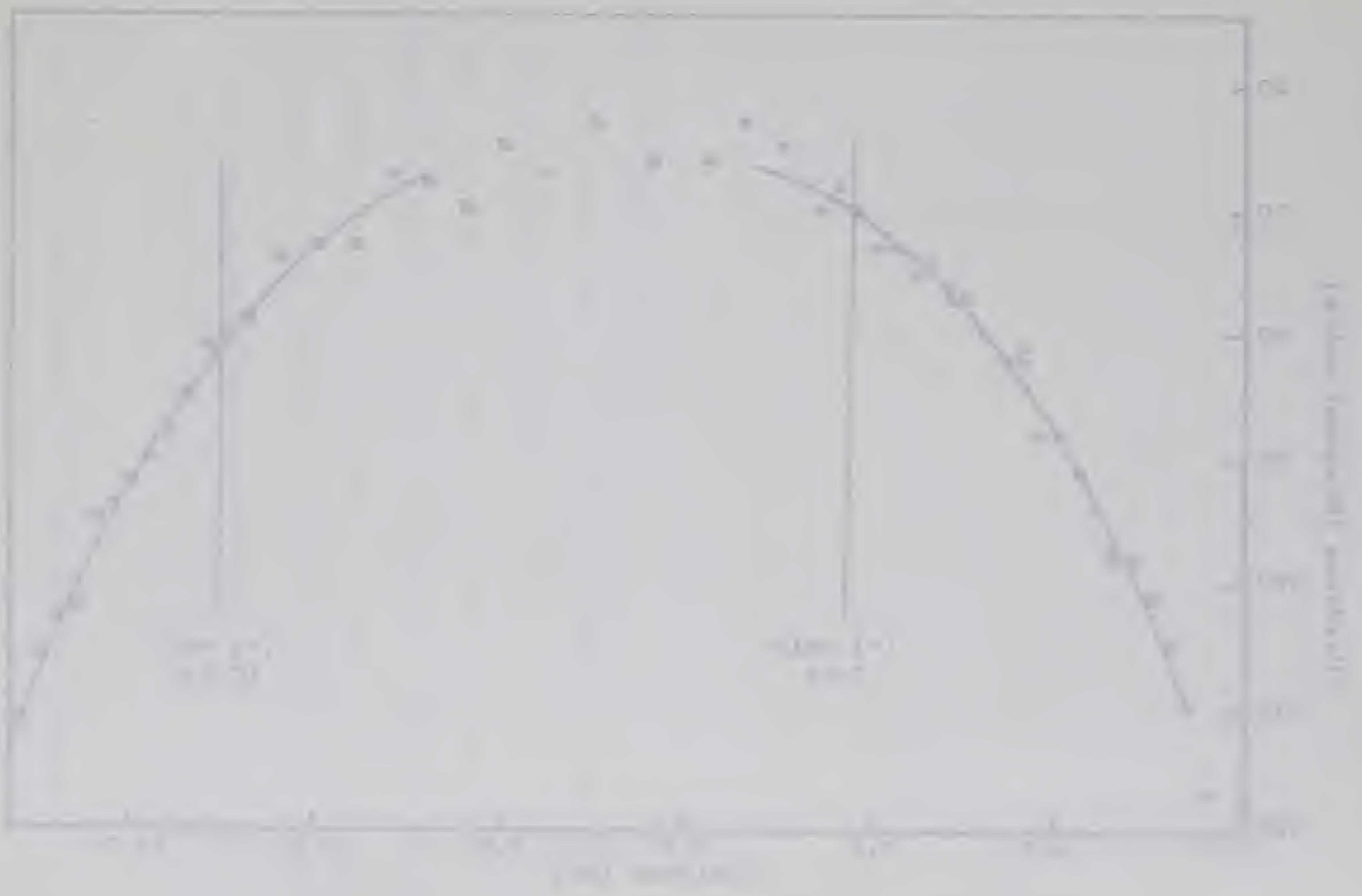

[illegible]

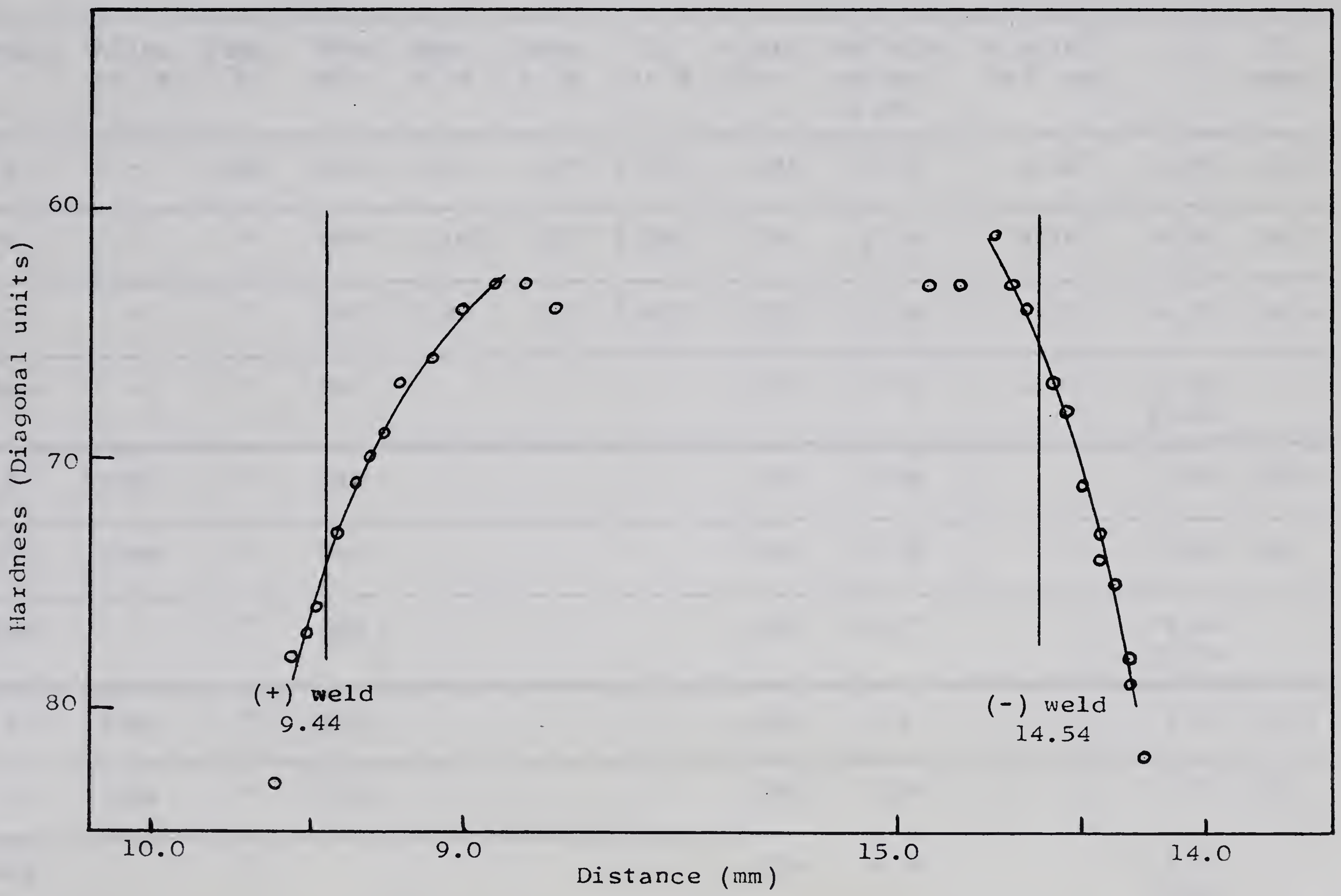

Figure 16. Hardness Traverse for Fe-2% Si-C Couple F, Traverse (a)

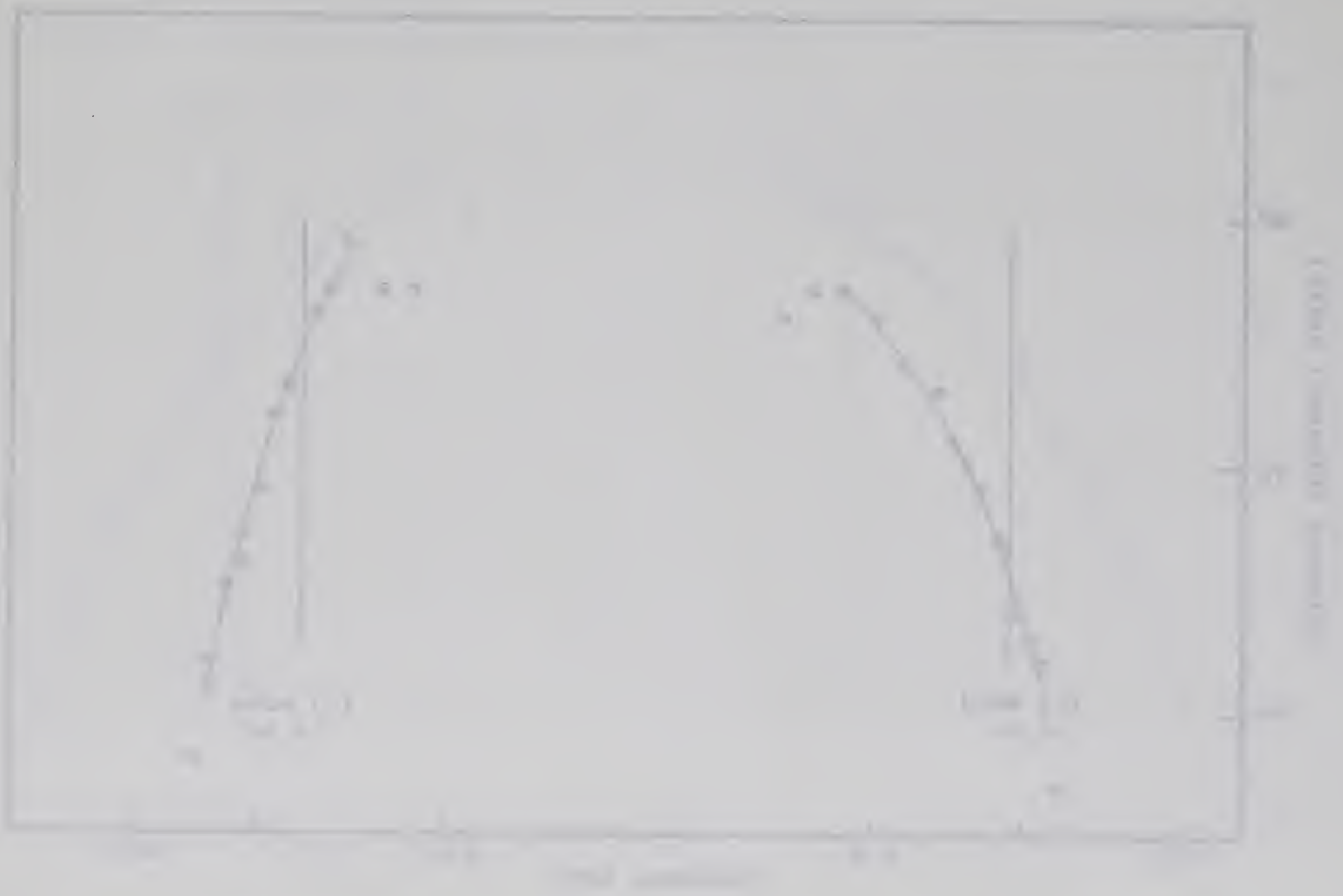

[illegible]

TABLE 3

Sample	Alloy wt. %	Temp. ^{o}C	Time min.	Cmax at %	Cmin at %	C_o at %	Field V/cm	Velocity cm/sec. x 10	D x 10^{+7} cm^2/sec.	q	I amps
A	-	950	180	2.51	.137	2.373	.235	2.76	2.42	6.70	28.5
B	-	"	180	1.162	.137	1.025	.23	2.74	2.10	6.81	26.3
C	-	"	180	1.96	.137	1.823	.232	2.59	1.12	6.36	24.4
Ave.	-	"	180				.232	2.72	1.88	6.69 ±0.22	
D	4-Mn.	"	180				.22	3.66		9.52	40.7
E	4-Mn.	"	180				.225	3.49		8.85	40.
Ave.		"	180				.222	3.57		9.19 ±0.34	
F	2-Si.	"	120				.255	1.9		4.35	21.5
G	2-Si.	"	135				.253	2.26		5.11	21.
Ave.		"					.254	2.08		4.73 ±0.38	

V. DISCUSSION

(1) Experimental Errors

There were certain factors that were of major concern in determining the experimental results. These were as follows:

(1) temperature control and measurement

(2) electric field across the couple

(3) prevention of decarburization during the run.

To maintain a constant temperature it was necessary to have a constant non-varying power supply. Power was supplied by the rectifier type direct current welding generator mentioned earlier. The small load offered by the electro-migration couples was not sufficient to choke the peaks of the power supply. Insertion of a 1.5 ohm resistor in series with the sample was a large enough load to eliminate any peaks in the power supply. A rheostat on the D.C. generator permitted regulation of the power supply to the electro-migration couples for temperature control. The power necessary to keep the couple at 950° C increased slowly through the course of the experiment. This was noticed by an increase in both the voltage and the current. The reason for this increase can be explained by the heating up of the terminal ends of the electro-migration couple. The temperature was measured by the three

wire thermocouple arrangement as described earlier. There was no difficulty in keeping the temperature to within ± 4° C.

Knowing the electric field applied to the sample is obviously important in regard to determining the effective charge q. The field was measured by means of two probes spot welded to the side of the couple with the leads running to the potentionmeter used for measuring the temperature. The two Alumel thermocouple wires were used as the probes. These wires were welded approximately 0.040 inches apart, giving a millivolt reading of approximately 20 for which there was no significant reading error. A micrometer, accurate to ± 0.0005 inches, was used with the aid of x30 binoculars to measure the distance between the wires. A correction for thermal expansion was applied to this reading for calculating the volts per centimeter. The voltage increased slightly over the length of the run as mentioned above. To obtain an average voltage for use in the calculations a time average was calculated. Figure 28 shows the typical time variation of the voltage.

The iron lattice seems reluctant to hold carbon atoms in it at elevated temperatures if there is any oxygen or hydrogen in the atmosphere. This necessitated electro-depositing a protective layer of copper on the sample to prevent the loss of carbon. A low electro-deposition current density across

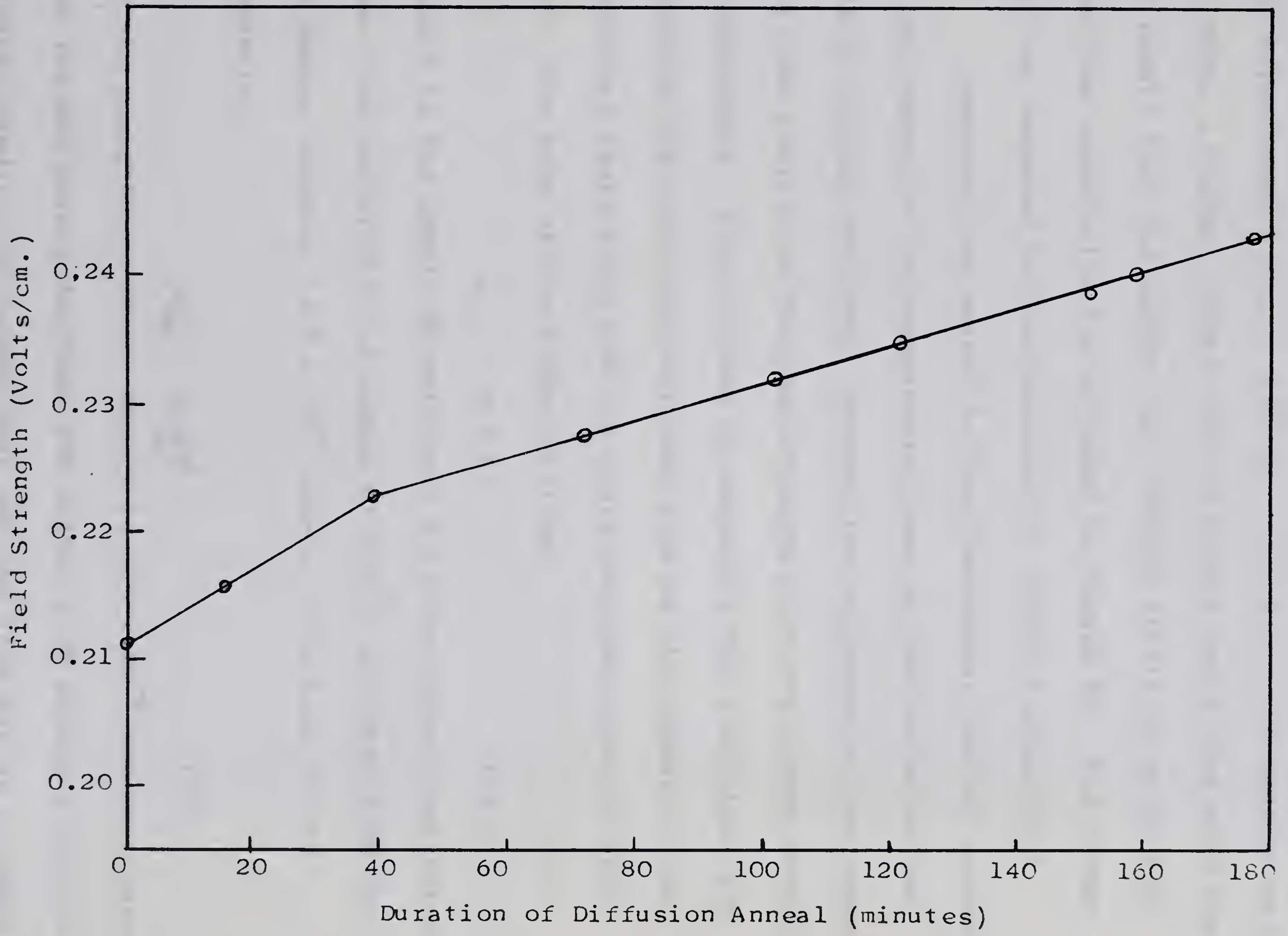

Figure 28. Variation of Electric Field with Time.

[illegible]

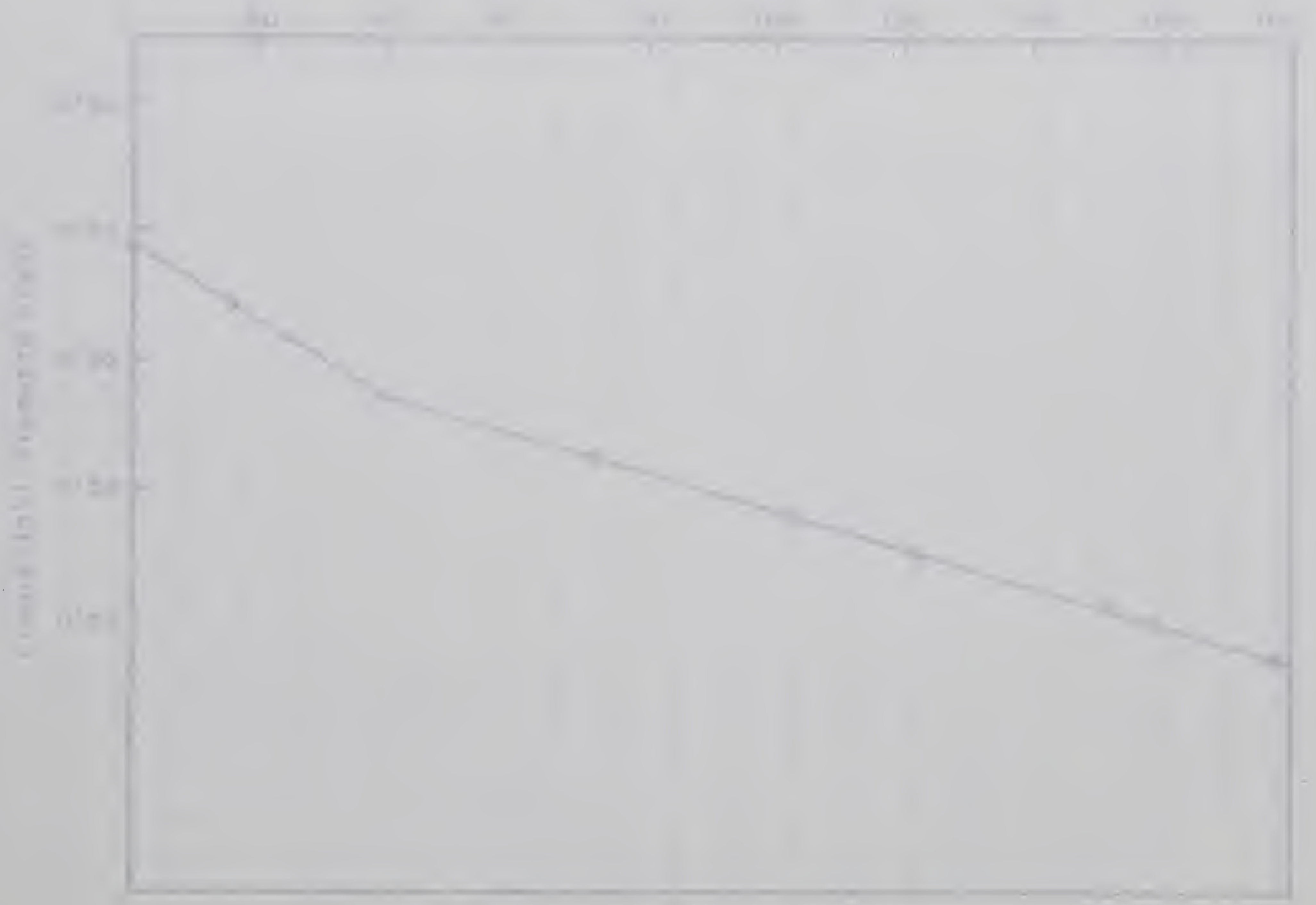

the electrodes gave a solid copper coating that remained intact after three hours at 950° C. If the current density was too high, a coarse, porous coat of copper would form with the net result that the copper coat offered little or no protection from decarburization as shown in Figure 29. The copper coat was measured to be approximately 0.0007 inches thick.

Comparing the actual to the theoretical current carried by the copper in the experiments gives an indication of the type of coating obtained. Knowing the thickness of the copper coat, the portion of the current carried by the copper should be calculable. This is done by comparing the electrical resistivity and the cross sectional area of the copper to the electrical resistivity and the cross sectional area of the iron. The area of the copper will be,

$$A_{Cu} = \pi d t , \tag{16}$$

where d is the sample diameter and t is the copper coat thickness. The resistivity of copper at 950° C as taken from the ASM Metals Handbook is 9×10^{-6} ohm-cm. The area of the sample is,

$$A_{Fe} = \pi \left(\frac{d}{2}\right)^2 , \tag{17}$$

and the resistivity of the sample is 119×10^{-6} ohm-cm, (taken from the ASM Metals Handbook and within 2.5% accuracy for the material used). The copper coat and the iron act as a parallel

circuit so the volts per centimeter will be the same in both. Thus

$$E_{Cu} = E_{Fe} ,$$

$$\frac{I_{Cu}\,\rho_{Cu}}{A_{Cu}} = \frac{I_{Fe}\,\rho_{Fe}}{A_{Fe}} ,$$

and

$$\frac{I_{Cu}}{I_{Fe}} = \frac{A_{Cu}\,\rho_{Fe}}{A_{Fe}\,\rho_{Cu}} \approx 0.75$$

From this calculation one would expect the copper coat to carry nearly 43% of the current. Noting the field voltages and the corresponding currents for the Fe-C samples it was concluded that the copper coat does not carry the expected 43% of the current. Calculating the current I for Couple A from the measured voltage, area, and resistivity yields a current of 25 amps. This means that the sample carries (25/28.5) x 100 = 88% of the current. Calculations for the other couples give similar results. This indicates that the copper coat is made up of small spheres forming a porous coat even though it offers ample protection from decarburization. Figure 30 shows the copper coat and also illustrates the absence of decarubrization. To check the above calculations, a sample of Armco iron wire of 0.050 inches diameter was heated to 950° C by the direct current apparatus. The field voltage was 0.22 V/cm. with a current of 24.35 amps recorded. The resistivity calculated from these figures is,

Figure 29. Decarburized Couple Due to Porous Copper Coat.

Figure 30. Copper Coat Preventing Decarburization.

$$Fe = \frac{E \times A}{I} = 114.9 \times 10^{-6} \text{ ohm-cm.}$$

The resistivity of pure iron at 950° C is 114.2 x 10^{-6} ohm-cm. as taken from the ASM Metals Handbook.

(2) Carbon Diffusivity

The diffusion constant D for carbon in iron, used for calculating the effective charges, was taken from Wells et al.[21]. The D values determined for three temperatures and two concentrations are listed below,

T °C	Atomic % C	D cm^2/sec x 10^7
950	1	1.74
	2	2.15
956	1	1.89
	2	2.20
958	1	1.33
	2	1.74

An average value of 1.85 x 10^{-7} cm^2/sec. is used for all the results. Wells et al. showed that there is a systematic but insignificant increase in D between 1 and 2 atomic percent carbon. The addition of 2% silicon was found to have no effect on the value of D.

Values for D in Jost show that for 4% manganese in iron there is no effct on the diffusion constant of carbon. It was possible to calculate values for D from the carbon penetration curves given in Figures 14, 17, 18, 19, and 21. The Matano method was used to calculate the D values. The average

values of 2.42×10^{-7} cm^2/sec. for couple A, 2.10×10^{-7} cm^2/sec. for couple B, 1.12×10^{-7} cm^2/sec. for couple C do not vary significantly from those found by Wells et al. The diffusion constants calculated here were not used in the calculations. The similarity between the calculated D values and the values from Wells et al. indicate that the external force in electro-migration is the same for each ion.

(3) The Hardness vs. Carbon Concentration Curve

According to Figure 12, increasing carbon content increases the hardness of Fe-C alloys in the martensitic condition up to approximately 0.55% C, beyond which hardness becomes insensitive to carbon content. Below 0.15% C it is probably more difficult to reproduce hardness vs. concentration results.

Some factors could be considered variables in the reproduction of hardness values in Fe-C alloys. These factors are soaking time, quenching temperature, carbon content, alloy content* and cooling rate, which will be represented by the letters S,T,C,A, and R respectively. An expression h = f(S,T, C,A,R) can now be written to indicate the dependence of hardness h upon the variables. Thus

---

*Alloy content refers to alloys other than carbon.

$$dh = \frac{\partial h}{\partial S} dS + \frac{\partial h}{\partial T} dT + \frac{\partial h}{\partial C} dC + \frac{\partial h}{\partial A} dA + \frac{\partial h}{\partial R} dR \quad (18)$$

Investigations were carried out to show that the various coefficients (i.e., partial derivatives) are negligible, except that associated with the change in carbon concentration.

For the first term, $\frac{\partial h}{\partial S}$, a specimen was soaked at 1000° C for periods of time varying from 5 minutes to 30 minutes and then quenched in water. It was observed that the hardness was the same in each case. It is necessary to protect the sample from decarburizing during the soaking period. A tantalum lining in the furnace tube and maintaining an inert atmosphere by passing argon gas through the furnace tube prevented decarburization.

For the temperature effect, $\frac{\partial h}{\partial T}$, samples were soaked at different temperatures in the range 1000° C to 1075° C before quenching. Results indicate that the hardness of each sample was not affected by the soaking temperature.

The term, $\frac{\partial h}{\partial R}$, is effectively zero for the present work. A cooling rate of 40° C to 180° C per second is required to quench steel from austenite to martensite.[22] A water quench gives a cooling rate of 1000° C per second at the surface of the sample. The surface on quenched samples seems to be approximately 0.050 inches thick. The thickest sample quenched in this work was 0.075 inches thick so it is safe to conclude

that the cooling rates obtained in this work were greater than the critical cooling rate in each case. Any change of cooling rate with sample size was therefore of no consequence in affecting maximum hardness.

The fourth term, $\frac{\partial h}{\partial A}$, is not necessarily zero. According to Bain[1], the addition of alloys will increase the maximum hardness of steel. Nehrenberg,[2] in contrast, finds that the addition of alloys does not increase the maximum hardness. The present work shows that 4% manganese and 2% silicon increases the maximum hardness. Hardnesses for equal carbon concentrations in Fe, Fe-Mn, and Fe-Si alloys will be different because dA does not equal zero when comparing the compositions of the three samples relative to one another. If hardnesses for equal carbon concentrations are taken on any one of the samples, the hardness will be the same because dA equals zero from one part of the sample to another. For a given diffusion couple therefore, $\frac{\partial h}{\partial A}$ is zero.

Thus it is evident that the variation in carbon content is reponsible for the changes in hardness in the hardness traverses.

Approximately 75 to 100 microhardness measurements were taken on samples of known carbon content to construct the calibration curve. The measurements had an R.M.S. deviation of

1.1 for an average hardness measurement of 80 diagonal units. The measurements were sufficient to test the sample for homogeneity and to obtain an average hardness. The carbon analyses done on the calibration samples can be considered to be accurate to ± 0.01%. The spread of the calibration points at the 0.15% to 0.20% carbon level indicates a decreasing sensitivity of hardness with carbon content.

The use of microhardness and the availability of calibration curves such as Figure 12 provides an extremely good method of determining carbon concentration distribution curves. A simple calculation will illustrate the possible number of hardness readings, and therefore carbon concentration determinations, for a hardness traverse of a couple (diffusion zone) that is 0.2 cm by 0.0625 cm. Consider an indentation diagonal of 100 units to be the maximum size that is useful in determining carbon concentrations. A factor of 0.161 microns per unit is used to convert diagonal units to centimeters. If a space equal to five times the diagonal length is left between each indentation, it may be noted from the following calculation,

$$\left(0.161 \frac{\mu}{\text{unit}} \times 5 \times 100 \frac{\text{units}}{\text{indentation}} \times 10^{-4} \frac{\text{cm}}{\mu}\right)^{-2} \times 0.2 \times 0.0625\text{cm}^2$$

that there is a possible 200 carbon analyses on one plane of

the sample. From the geometry of the diamond indenter and a factor of 5 it can be calculated that a new plane of the sample can be prepared for hardness measurements every 1.5 x 10^{-3} centimeters. These approximate calculations demonstrate that the small couple size used introduces no errors in carbon analyses when determined by microhardness techniques.

(4) Electro-Migration of Carbon in Pure Iron

The displacement of the carbon ions due to the electromigration is one half the difference in distance calculated between the concentration-penetration curve shift from the (-) weld and the concentration-penetration curve shift from the (+) weld. Figure 31 shows the displacement of the carbon ions and illustrates how the preceeding statement can be stated in an expression.

Consider $D_D - D_E$ to be the displacement of the carbon ion away from the positive weld, or to the left in Figure 31. Then $D_D + D_E$ to be the displacement of the carbon ion away from the negative weld, or to the right in Figure 31. Subtracting the two displacements,

$$(D_D + D_E) - (D_D - D_E) = 2D_E, \qquad (19)$$

yields twice the displacement due to the field. In Figure 13 it is assumed that equal hardness diagonals indicate equal

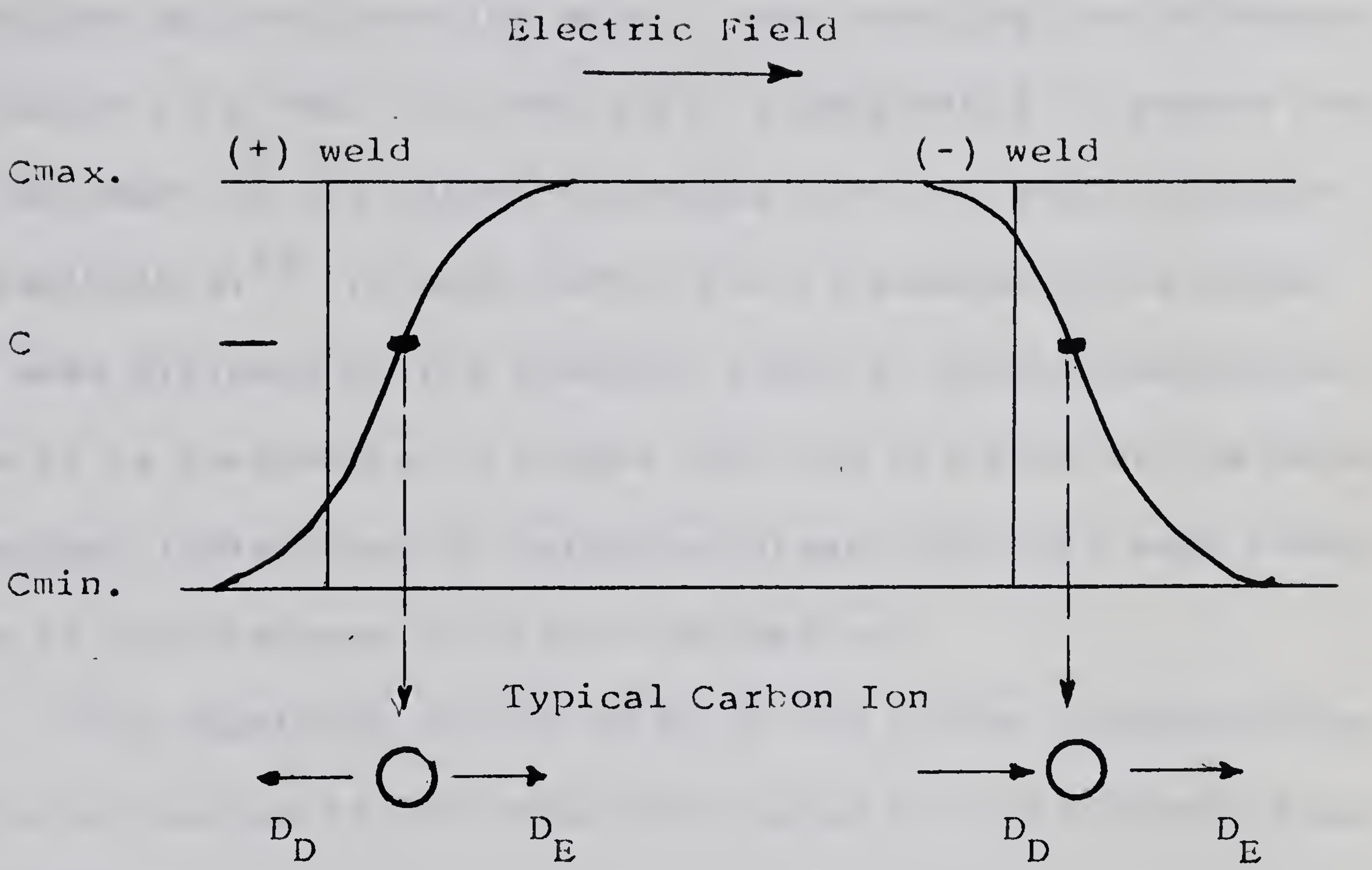

D_D = displacement of carbon ion due to diffusion

D_E = displacement of carbon ion due to electric field

Figure 31. Carbon Ion Migration Under the Influence of an Electric Field and a Diffusion Gradient.

carbon concentrations.

Another procedure used to determine the magnitude of electro-migration was to measure the distance that the Matano Interface shifted from the weld. When studying the diffusion of carbon in a Fe-C, Fe couple it is reasonable to assume that the movement of the Matano Interface from the weld interface is negligible.[23] If each carbon ion is assumed to be moved the same distance by the electric field in electro-migration, then it is reasonable to assume that the distance of the Matano Interface (determined by balancing areas) from the weld interface is the distance of electro-migration.

The magnitude of the shift of the carbon concentration curve is related to the effective charge by the Einstein relationship,

$$\mu = \frac{D}{kT}\ , \qquad (14)$$

where μ is the mobility. In this case the force is considered to be the field force eE times q, the effective charge. The expression for the charge is therefore

$$q = \frac{vkT}{eED}\ , \qquad (20)$$

where D is the diffusion constant of carbon in iron and v is the velocity. The numerical value of v is obtained by dividing the observed displacement by the time of the electro-diffusion anneal.

The results of the Fe-C couples indicates an effective charge of 6.69 ± 0.22* for the carbon ions at 950° C with a field strength of 0.23 V/cm. The results of Couple A were plotted as hardness diagonal vs. distance as well as atomic percent C vs. distance. For hardness diagonals of 70, 76, and 86 the effective charge was found to be 6.54, 6.87, and 7.21 respectively. At 1.75%, 1.30%, and 0.75% C, corresponding to the above hardness values, the effective charge was found to be 6.2, 6.6, and 6.92. The latter charges are seen to be approximately 0.30 smaller than the charges determined from the hardness traverse. The difference is due to the experimental errors in drawing the best fit lines through probability plots and in the hardness traverse of Figure 13. Values of q determined by measuring the Matano Interface shift in Couple A are 6.52 for the negative weld and 6.75 for the positive weld.

In the Fe-C Couples B and C, only one weld in each couple was effective. In Couple B the negative weld was not welded completely across the whole section. This was evident only after the sample had been mounted and polished. The positive weld was sound as indicated by a continuous hardness change along the length of the hardness traverse, which indicates a continous changing carbon concentration.

---

*All deviations are standard deviations.

The effective charge determined by measuring the Matano Interface shift was 6.69 and 6.94 for each of two hardness traverses taken on the sample.

A poor weld on the positive end of Couple C was indicated by an arrest in the hardness diagonal vs. distance curve at the weld as seen in Figure 20. The negative weld appeared to be satisfactory as shown by a continuous hardness change. The effective charge determined by measuring the Matano Interface shift was 6.36.

Of all the carbon ion charges calculated for the Fe-C couples, only one varies from the mean by as much as 0.5. A standard deviation of 0.22 was determined for eleven calculations. This allows a degree of confidence in reporting the charge on the carbon ion to be 6.7 in iron at 950° C at 0.35% C.

It is interesting to compare the results obtained for the effective charge on carbon here with some of the results reported in the literature. The reported velocities will also be considered.

Probably the first electro-diffusion velocity for carbon ions reported was that by Seith and Kubaschewski.[5] They report a velocity of approximately 2×10^{-6} cm/sec. at a temperature of 1000° C. and a field of 0.1 V/cm. Using the Einstein relation, this would give an effective charge near

the value found in the present work. A large velocity and correspondingly high effective charge was determined by Kalinovich.[12] He reports a velocity of 8.1×10^{-6} cm/sec. with a corresponding charge of 13.4 at 950° C. The procedures followed by these investigators were similar to that used in the present work in that they measured the magnitude and direction of the shift of a carburized zone in an iron wire under the influence of an electric field. Seith and Kubaschewski observed the carbon migration by metallographic means. Kalinovich used radioactive carbon in his experiments to measure the displacement of the carbon distribution curve. A third set of results obtained by a different procedure has been reported by Dayal and Darken.[16] Their procedure was outlined in the literature review. At a temperature of 920° C they did not observe any migration of carbon ions. It is useful to apply Kalinovich's velocity to the calculations of Dayal and Darken's method to determine what carbon concentration variation to expect between the anode half and cathode half of a sample. Dayal and Darken,[16] express the mobility as,

$$B = (C_c - C_a)V/tC_oAE, \qquad (21)$$

where C_c is the carbon concentration of the cathode half, C_a is the carbon concentration of the anode half, V is the volume of the sample, t is the duration of the experiment, C_o is the

concentration at the central plane, A is the cross-sectional area of the specimen perpendicular to the direction of the field, and E is the potential gradient. From this expression we see that the difference in carbon concentration between the anode half and the cathode half is,

$$\Delta C = \frac{v\ t\ C_o}{l}\ , \qquad (22)$$

where v is the velocity, and l is the length of one half of the sample.

One run by Dayal and Darken was at 920° C for a duration of eight and one half hours. Considering the decrease in velocity with temperature in Kalinovich's paper, we would expect a velocity of approximately 6.5×10^{-6} cm per sec. at 920° C. Using this value in expression (22) we get ΔC equal to 0.047%. If Kalinovich's velocity was correct it would be expected that Dayal and Darken would have observed a carbon concentration difference of some extent in spite of the decarburization that occurred. If the velocity reported in this thesis is substituted in expression (22) a value of 0.02% is obtained for ΔC.

These calculations emphasize the disagreement between Kalinovich's results, Dayal and Darken's results and the results reported in this work. At the same time they illustrate

the inability of Dayal and Darken's method to measure accurately small mobilities of carbon ions. This also casts some doubt on the accuracy of the higher mobilities determined by Dayal and Darken.

To explain an effective charge of 6.7 for an element of atomic number 6, one might invoke Fiks' theory supplemented by Glinchuk's hole-wind effect, where the force on the ion is given by

$$F = eE(q - n_e l_e \sigma_{ie} + n_p l_p \sigma_{ip}).$$

This offers the ready explanation that the carbon ions have moved under the force of the electric field plus the force of the hole-wind. The hole-wind predominates over the electron wind because iron is said to be mainly a p-type conductor. Kalinovich justifies his charge of 13 for carbon ions in this way.

Another very interesting possibility for explaining the high charge obtained for carbon is suggested by the results of Gertsriken[15] and Frantsevich.[14] They have found that iron migrates to the anode in the presence of carbon whereas it is known that iron migrates to the cathode in pure iron. The movement of iron in the opposite direction to carbon suggests an interaction effect between the iron and carbon ions resulting in increased migration of carbon. A simple model is set

up in Figure 32 to illustrate the mechanism. The carbon will find itself associated with the three iron atoms on the down field side of the interstitial site. As one of the negatively charged iron atoms with which the carbon is associated with makes a diffusion jump in the direction of the anode, this will facilitate the movement of the carbon ion towards the next interstitial site in the direction of the cathode. The implication here is that the diffusivity increases, thus giving a large effective charge for carbon in electro-diffusion studies when using the Einstein relationship to calculate q.

(5) Electro-Migration of Carbon in Iron Alloys

The concentration distribution curves for the alloys of Fe-Mn-C and Fe-Si-C were plotted as hardness diagonals vs. distance. Because of the apparent small effect of manganese and silicon on the maximum hardness there was no effort made to construct true concentration distribution curves. It was considered valid, however, to assume equal hardness values mean equal carbon concentration since the manganese and silicon was relatively uniform across the entire diffusion couple.

An average value of q calculated from Figures 15, 22, 23, and 24 for Fe-4% Mn-C was 9.19 ± 0.34. Couples D and E had average q values of 9.52 and 8.85 respectively. The 7%

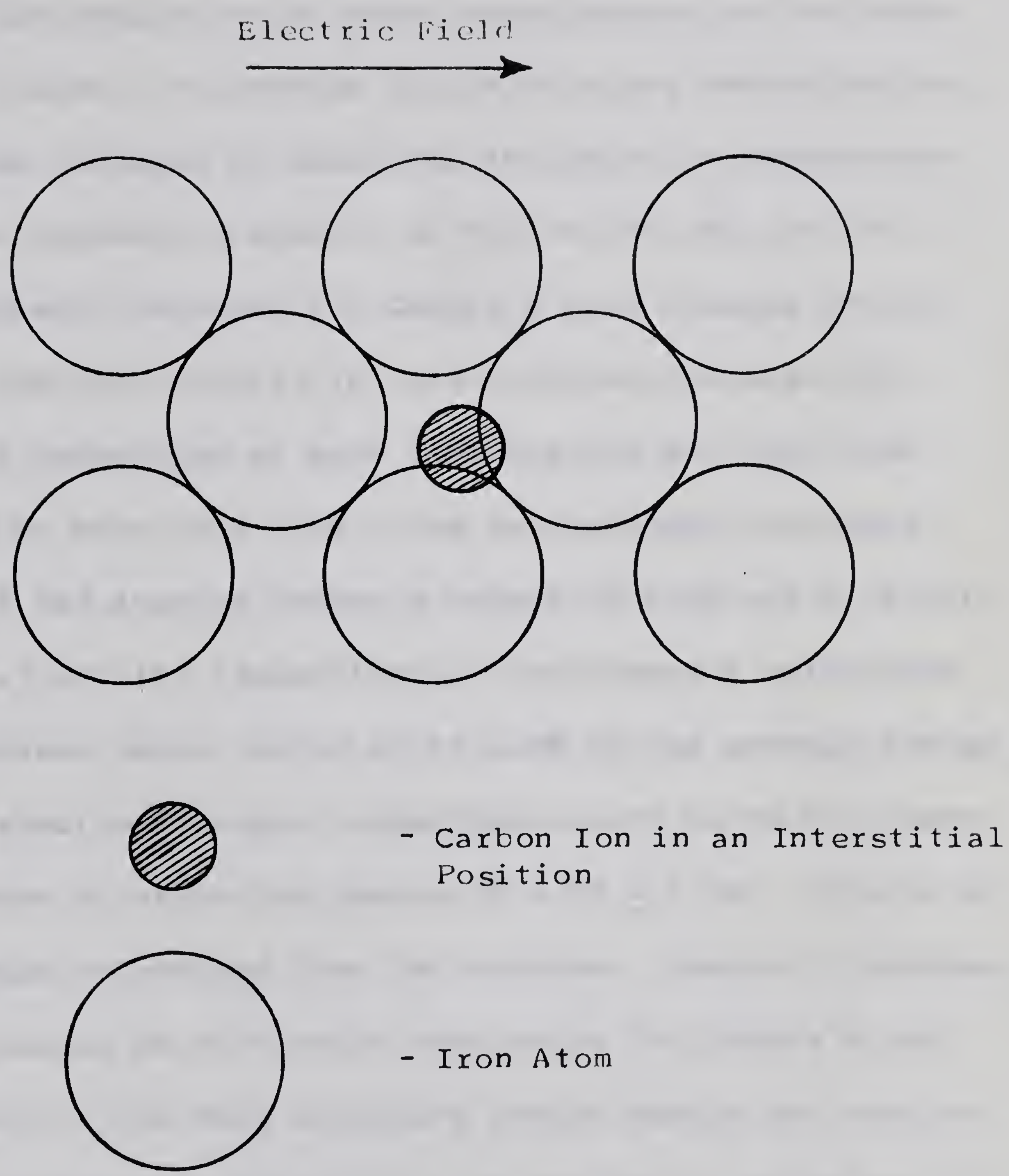

Figure 32. Arrangement of a Carbon Ion in Iron Under the Influence of an Electric Field.

difference between the charges is an experimental error that is probably an indication of some inconsistency in the soundness of the welds. An average charge of q was determined for each hardness traverse by measuring the shift in carbon distribution at hardness diagonals of 75, 80, 85, 90, and 95. The two hardness traverses for Couple D gave average charge values of 9.49 for traverse (a) and 9.55 for traverse (b). The charge q calculated at each hardness did not vary from the average by more than 2.5%. The two hardness traverses for Couple E had average charge q values of 8.94 and 8.76 for traverses (a) and (b) respectively. The charge q calculated at each hardness value varied up to 4.5% of the average charge q.

The electro-transport experiments with Fe-2% Si-C show carbon to have an effective charge of 4.73 ± 0.38. This is an average charge determined from two couples. Couple F produced an average charge of 4.35 while the charge for Couple G was higher at 5.11. The more elaborate couple design for the Fe-Si alloy increases the possibility of one of the welds not being sound, therefore increasing the possible experimental error. The charges were determined at hardness diagonals of 68 and 72 for two different hardness traverses on each sample. A standard deviation of 0.38 was determined for eight calculations of the effective charge q.

In considering the effect of Mn and Si on the effective charge of carbon in iron it is instructive to consider the donor-acceptor relationship in transition metal alloys, which results in the transference of charge from carbon to iron. In this respect, Pauling's theory on the valencies of transition metals is pertinent.

Beginning with the alkali metal potassium and moving to the right in the periodic chart to chromium, the number of valence electrons can be considered to increase from one to nearly six. Because of the close relationship between the inter-atomic distances and bond type, and observing that the inter-atomic distances of the crystals decrease from K-4.62A to Cr-2.49A, it is suspected that all the valence electrons are taking part in bond formation. This conclusion is supported by the magnetic properties for the metals. For example, vanadium has a normal atomic configuration of $3d^3 4s^2$ for the valence electrons. If only the $4s^2$ electrons were involved in bond formation the $3d^3$ configuration of the ion core would have a strong dipole moment resulting in vanadium showing ferromagnetism. Because vanadium does not show ferromagnetism it is assumed that the electrons must be involved in bond formation. The bonds are considered to be formed by hybridization of 3d, 4s, and 4p orbitals.

There are 5 d orbitals, 1 s orbital and 3 p orbitals available for hybridization which means that as many as nine outer electrons could possibly take part in bonding. Continuing on from chromium, this would mean the number of bonds would be seven for manganese, eight for iron, nine for cobalt, and then begin to decrease with eight for nickel and so on because some orbitals now have two electrons. The fact that the interatomic distances do not continue to decrease with the increased bonding, (as concluded from the increased cohesive strength) and the fact that the variation of the magnetic properties deviates from the proposed scheme in the middle region of the period, leads Pauling to conclude that the elements from chromium to nickel all have similar valencies of nearly six. From values of the atomic saturation magnetization, σ_A, for iron, cobalt, and nickel, Pauling arrived at the number of d orbitals that do not take part in bonding. The orbitals that do not take part in bonding are called atomic orbitals and the remainder bonding orbitals. When the atomic saturation magnetization is expressed in Bohr magnetons, the numbers are the average number of unpaired electron spins in the metal. The

values for iron, cobalt, and nickel are 2.22, 1.71, and 0.61 Bohr magnetons respectively. As electrons are taken into atomic orbitals they will follow Hund's rule and tend to

remain unpaired. Thus for nickel there are 0.61 unpaired electrons and for cobalt there are 1.71 unapired electrons. (Pauling suggests that the reason for σ_A for cobalt differing by more than unity from σ_A for nickel is because of experimental error in determining σ_A for cobalt). Assuming the removal of one electron for each step to the next element, a value of 2.61 would be expected for iron instead of 2.22. This means that there are fewer than 2.61 orbitals in the atomic orbital class but necessarily more than 2.22. Figure 33, after Pauling, shows that the number of atomic orbitals is 2.44. This means that there are 2.56 d orbitals that are available for bonding. The expected diamagnetism for copper is observed as at this point all the 2.44 atomic orbitals are filled with paired electrons.

Some of the details of Pauling's scheme are criticized by Hume-Rothery because the valencies of nearly six are not in general agreement with the chemistry of the elements. Hume-Rothery does however concede that Pauling's scheme contains much truth and he does not offer any attractive alternative of his own.

Pauling's theory infers that at high temperatures sufficient to destroy ferromagnetism in iron, we will find iron and manganese acting as acceptors of electrons in the 3d atomic

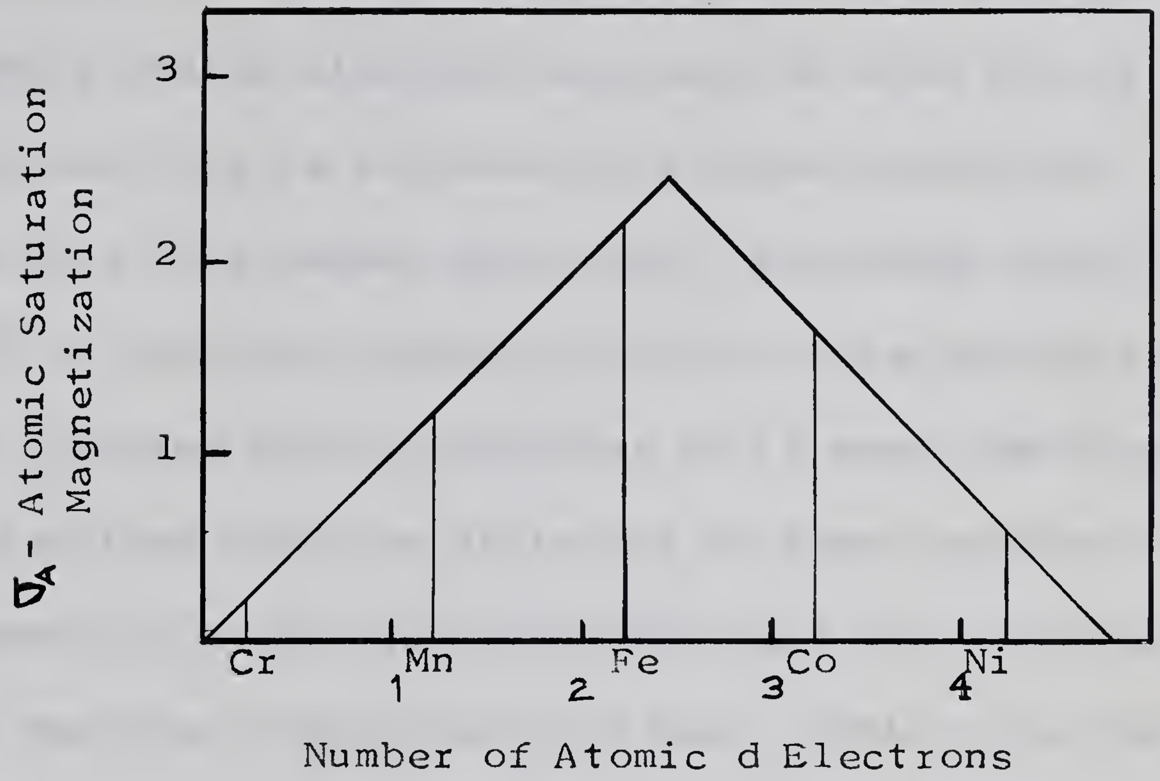

Figure 33. Predicted Dependence of Atomic Saturation Magnetic Moment, σ_A, as a Function of Atomic d Electrons (After Pauling).

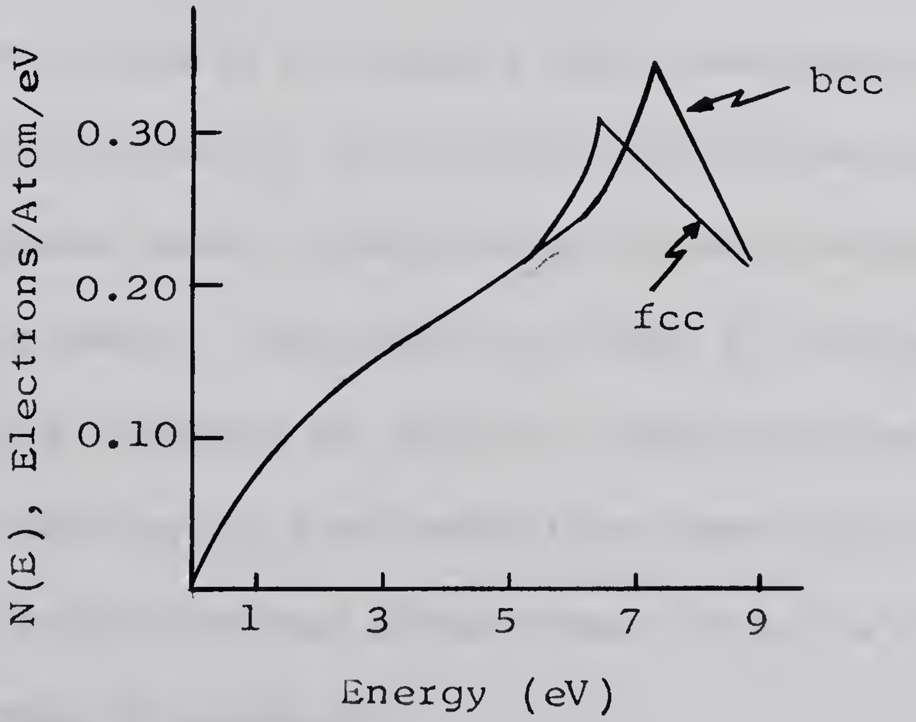

Figure 34. N(E), Number of States per Unit Energy Range for fcc and bcc Lattices as a Function of Energy.

orbitals. This agrees with the reasoning behind the phase change in iron from body centered cubic to face centered cubic. When iron is heated electrons are excited from the 4s to the 3d shell, and this is followed by a phase transition (bcc ⟶ fcc) to a denser structure. Following Jones' calculations[24] of electron concentration for face centered cubic and body centered cubic structures it is seen that the transfer of electrons from the 4s to the 3d level reduces the electron concentration in the conduction band and therefore makes the face centered cubic structure more stable from the point of view of electronic or Fermi energy. This is illustrated by the curves in Figure 34 showing N(E), the number of electrons per atom, as a function of the energy and crystal structure.

The above also implies that manganese, which can accept one more electron in the 3d band than iron, will stabilize the face centered cubic structure by drawing electrons from the conduction band. The effect of this is to open the gamma field. The tendency of silicon, which can only increase the electron density in the conduction band, is to close the gamma loop, or stabilize the alpha iron. This is also explained in view of this discussion.

With an appreciation of the proposed electronic

distribution and bonding mechanism, it is now possible to discuss how a carbon ion might display an effective charge as high as the presently reported value.

At 950° C., we find the carbon evenly distributed among the iron atoms and the valence electrons of the carbon will be accepted by the iron in the 3d band and will enter the conduction band. When a field, E, is put across the sample, the positively charged carbon ions will tend to migrate towards the cathode (agreeing with the experimental results). The iron has been observed to move to the anode i.e. migrate as though it had a negative charge. This justifies referring to iron as an acceptor of electrons.

When manganese is added to the iron there are more positions available in the 3d shell for electrons. This will result in the carbon atoms being more effectively stripped of their electrons i.e., the electrons find more openings in the 3d shell and fewer electrons will go to the Fermi level where they will screen the positive charge of the carbon ion from the effect of the field. It is apparent from this that the carbon will now migrate faster towards the cathode.

When silicon is added to the iron it is expected to act as an electron donor. This follows Jones' theory that increased electron concentration increases the tendency to form

a body centered cubic structure, which is the case for silicon in iron. The carbon atoms will not be stripped of their electrons as effectively in iron-silicon alloys as they were in iron-manganese alloys and the increased electron concentration will tend to screen the positive charge of the carbon ions. Electro-migration of carbon ions will certainly be expected to decrease under these circumstances, hence the lower effective charge for carbon ions in the presence of silicon.

This model is very qualitative but it offers a reasonable alternative to the idea of hole-wind as an added driving force on the ions. The results reported in this work and the work of Frantsevich[14] and Gertsriken[15] reported on iron migration agree with the mechanisms of the above model.

VI. SUMMARY AND CONCLUSIONS

1. Advantage was taken of the reproducible relationship between carbon concentration in iron and the hardness of the material in the martensitic condition to construct a calibration curve for use in carbon analyses by a microhardness technique. It was found that a microhardness technique was a powerful method of determining carbon concentration distribution curves in small diffusion couples.

2. The electrical mobility of carbon in pure iron at 950° C and a field strength of 0.23 V/cm was related to an effective charge q of 6.69 ± 0.22 by use of the Einstein equation.

3. The effects of 4% Mn and 2% Si on the electrical mobility of carbon in iron at 950° C were studied at a field strength of 0.22 V/cm and 0.25 V/cm respectively. Manganese increased the effective charge of carbon by 2.5 to 9.19 ± 0.34, and silicon decreased it by 1.96 to 4.73 ± 0.38.

4. The large effective charges reported for carbon ions leads to the conclusion that the electric field is not the only force acting on the carbon ions. Consideration of the results reported here, the results from the literature on electro-migration of Fe in Fe-C, and Pauling's theory on the valencies of transition metals, suggests an explanation for

the high electrical mobility of carbon. It is considered that the tendency of iron to migrate to the anode under the influence of an electric field facilitates the migration of carbon ions towards the cathode resulting in a large velocity for carbon ions. The effects of Manganese and silicon on electro-migration of carbon are considered to be the result of altered electron distribution. In the presence of Mn carbon is more effectively stripped of electrons since Mn can accept an extra electron in its 3d shell, thus giving carbon a higher effective positive charge. In the presence of silicon, which acts as an electron donor, the carbon ion can not be as effectively stripped of its electrons. Electrons from Si enter the conduction band with the consequent result that the carbon charge is more effectively screened.

BIBLIOGRAPHY

1. E.C. Bain, "Alloying Elements in Steel", American Society for Metals, Metals Park, Ohio (1948).

2. Nehrenberg, Payson and Lillys, Trans. ASM., 47, 791 (1955).

3. "Metals Handbook" - American Society for Metals, Metals Park, Ohio (1948).

4. W. Jost, "Diffusion in Solids, Liquids, Gases", Academic Press, New York (1960).

5. R.P. Johnson, Phys. Rev., 53, 54, 766, 459 (1938).

6. W. Seith and O. Kubaschewski, Z. Elektrochem., 40, 829 (1934).

7. V.B. Fiks, Soviet Physics-Solid State, 1, 14 (1959).

8. N.F. Mott and H. Jones, "The Theory of the Properties of Metals and Alloys", Oxford (1936).

9. J. Frenkel, "Kinetic Theory of Liquids", Dover Publications, New York (1955).

10. A. Einstein, Ann. Physik., 17, 549 (1905).

11. M.D. Glinchuk, Ukrain. Fiz. Zhur., 4, 684 (1959).

12. D.F. Kalinovich, Soviet Physics-Solid State, 3, 812 (1961).

13. H. Wever, Z. Electrochem., 60, 1170 (1956).

14. I.N. Frantsevich, D.F. Kalinovich, I.I. Kovensky and M.D. Smolin, Soviet Physics-Solid State, 1, 58 (1959).

15. S.D. Gertsriken, I. Ya. Dekhtyar, V.S. Mikhalenkov and V.M. Fal'chenko, Ukrain. Fiz. Zhur., 6, 129 (1961).

16. P. Dayal and L.S. Darken, AIME Trans., 188, 1156 (1950).

17. W. Hume-Rothery, J. Iron and Steel Inst., 188 (2), 113 (1958).

18. I.N. Frantsevich, D.F. Kalinovich and I.I. Kovensky, Physics Metals Metallography, 8 (4), 94 (1959).

19. O.A. Boedtker and P. Duwez, Report No. 3 to O.N.R., C.I.T., (Pasadena) March 1962.

20. "Metals Handbook" - American Society for Metals, Metals Park, Ohio, p. 309 (1948).

21. C. Wells, W. Batz and R.F. Mehl, AIME Trans., 188, 553 (1950).

22. "Metals Handbook" - American Society for Metals, Metals Park, Ohio, p. 620 (1948).

23. "Atom Movements", - American Society for Metals, Cleveland, Ohio, (1951).

24. H. Jones, Proc. Phys. Soc., 49, 250 (1937).

APPENDICES

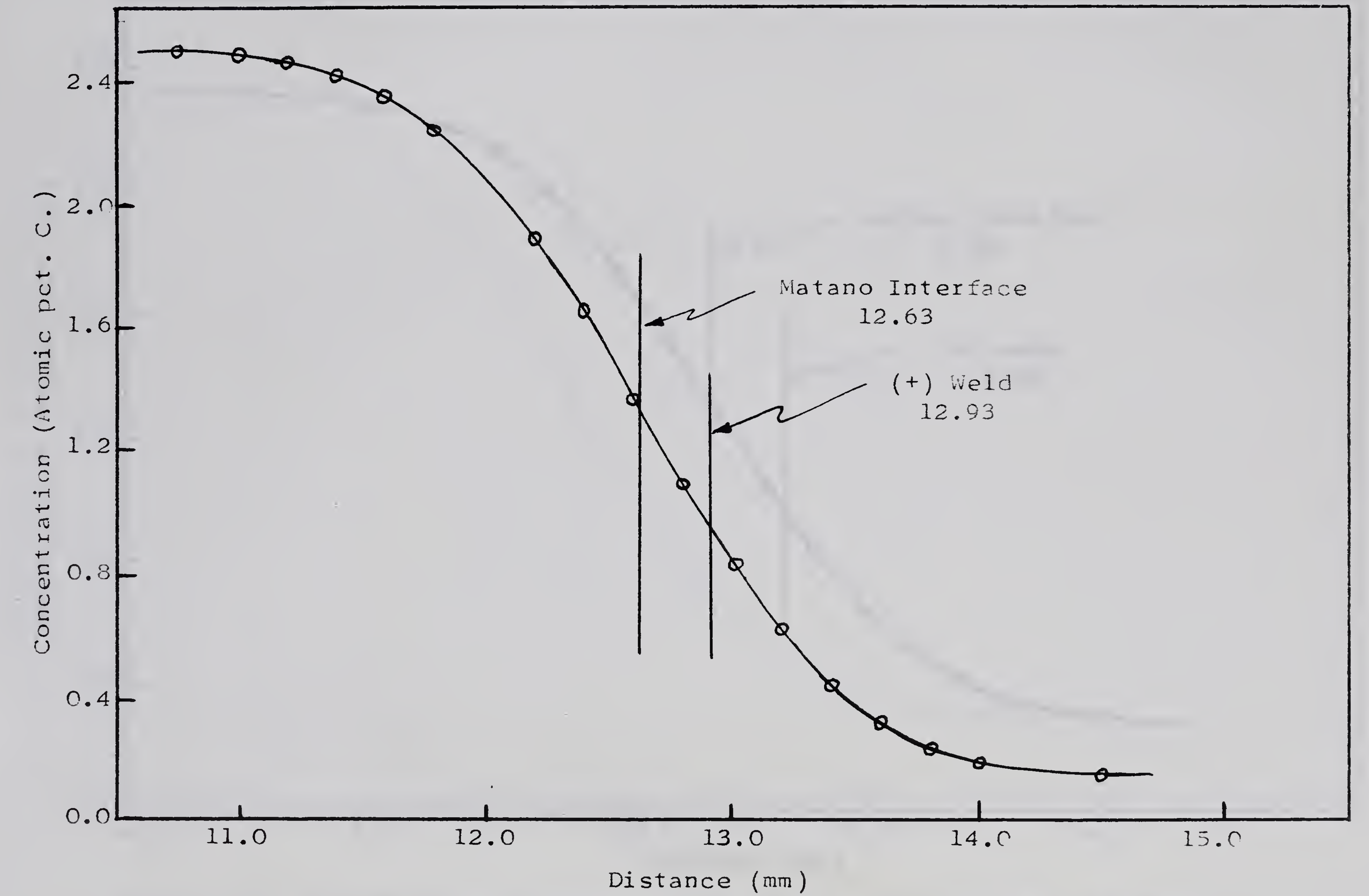

Figure 17. Concentration-Penetration Curve for Fe-C Couple A, (+) weld.

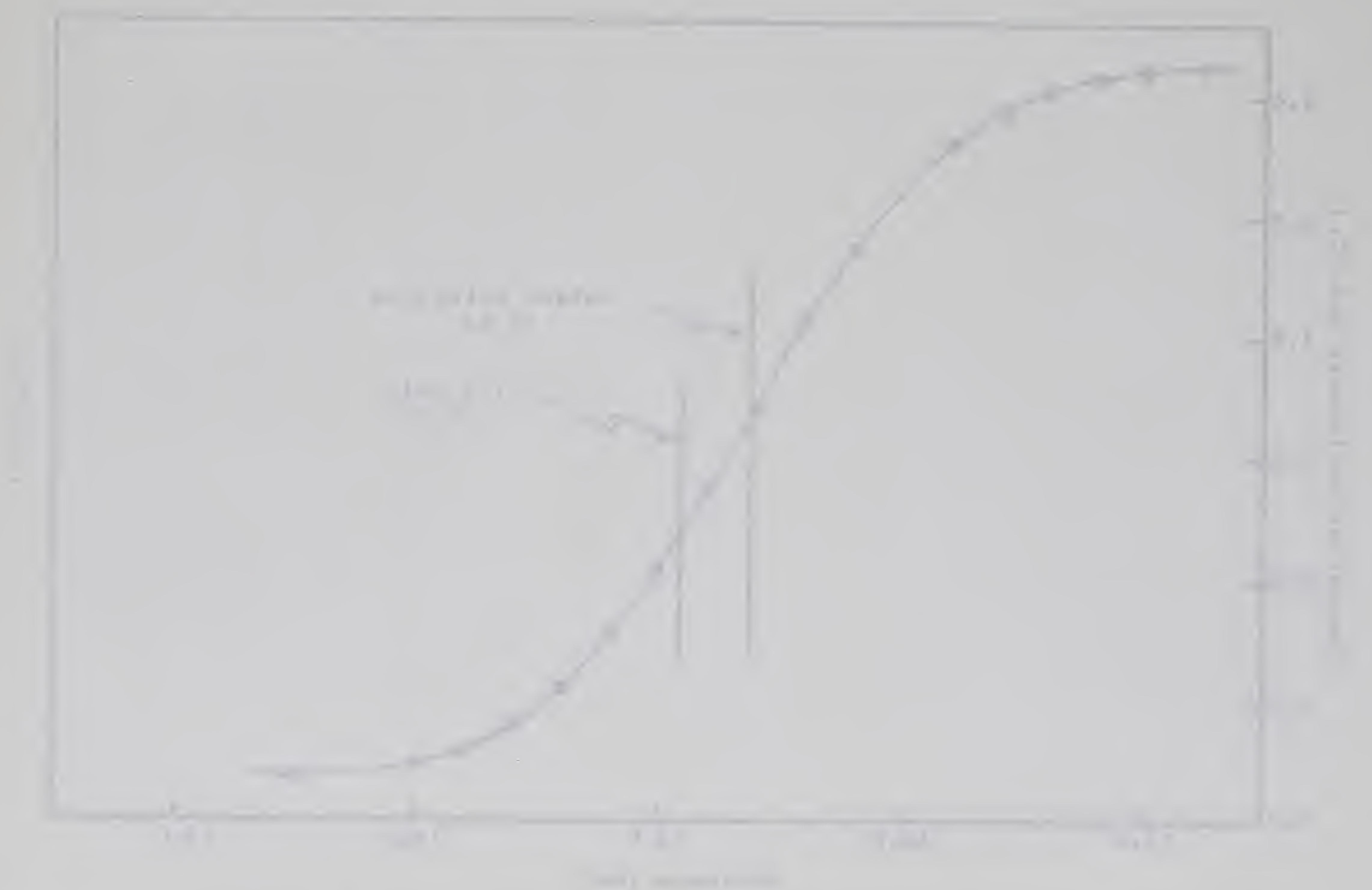

[illegible]

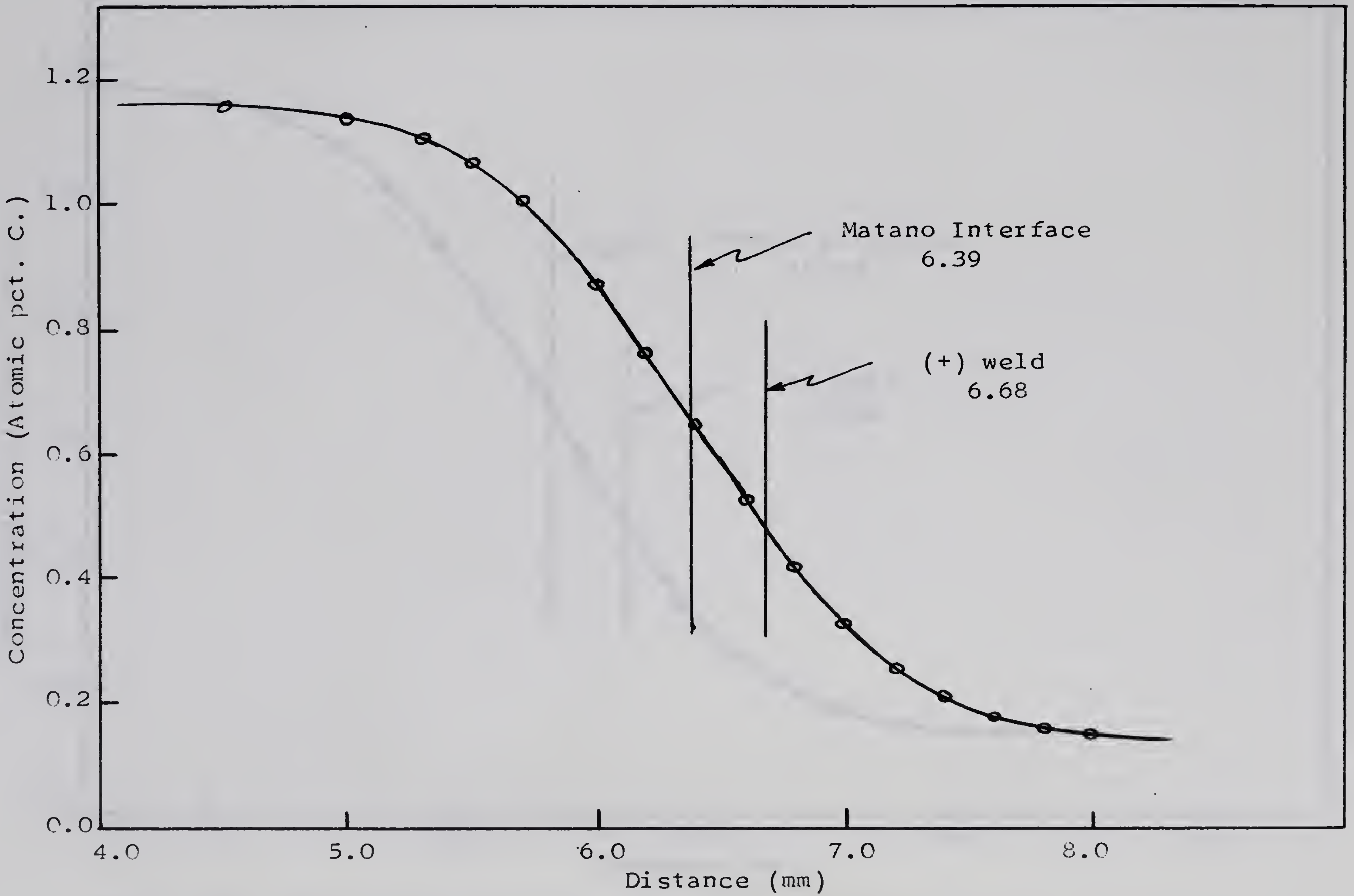

Figure 18. Concentration-Penetration Curve for Fe-C Couple B, (+)weld, Traverse (a).

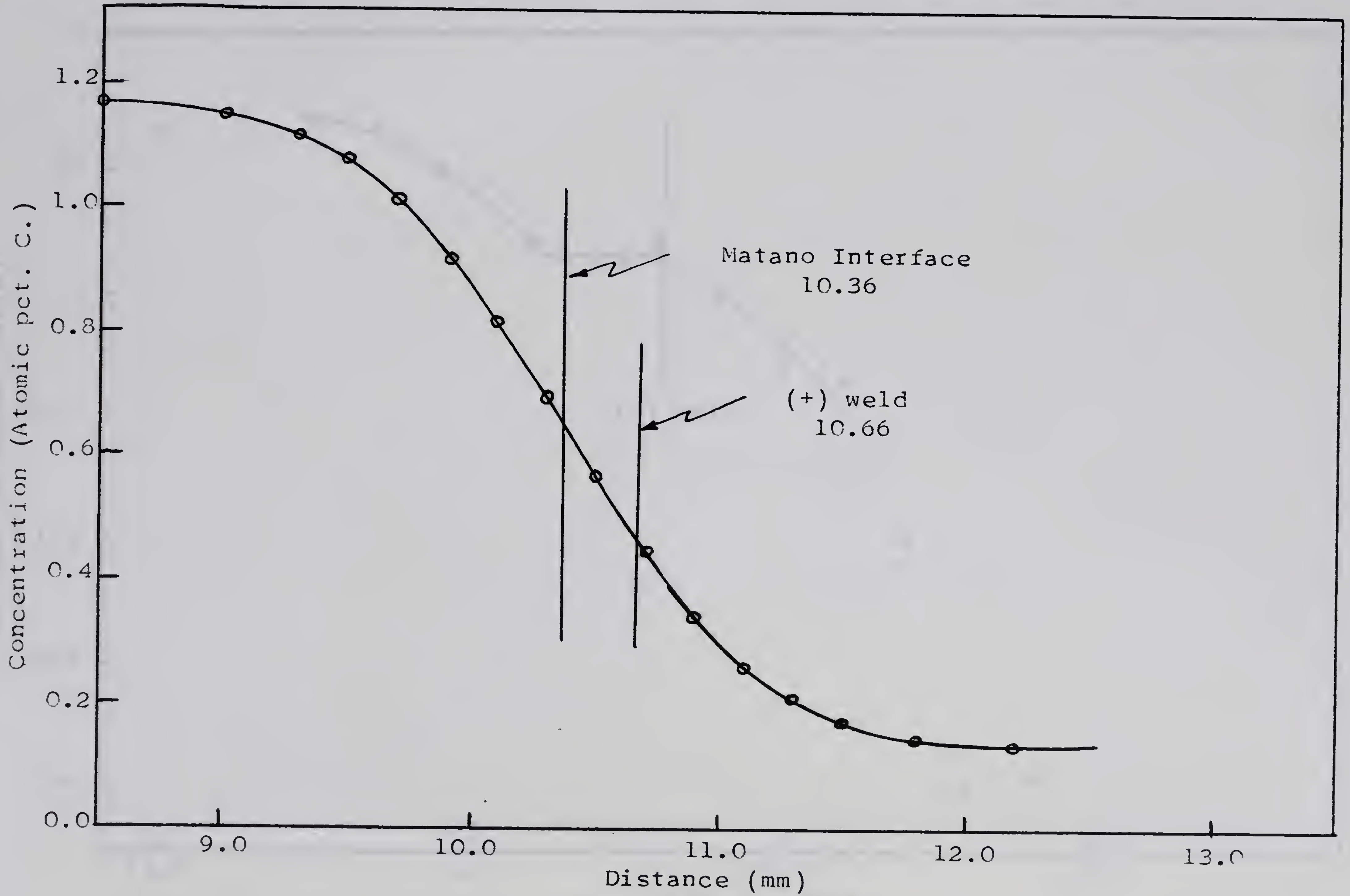

Figure 19. Concentration-Penetration Curve for Fe-C Couple B, (+) weld, Traverse (b).

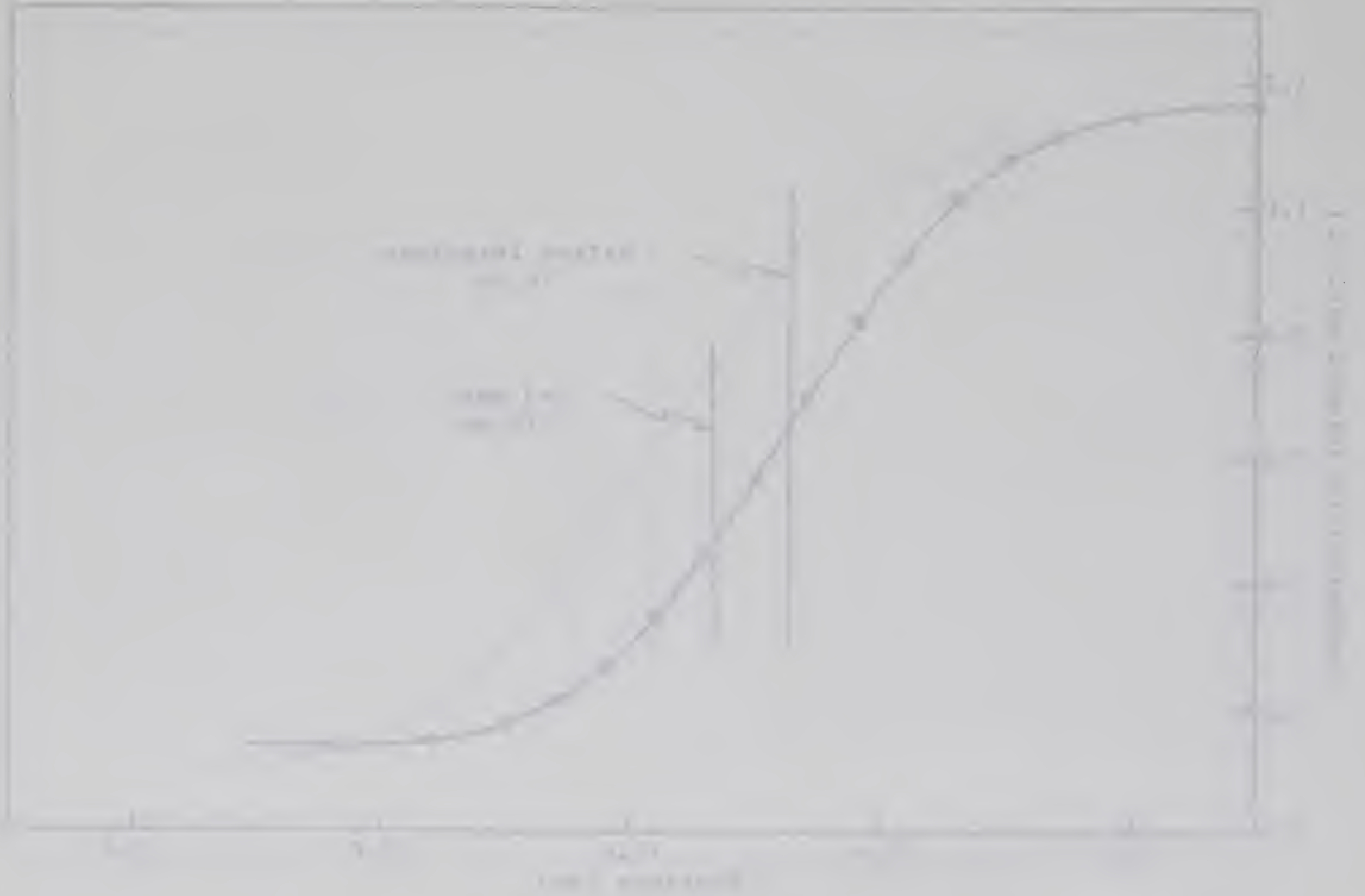

[illegible]

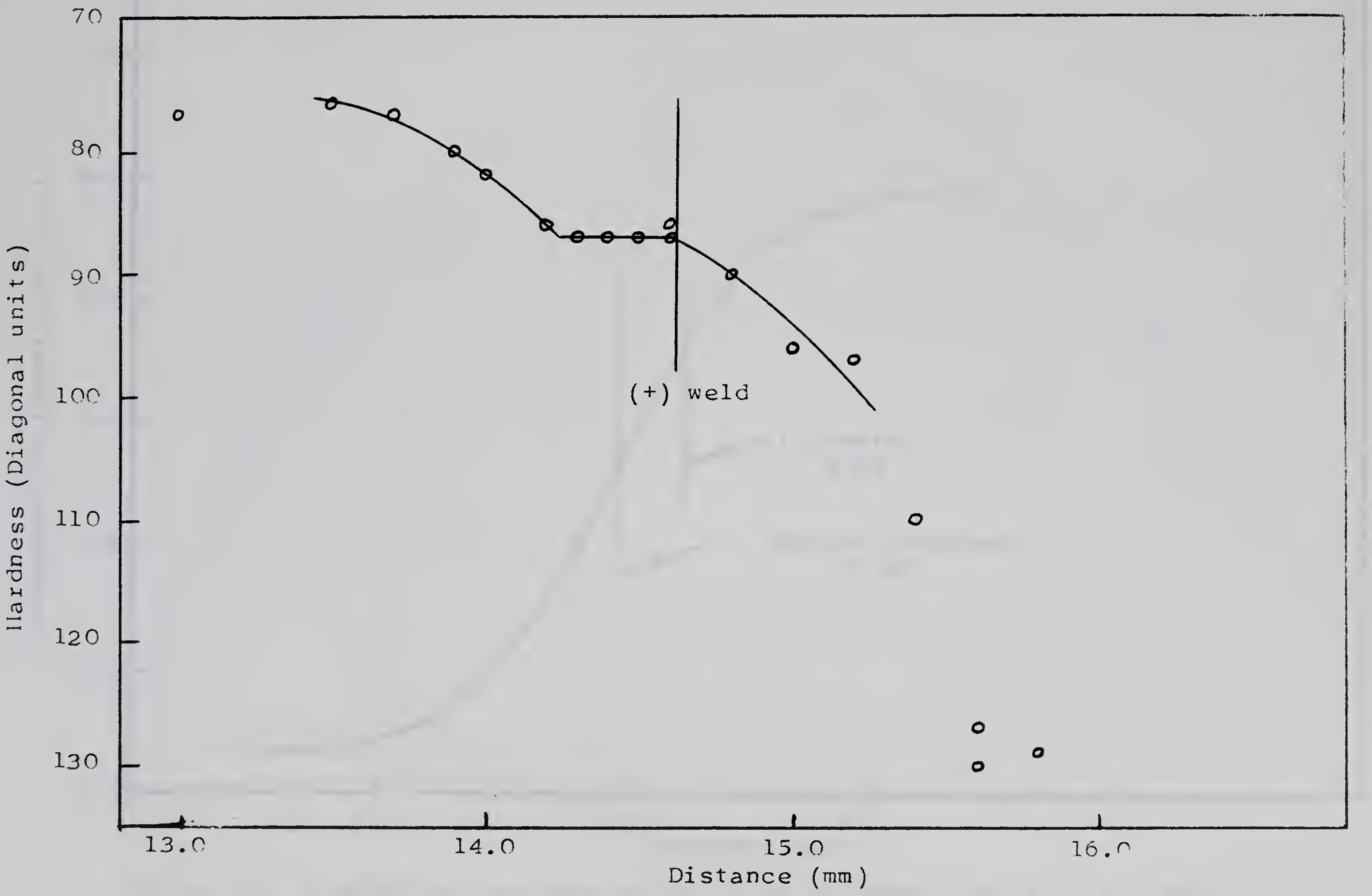

Figure 20. Hardness Traverse for Fe-C Couple C, (+) weld, Traverse (a).

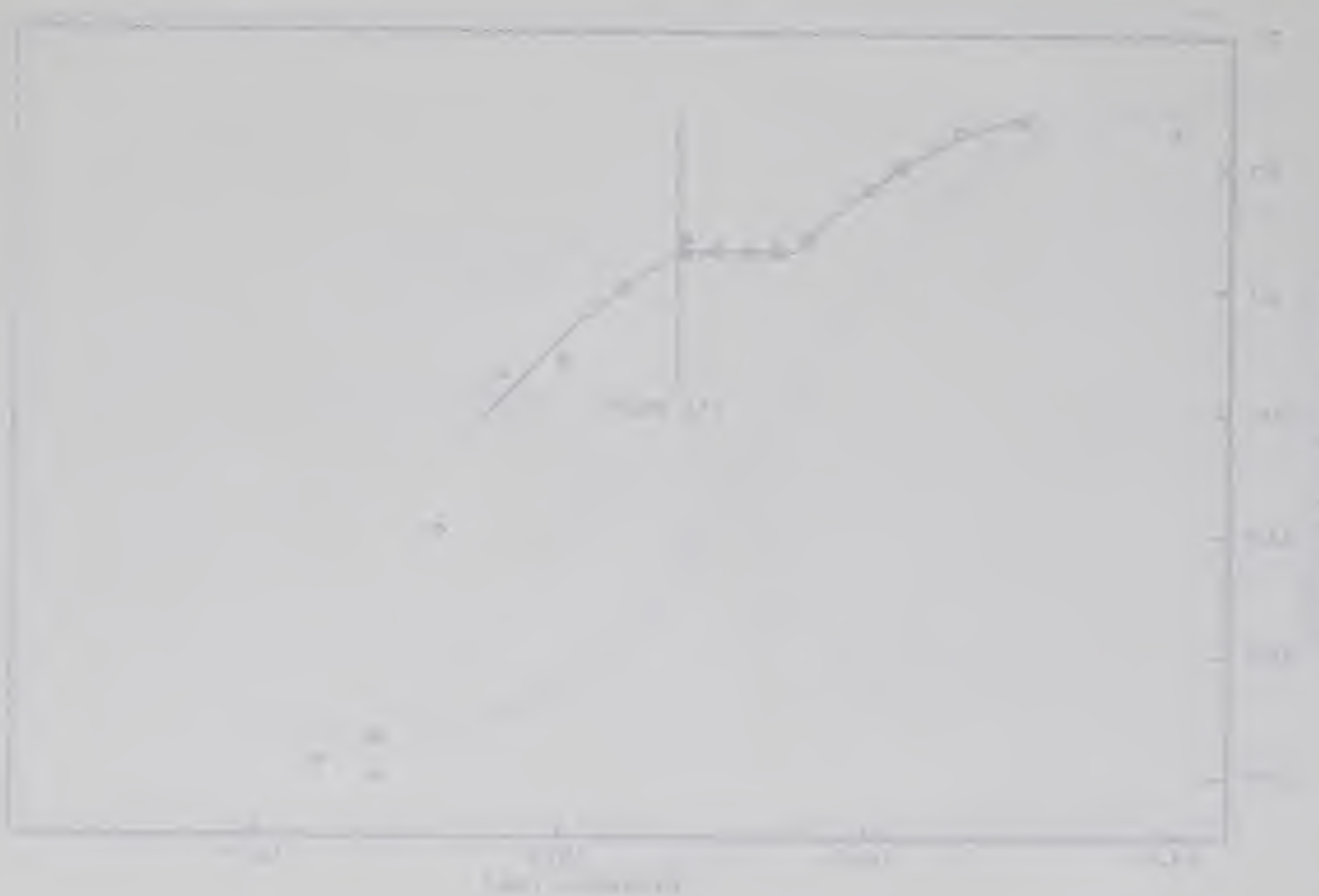

[illegible]

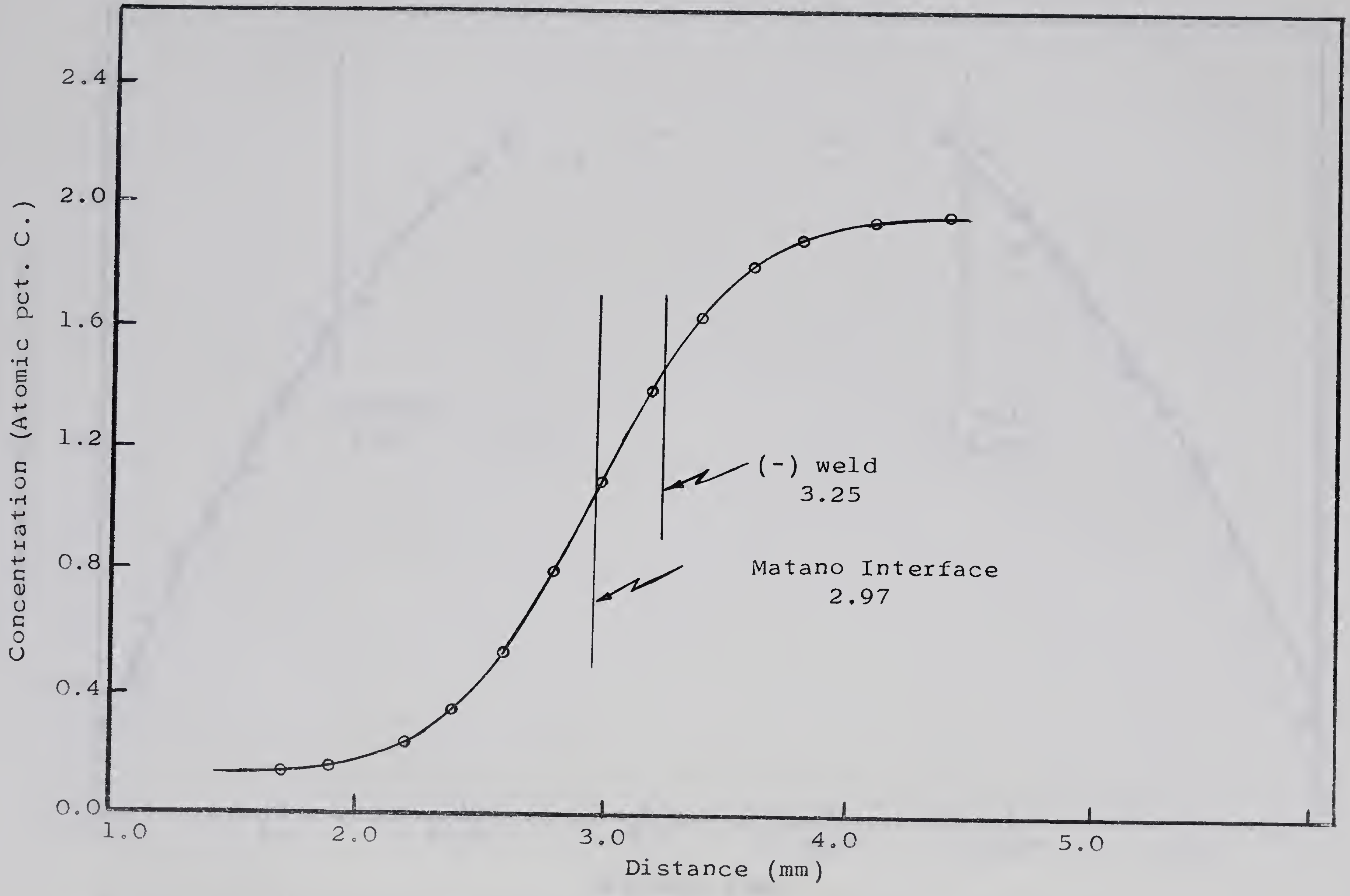

Figure 21. Concentration-Penetration Curve for Fe-C Couple C, (-) weld, Traverse (a) & (b).

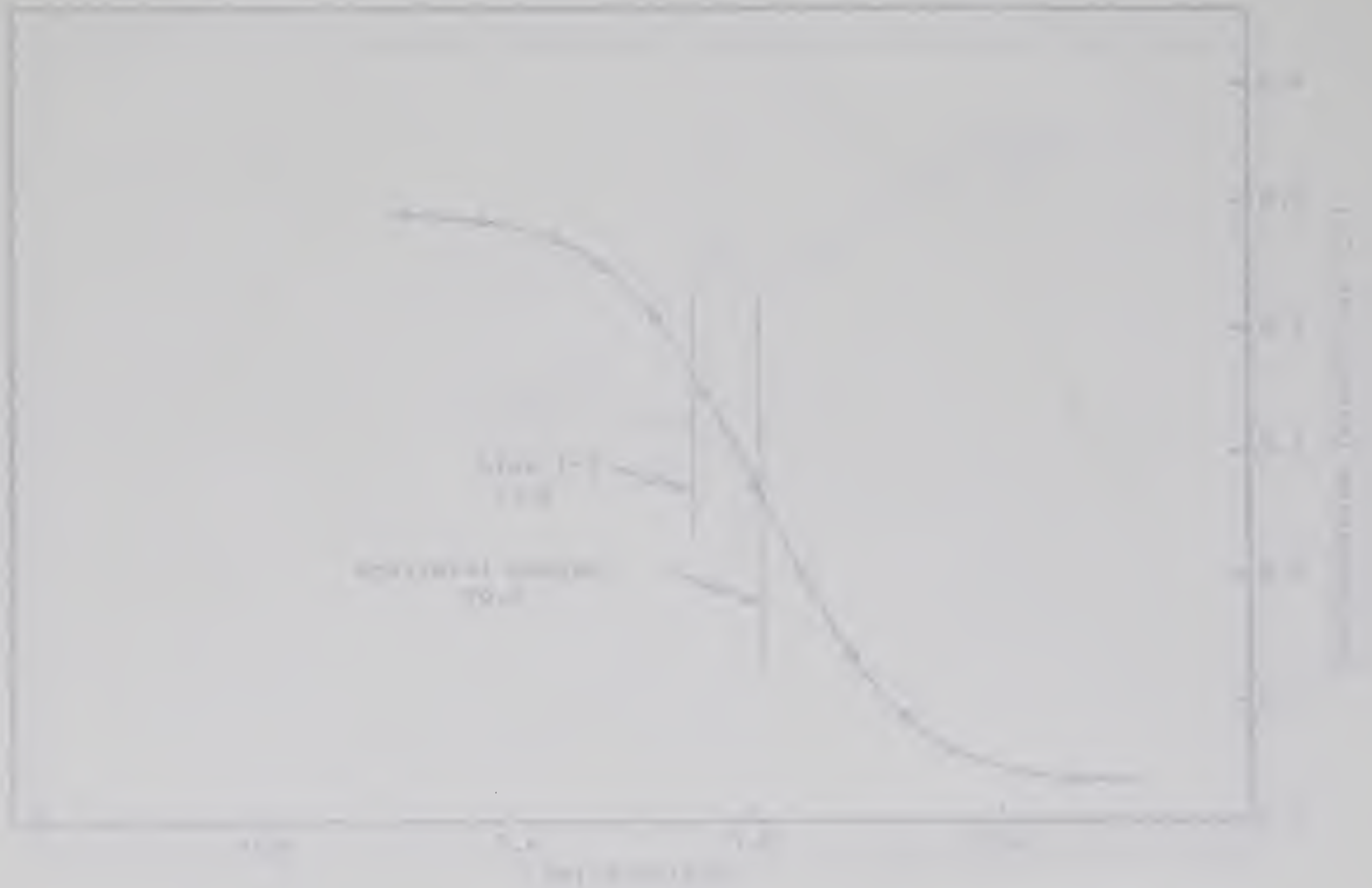

[illegible]

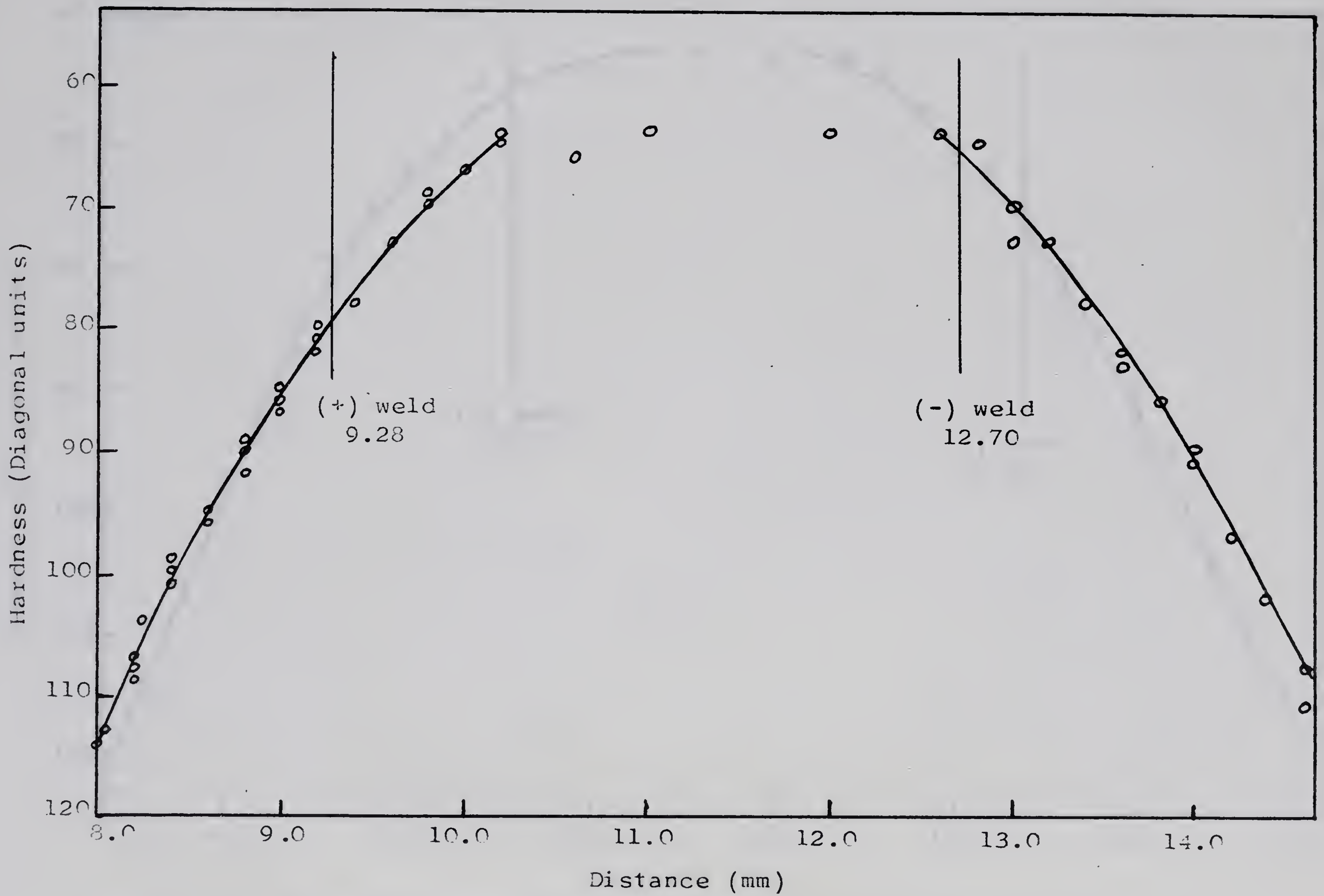

Figure 22. Hardness Traverse for Fe-4% Mn-C Couple D, Traverse (b).

[illegible]

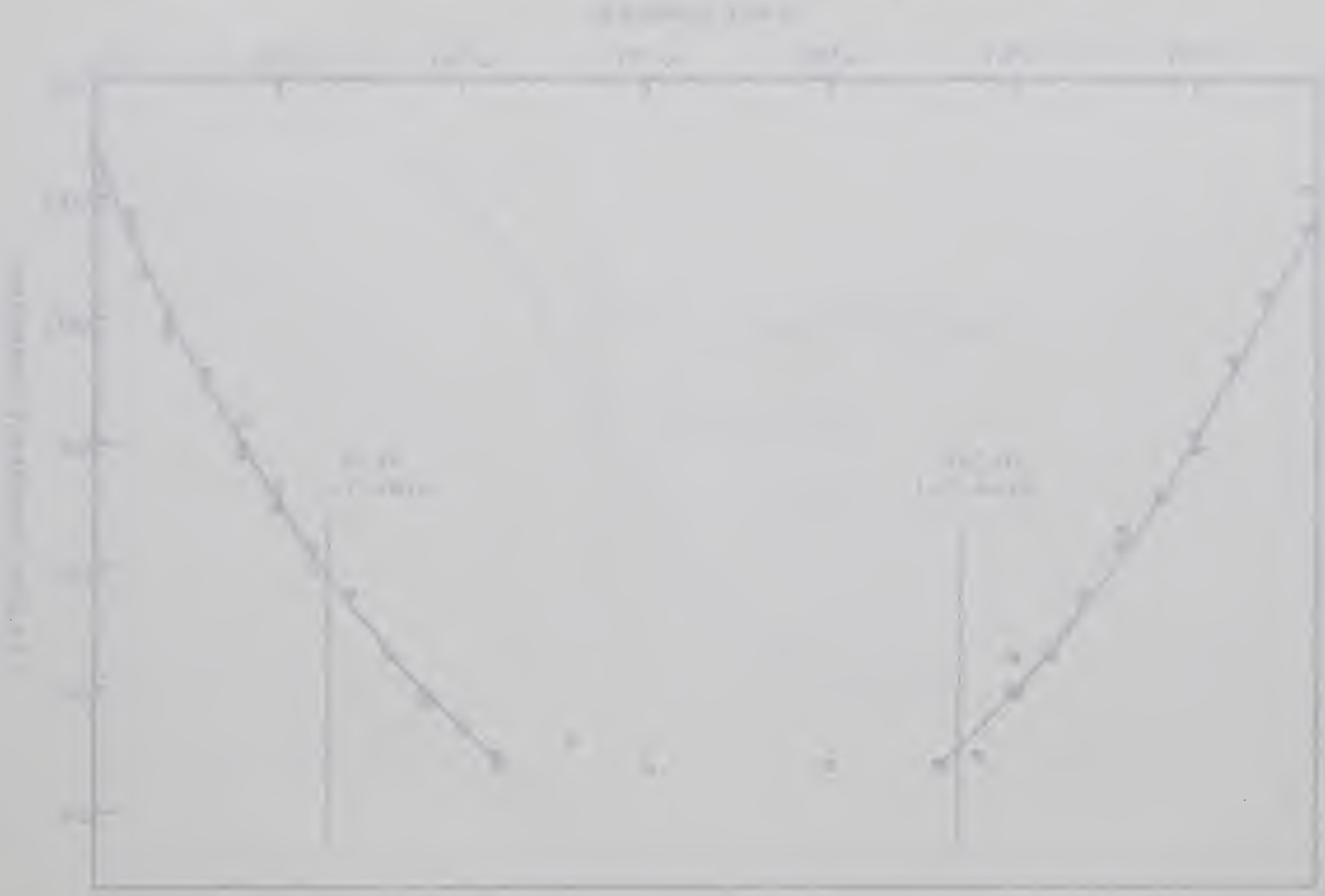

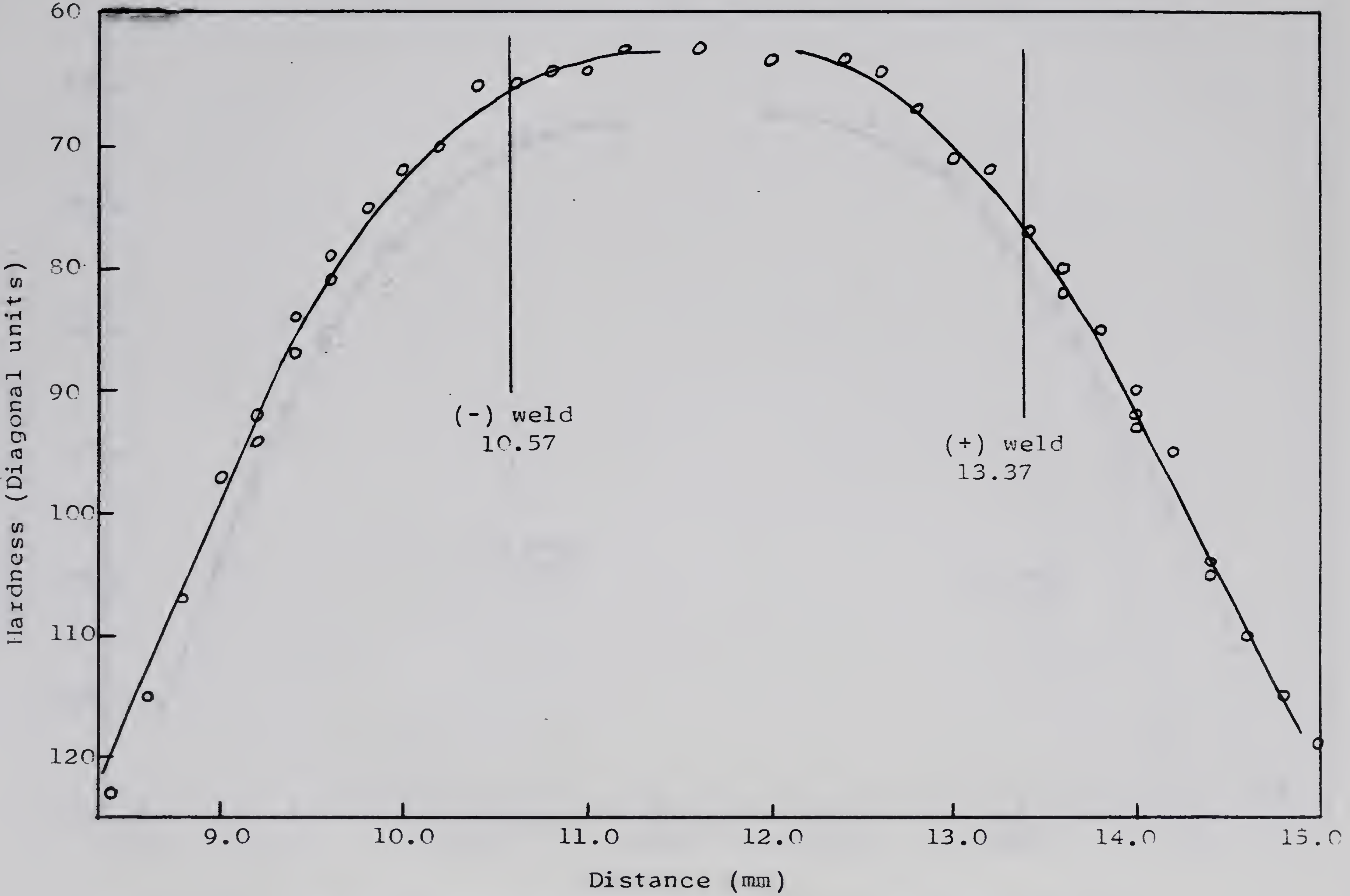

Figure 23. Hardness Traverse for Fe-4% Mn-C Couple E, Traverse (a).

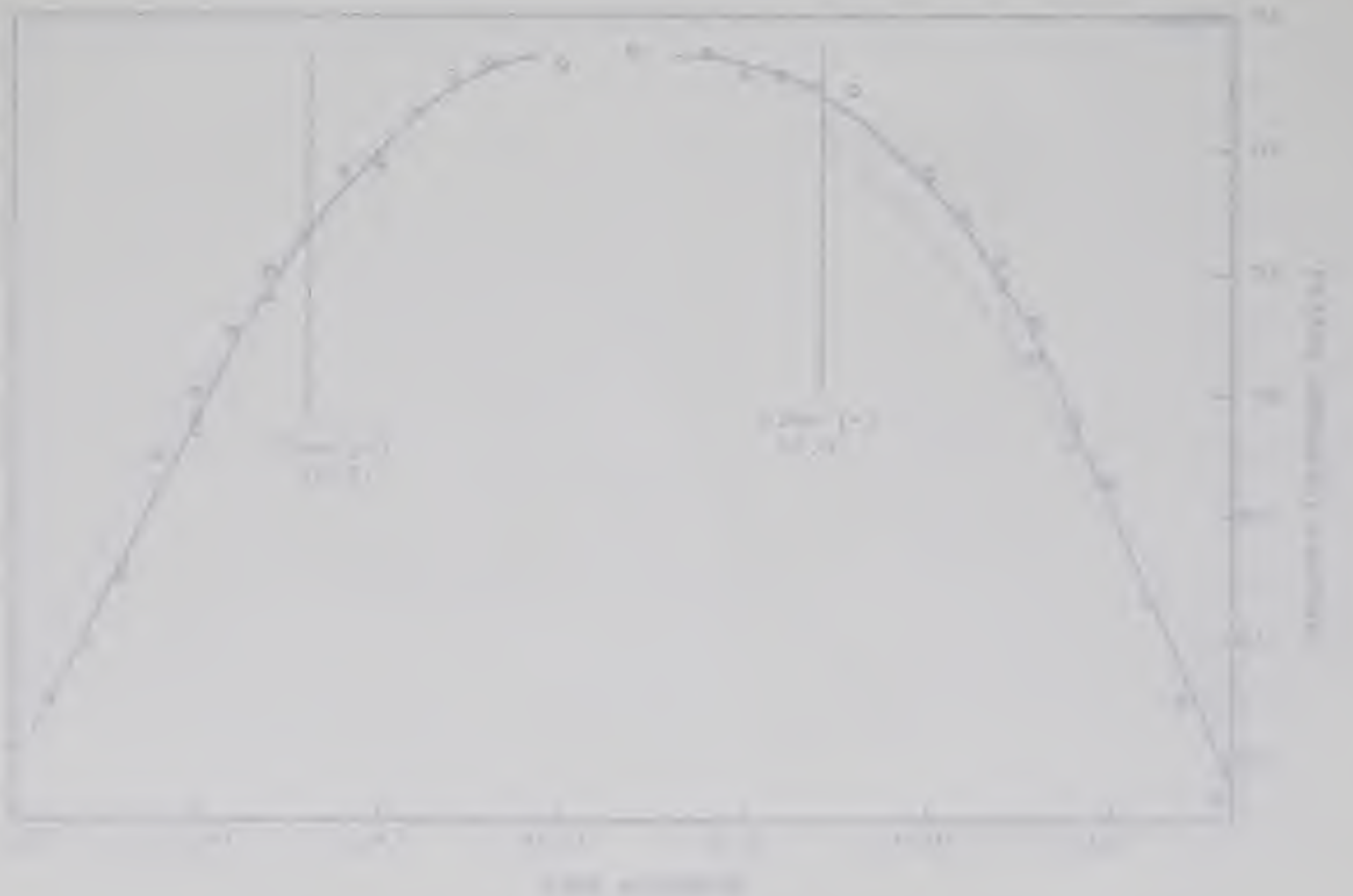

[illegible]

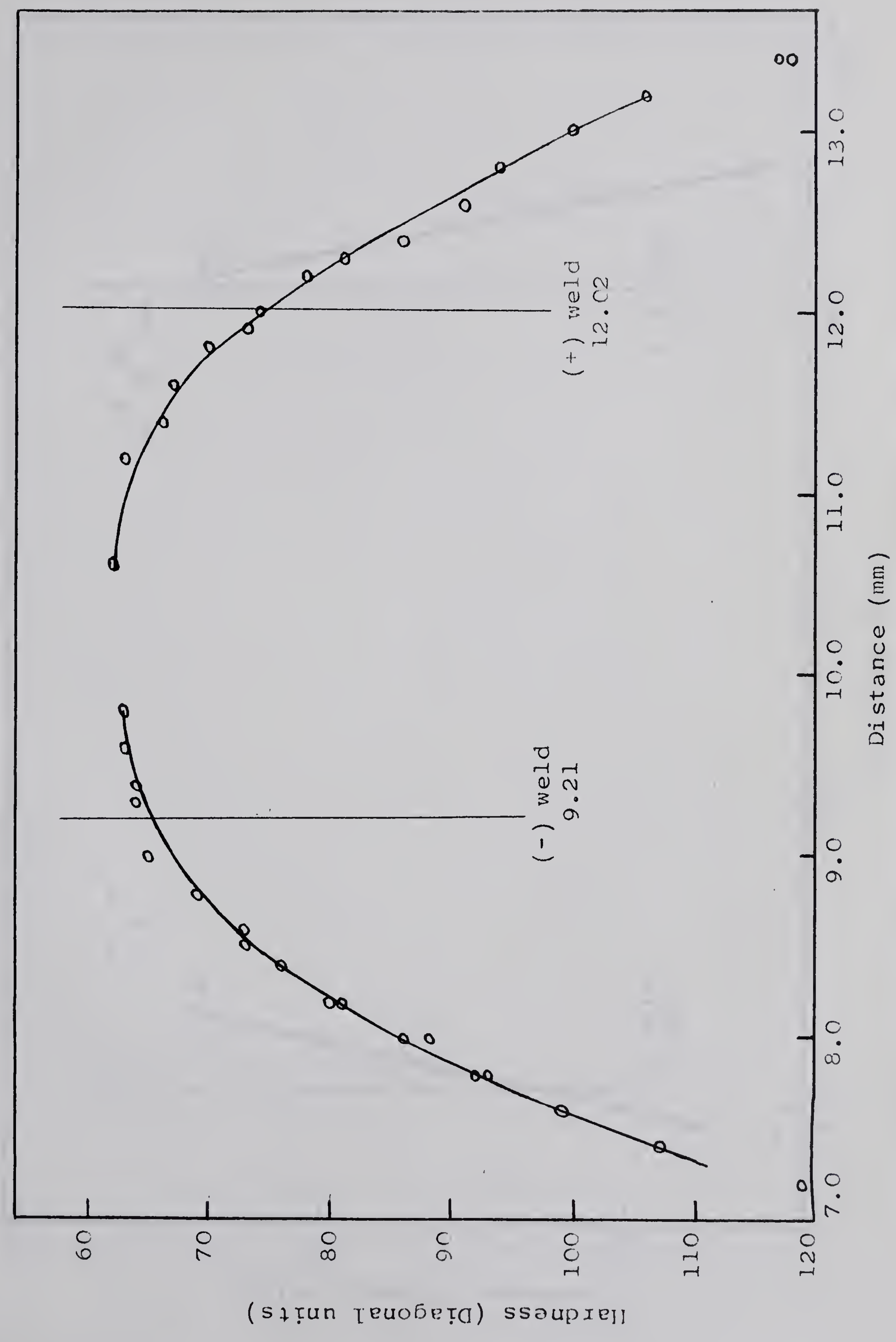

Figure 24. Hardness Traverse for Fe-4% Mn-C Couple E, Traverse (b).

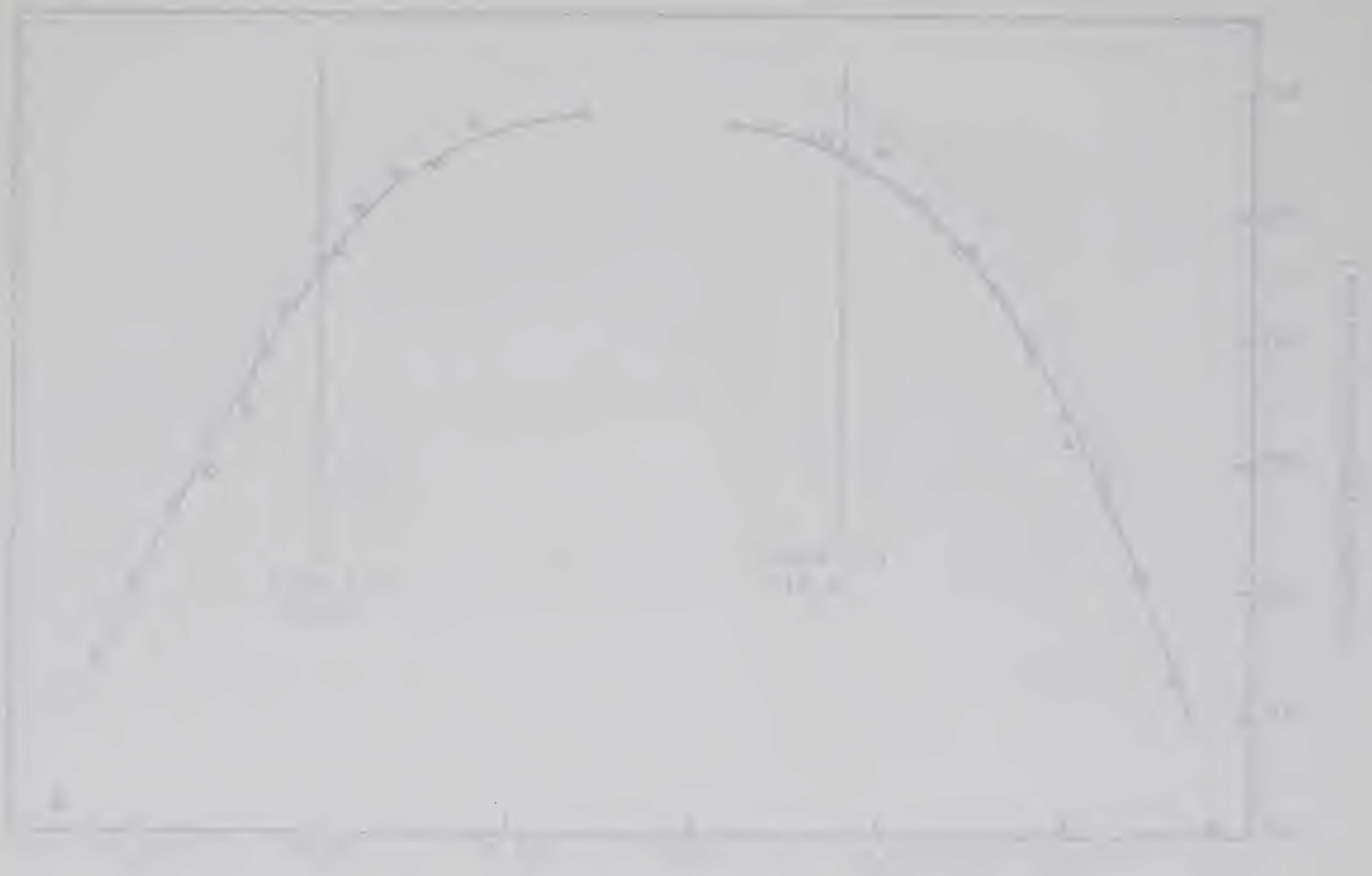

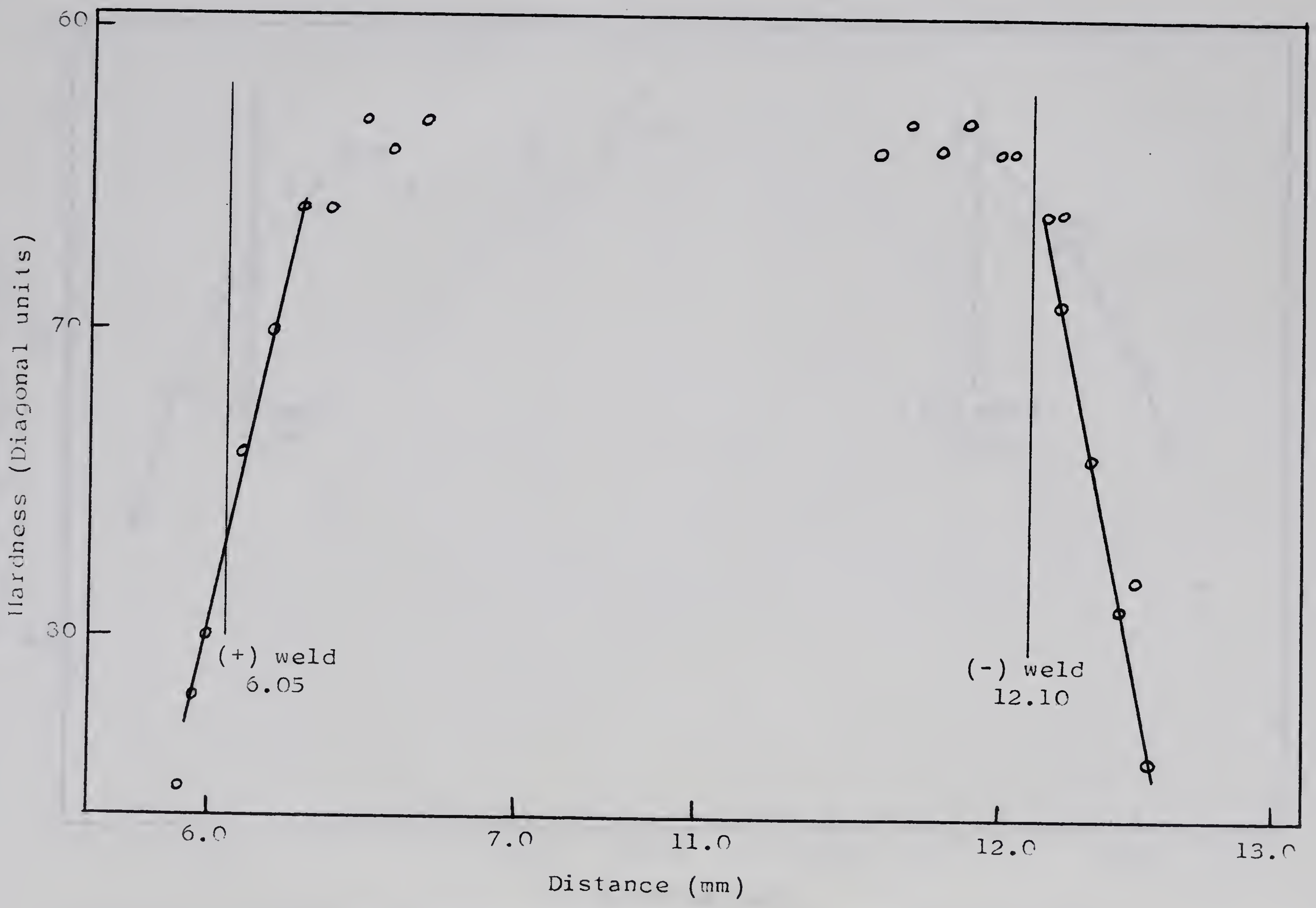

Figure 25. Hardness Traverse for Fe-2% Si-C Couple F, Traverse (b)

[illegible]

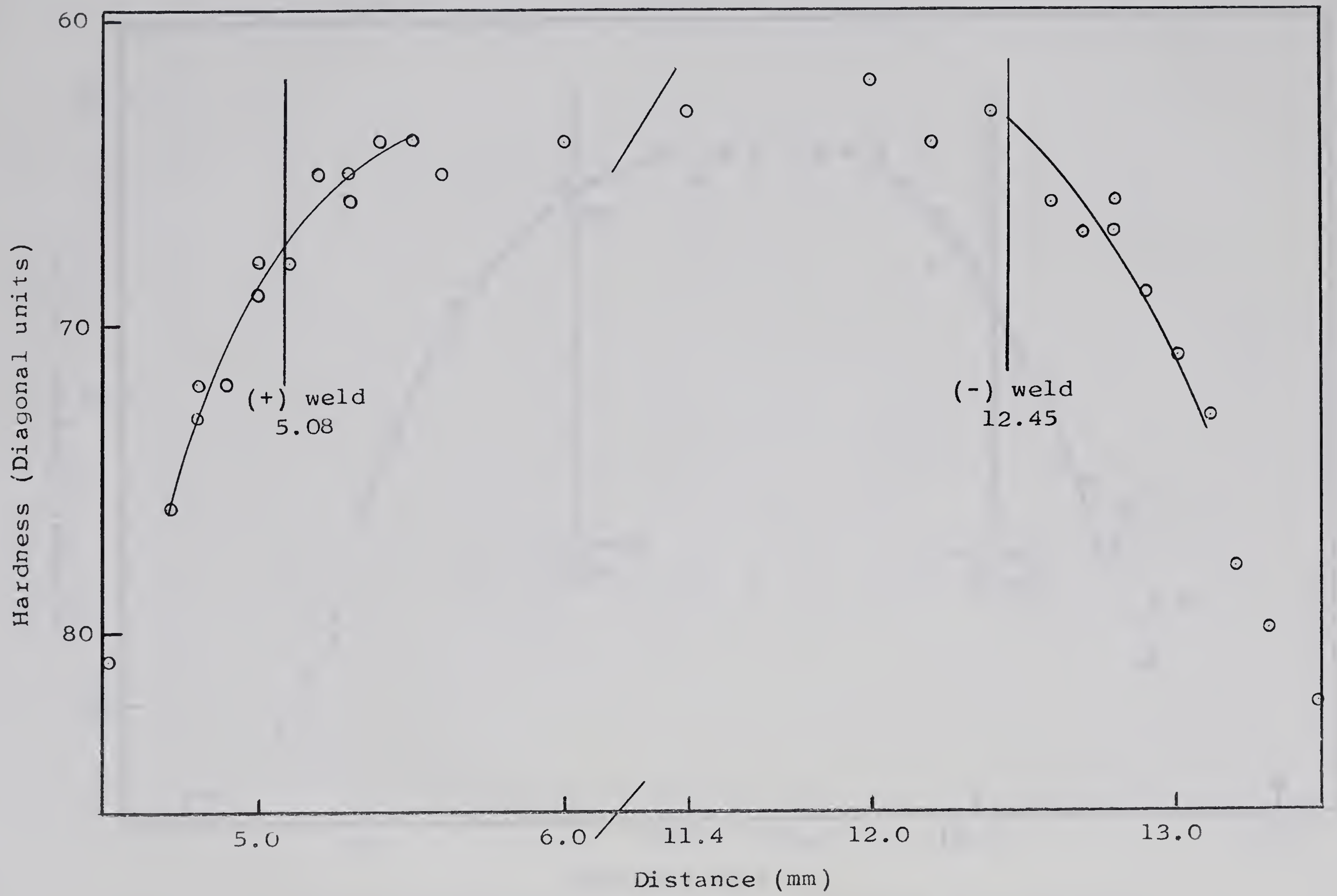

Figure 26. Hardness Traverse for Fe-2% Si-C Couple G, Traverse (a)

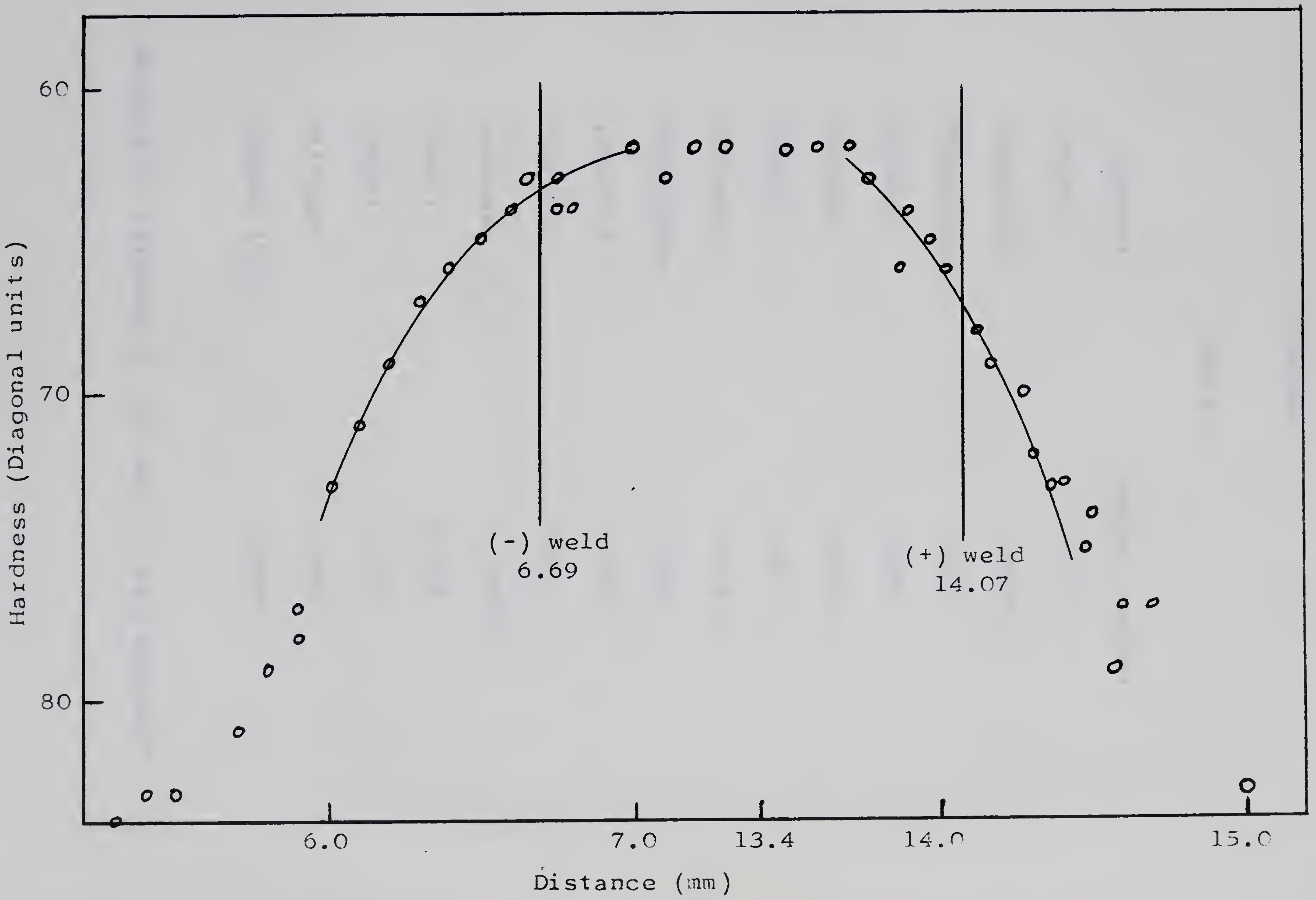

Figure 27. Hardness Traverse for Fe-2% Si-C Couple G, Traverse (b).

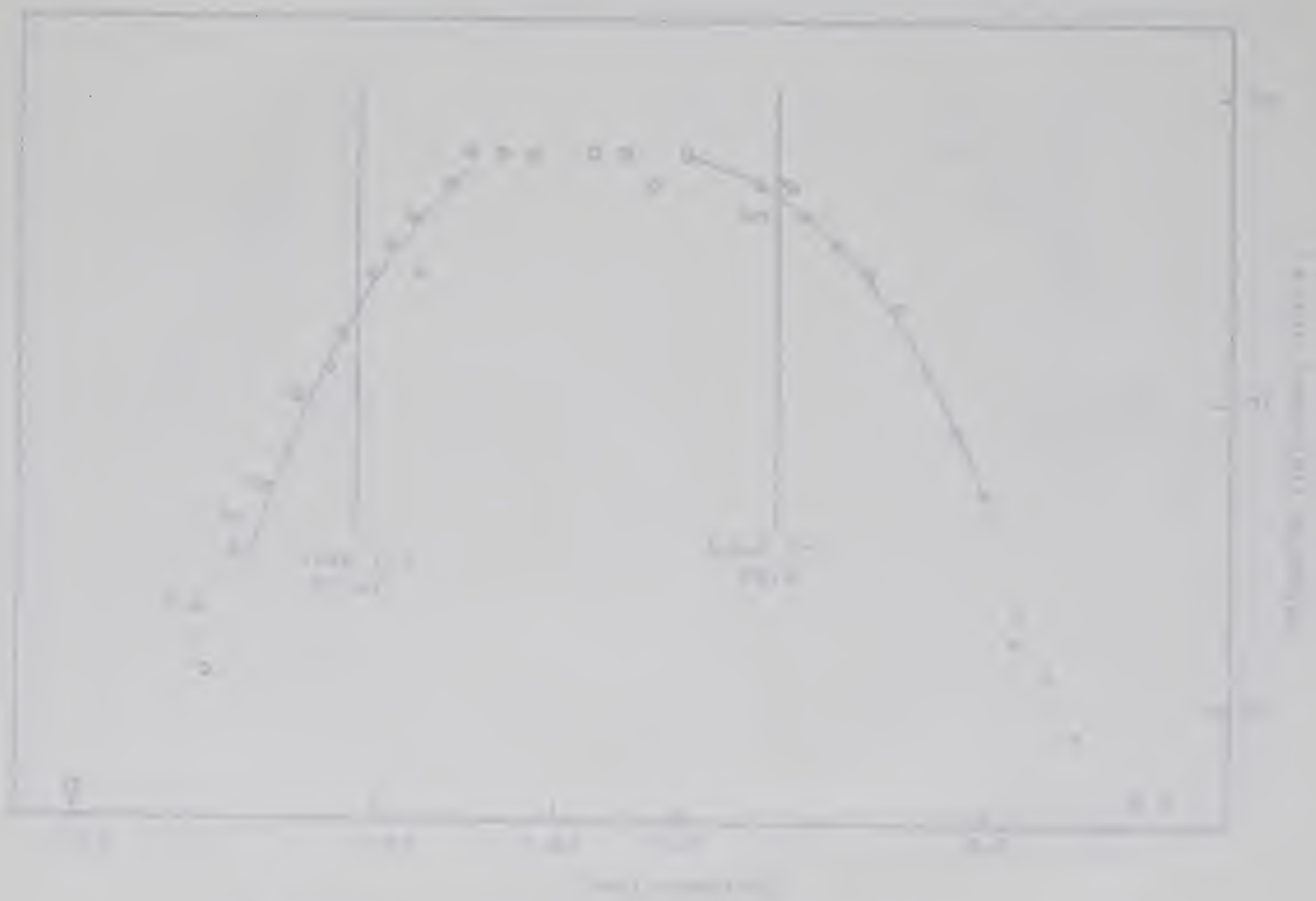

[illegible]

APPENDIX II

TABLE 1

Element	Weight percent
Carbon	0.010
Manganese	0.0005
Phosphorous	0.003
Sulphur	0.006
Silicon	0.006
Nickel	0.03
Chromium	0.003
Molybdenum	0.001
Vanadium	0.004
Tungsten	0.02
Hydrogen (H_2)	0.000027
Cobalt	0.005
Copper	0.001
Nitrogen	0.0002
Oxygen (O_2)	0.0034

Material: Ferrovac E CD Nat. "as received"

TABLE 2

Element	Weight percent
Carbon	0.030
Chromium	0.01
Copper	0.07
Manganese	0.03
Nickel	0.05
Oxygen	0.108
Phosphorous	0.010
Silicon	0.005
Sulphur	0.014

Material: Armco iron "as received"

B29836